HOW TO OVERCOME THE FEAR: CHARACTERIZATION OF SEPTAL OXYTOCIN RECEPTOR EXPRESSION AND IMPLICATIONS IN SOCIAL FEAR EXTINCTION

Dissertation zur Erlangung des Doktorgrades der Naturwissenschaften (Dr. rer. nat.) der Fakultät für Biologie und Vorklinische Medizin der Universität Regensburg

Vorgelegt von
Theresa Schäfer (geb. Süß)

aus
Ingolstadt

im Jahr
2023

Das Promotionsgesuch wurde eingereicht am:

23.11.2023

Die Arbeit wurde angeleitet von:

Prof. Dr. Inga Neumann

Unterschrift:

X

Theresa Schäfer

CONTENTS

ABSTRACT

Social interactions play a pivotal role in an individual's survival and well-being. However, when responses to social cues become maladaptive, as seen in social anxiety disorder (SAD) it becomes a pathological concern. Although cognitive behavioral therapy (CBT) combined with pharmacological treatments are commonly used to aid patients, these interventions lack specificity and often therapy success due to incomplete understanding of the disease.

To unravel the intricate neuronal and molecular mechanisms underlying SAD, the social fear conditioning paradigm (SFC) has been developed to model the core symptoms of the disease in mice. This paradigm uses a combination of operant conditioning to induce social fear and consequently avoidance of the associated stimuli and repeated social exposure afterwards (reflecting the CBT in humans) where the animals gradually override the feared situation. Using the SFC paradigm it has been shown, that Oxytocin (OXT) signaling mediated by binding to the corresponding oxytocin receptor (OXTR) in the dorsal part of the lateral septum (LS) reverses social fear expression in mice. Furthermore, alterations in OXTR binding in the LS were observed during repeated presentation of social cues to conditioned animals. This suggests, that OXTR mediated signaling in the LS is involved in the expression and extinction of social fear.

Building up on these findings I aimed to characterize OXTR expressing cells ($OXTR^+$) within the LS regarding their spatial distribution, molecular identity and further connectivity and specify the involvement of $OXTR^+$ cells within the SFC regarding their temporal involvement and downstream signaling cascades.

Using receptor autoradiography, in situ hybridization, and tracing techniques, I characterized $OXTR^+$ cell populations within the LS, and found approximately 20% of the LS cells expressing OXTR, with a heterogeneous distribution pattern on protein and mRNA levels, concentrated in the intermediate caudal part of the LS. Notably, $OXTR^+$ neurons projecting to the medial habenula were identified within the caudal part of the LS (LSc). Infusion of synthetic OXT or an OXTR-Gαi agonist in the LSc prior to social fear extinction facilitated extinction and stabilized the extinction memory (OXTR-Gαi agonist), while OXTR-Gαq activation had no impact on extinction or recall. These findings indicate that OXT modulated social fear extinction via specific OXTR-mediated pathways. Using in vivo calcium imaging, I further demonstrated that LSc-$OXTR^+$- neurons exhibit selective responses to social interaction, which changed after animals experienced a socially traumatic event. Therefore, LSc-$OXTR^+$ neurons showed a decreased activation prior to social fear acquisition, which

was increased afterwards and normalized with successful extinction of social fear. Categorization of behavioral subgroups, revealed differential modulation of LSc-OXTR$^+$ neurons following social fear induction in animals with a rapid, or slow extinction success, highlighting their contribution to variable extinction outcomes.

This work describes a population of OXTR$^+$ neurons in the LS and the involvement of this cells in the regulation of social interaction and social fear extinction. Furthermore, it provides novel insights into the dynamic activity patterns of LSc-OXTR$^+$ neurons before and after a socially traumatic event with a high temporal resolution, and advances our comprehension of the LSc-OXTR mediated signaling in individual therapy efficacy.

ZUSAMMENFASSUNG

Soziale Interaktionen spielen eine zentrale Rolle für das Wohlbefinden und Überleben bei vielen Spezies. Beim Krankheitsbild der sozialen Angststörung, wird die Reaktion auf einen sozialen Reiz unproportional. Aktuell wird eine Kombination aus Verhaltenstherapie und Pharmakotherapie als Behandlungsstrategie für Patienten angewandt, allerding zeigen hohe Rückfallquoten und geringe Therapieerfolge die mangelnde Spezifität dieser Anwendungen auf. Dieser Umstand ist auf das unzureichende Verständnis der zugrundeliegenden neuronalen Mechanismen zurückzuführen.

Um diese neuronalen Mechanismen besser untersuchen zu können wurde ein Tiermodel entwickelt, welches spezifisch die Symptome der Krankheit in männlichen Mäusen wiederspiegelt entwickelt, das sogenannte social fear conditioning (SFC) Paradigma. Das Model basiert auf operanter Konditionierung und induziert spezifische Angst vor Artgenossen und folglich Vermeidung dieser in den experimentellen Tieren. Allerdings führt eine wiederholte Konfrontation mit Artgenossen im Anschluss zu einer graduellen Extinktion der induzierten Angst. Durch Verwendung dieses Tiermodels, konnte bereits gezeigt werden, dass Bindung von Oxytocin (OXT) an den Oxytocin Rezeptor (OXTR) im lateralen Septum (LS) den Extinktionsprozess verbessern kann.

In der vorliegenden Arbeit charakterisiere ich Zellen im LS welche OXTR exprimieren hinsichtlich ihrer räumlichen Verteilung innerhalb verschiedener Subregionen im LS, als auch im Hinblick auf ihre Konnektivität und Expression anderer Neurotransmitter. Weiterhin untersuche ich inwiefern OXTR mediierte Signale bei der Extinktion sozialer Angst involviert sind unter Verwendung the SFC Paradigmas.

Unter Verwendung von OXTR-Autoradiographie, *in situ* Hybridisierung und viraler Vektoren, konnte ich zeigen, dass ca. 20% der Zellen im LS OXTR exprimieren, diese akkumuliert im kaudalen Teil des LS auftreten und weiterhin zu einer Region projizieren, die als mediale Habenula bekannt ist. Infusion von OXT in den kaudalen Teil des LS führte zu einer beschleunigten Extinktion der sozialen Angst. Außerdem konnte derselbe Effekt durch identische Verabreichung eines OXTR-Gαi Agonisten erzeugt werden, während die Injektion eines OXTR-Gαq keinen Effekt aufwies. Diese Ergebnisse weisen darauf hin, dass OXT Bindung im kaudalen Teil des LS zu einer erleichterten Extinktion sozialer Angst führ und zwar spezifisch über einen weiterführenden OXTR- Gαi mediierten Signalweg. Durch in vivo Messung von Kalzium Influx konnte ich weiter demonstrieren, dass OXTR+ Neuronen im kaudalen Teil des LS spezifisch auf soziale Interaktionen aktiviert werden. Nach Induktion eines sozialen Traumas mithilfe des SFC Paradigmas zeigten OXTR+ Neuronen

reduzierte Aktivität, welche jedoch mit zunehmenden Extinktion Erfolg wieder anstieg. Zusätzlich konnte ich unter den experimentellen Tieren zwei Gruppen identifizieren, eine Gruppe mit schnellem und eine mit verzögertem Extinktionserfolg. Die Gruppen zeigten eine unterschiedliche Regulierung der OXTR+ Neuronen im kaudalen LS bei sozialem Kontakt während des Extinktionstraining, was darauf hindeutet, dass eine temporal spezifische Regulierung dieser Neuronen in variable Extinktionserfolge involviert ist.

Diese Arbeit beschreibt eine Population von Neuronen im LS die OXTR exprimiert und untersucht die Regulation dieser Zellen im Hinblick auf soziale Interaktion und der Extinktion von Trauma induzierter sozialer Angst. Zum ersten Mal werden hier Aktivitätsmuster OXTR+ Neuronen im kaudalen Teil des LS vor- und nach einem sozialen Trauma beschrieben. Diese Erkenntnisse könnten signifikant zu unserem Verständnis individueller Therapieansätze für Patienten mit sozialer Angststörung beitragen.

ABBREVIATIONS

5-HT ..... *Serotonin*
AAV ..... *Adeno Assoicated Virus*
AH ..... *Anterior Hypothalamus*
AMY ..... *Amygdala*
AON ..... *Anterior Olfactory Nucleus*
aSFC ..... *adapted SFC*
AVP ..... *Arginine Vasopressin*
BNST ..... *Bed Nucleus of the Stria Terminalis*
CA1 ..... *Cornu Ammonis region 1*
CA2 ..... *Cornu Ammonis region 2*
cAMP ..... *cyclic* Adenosine Monophosphate
CBT ..... *Cognitive Behavioral Therapy*
CNS ..... *Central Nervous System*
CRF ..... *Corticotropin Releasing Factor*
CS ..... *Conditioned Stimulus*
DA ..... *Dopamine*
DSM-5 ..... *Diagnostic and Statistical Manual of Mental Disorders*
ER ..... *Estrogen*
FEA ..... *Fast Extinction Animals*
fMRI ..... *functional Magnetic Resonance Imaging*
GABA ..... *Gamma-Aminobutyric Acid*
GECI ..... *Genetically Encoded Calcium Indicator*
GPCR ..... *G Protein Coupled Receptor*
GRIN ..... *Gradient Refractive Index*
HIP ..... *Hippocampus*
HPA ..... *Hypothalamo Pituitary Adrenal*
HYP ..... *Hypothalamus*
icv ..... *intracerebroventricular*
LHb ..... *Lateral Habenula*
LS ..... *Lateral Septum*
LSd ..... *LS dorsal part*

LSi ..... *LS intermediate part*

LSr ..... *LS rostral part*

LSv ..... *LS ventral part*

MAOI ..... *Monoamine Oxidase Inhibitor*

Mhb ..... *Medial habenula*

NAC ..... *Nucleus Accumbens*

Nts ..... *Neurotensin*

OB ..... *Olfactory Bulb*

OXT ..... *Oxytocin*

OXTR ..... *Oxytocin Receptor*

OXTR+ ..... *Oxytocin Receptor expressing*

PAG ..... *Periaqueductal Gray*

PFC ..... *Prefrontal Cortex*

PLCß ..... *Phospholipase C ß*

PVN ..... *Paraventricular Nucleus*

ROI ..... *Region Of Interest*

SAD ..... *Social anxiety disorder*

SEA ..... *Slow Extinction Animals*

SEM ..... *Standard Error of the Mean*

SFC ..... *Social Fear Conditioning*

SNRI ..... *Serotonin Noradrenaline Reuptake Inhibitor*

SON ..... *Supraotic Nucleus*

SSRI ..... *Selective Serotonin Reuptake Inhibitor*

SSt ..... *Somatostatin*

Str ..... *Striatum*

US ..... *Unconditioned Stimulus*

V1a ..... *Vasopressin receptor 1a*

V1b ..... *Vasopressin receptor 1b*

V2 ..... *Vasopressin receptor 2*

VDB ..... *Ventral Diogonal band of Broca*

Veh ..... *Vehicle*

VMH ..... *Ventromedial Hypothalamus*

VTA ..... *Ventral Tegmental Area*

WT ..... *Wild Type*

LIST OF TABLES

LIST OF FIGURES

1 INTRODUCTION

1.1 Fear and Anxiety

Fear and Anxiety are considered “emotional states” that trigger behavioral and physiological responses in order to reduce, or avoid harm and therefore increase the fitness and survival of an organism (Lewis and Haviland-Jones, 2008). While fear occurs upon a real and imminent danger, which requires rapid decision making and dissipates on removal of the threatening stimuli, anxiety can be triggered by an internally generated, or potential threat, with a high variability in persistence (Davis, 2006).

However, the concept and definition of emotion is a complex and highly debated topic. In the 19th century Charles Darwin proposed that emotions motivate people to respond quickly to stimuli in the environment, which helps to improve their fitness and survival (Darwin et al., op. 1998). Indeed, the ability to interpret a situation or the emotion of another animal correctly is crucial for the success of an individual. Compiling ideas and concepts from different researchers (Anderson and Adolphs, 2014; Darwin et al., op. 1998; Izard, 2009; Kleinginna and Kleinginna, 1981; LeDoux, 2000), Anna Zych and Nadine Gogolla defined emotion as this:

“Emotions are functional states that bear essential roles in promoting survival and thus have emerged through evolution. Emotions trigger behavioral, somatic, hormonal, and neurochemical reactions, referred to as expressions of emotion.” (Zych and Gogolla, 2021)

Therefore, an emotional state results in detectable and measurable physiological and behavioral adaptations. Fear and anxiety trigger strikingly similar responses across different species (Calhoon and Tye, 2015), which also reflect their importance as adaptations to potentially dangerous environments. Both, fear and anxiety elicit defensive behaviors and involve similar physiological processes, such as activation of the two key stress systems, i.e., the hypothalamo-pituitary-adrenal (HPA) axis and the sympathetic nervous system, in order to redirect energy to components required for physical activity. This includes, for example, an increased heart rate and respiration to provide the muscles with oxygen-rich blood in preparation for physical activity and increased glucocorticoid levels which consequently leads to increased glucose levels in the bloodstream (Öhman, 2008; Steimer, 2002).

Fear and anxiety have evolutionary benefits and are important for an individual's survival and well-being. However, when an emotion and its corresponding behavioral trait become inappropriate, either in terms of intensity or duration of the response to the perceived stimuli, it becomes a

pathological issue (Lewis and Haviland-Jones, 2008). Whenever the response to fear and anxiety become excessive and/or chronic it becomes a pathological condition, summarized under the term anxiety disorders in the Diagnostic and Statistical Manual of Mental Disorders (DSM-5) (Association, 2016). According to the DSMV, anxiety disorders include separation anxiety disorder, selective mutism, specific phobia, panic disorder, agoraphobia, generalized anxiety disorder and social anxiety disorder (SAD). All anxiety disorders display an immense burden for affected patients and among them, SAD is one of the most frequent psychiatric disorder (Cohen et al., 2007; Leichsenring and Leweke, 2017; Stein, 2022) and will be the focus of this thesis.

1.2 Social Anxiety Disorder

SAD, also known as social phobia, can be characterized by exaggerated and persistent fear and anxiety of being judged and humiliated in social situations. This results in patients developing an avoidance posture, which impairs their normal daily functioning, with severe consequences on their socio-economic status and their overall quality of life. The 12-month prevalence in the USA and Europe is estimated to be approximately 7% and 2.3% respectively, with a slightly higher prevalence in women (Ruscio et al., 2008)(Figure 1).

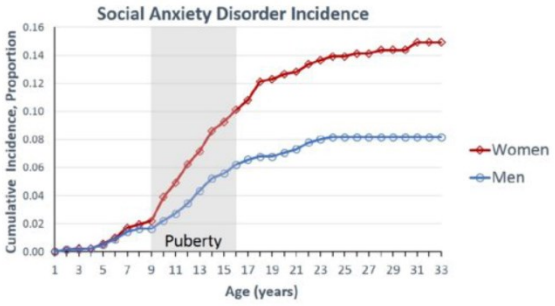

Figure 1: Onset of social anxiety disorder (SAD).Onset of SAD in men and women, image adapted from (Wright et al., 2020).

Onset and persistence of SAD have various factors, with most cases starting in juvenile age (between 8-15 years) (Kessler et al., 2005), and usually the experience of a specific traumatic event, such as bullying in school, or physical or psychological abuse. Additionally, there is also a genetic predisposition. If SAD occurs within families, relatives of the first degree have a 2-6 times higher

predisposition to develop the disease. Furthermore, the patient's ethnic background can play a role; for example, in Japan and Korea, a syndrome called *Taijin Kyofusho* can occur, which is characterized by the fear of the patient to cause unease in other people (e.g. “my look causes anger in other people so they avoid me and look away”). SAD also shows a high comorbidity with other anxiety disorders, major depression, and substance use disorders (Falkai and Hans-Ulrich Wittchen, 2014).

1.2.1 Treatment of Social Anxiety Disorder

SAD is typically treated with a combination of psychotherapy and pharmacotherapy. Cognitive behavioral therapy (CBT) is often the most effective type of psychotherapy for SAD (Acarturk et al., 2009; Barkowski et al., 2016; Powers et al., 2008), as it aims to teach patients a different way of thinking, behaving, and reacting to fearful situations through progressive confrontation (Choy et al., 2007; Craske, 2010). A CBT treatment program starts with psychoeducation, where the patient is informed about SAD, followed by cognitive restructuring with exposure exercises, where the patient is confronted with the feared situation, often in form of a role-play single persons or groups. Therefore, this specific type of CBT is also referred to as exposure therapy. The protocol includes 16 sessions (Hope et al., 2010) and the treatment outcome is then measured using the Liebowith Social Anxity Scale (LSAS) which assesses the reaction and performance of the patient in social situations (Heimberg et al., 1999). The effectiveness of of CBT in SAD is based on the promotion of therapeutic learning and memory modification. From a neuroscientifically point of view, that is based on experience-dependent plasticity mechanisms, whereas neuronal communication and consequently also the architecture of the the neuronal network mediating the behavioral and physiological response to a threat is modified (McKay and Tryon, 2017). However, the exact brain regions and neuronal mechanisms mediating this change are far from being understood.

Usually patients obtain the best results, when CBT is coupled with different types of medication (Fedoroff and Taylor, 2001; National Institute of Mental Health, 2023), including antidepressive and anxiolytic drugs, and beta-blockers:

- Antidepressants

  Antidepressants, such as selective serotonin reuptake inhibitors (SSRIs) and serotonin-noradrenaline reuptake inhibitors (SNRIs), are commonly used to treat SAD. These medications inhibit the reuptake of the neurotransmitters serotonin and noradrenalin, resulting in increased availability. Since SAD shows a high comorbidity with depressive disorder, due to isolation of

the patients, it can affect an individual's mood, and antidepressants can help alleviate these mood related symptoms. However, antidepressants generally have a slow onset of action. Additionally, they may cause side effects, such as headaches, nausea, or difficulty sleeping (Singewald et al., 2015).

Monoamine oxidase inhibitors (MAOIs), which inhibit the degradation of monoamines such as serotonin, dopamine, thyramine, and noradrenaline, are also used to treat SAD. However, due to limited effectiveness and several side effects, such as dry mouth, high blood pressure, nausea, and weight gain, MAOIs are considered a third-line treatment option for SAD (Sareen and Stein, 2000).

- Anxiolytics

Benzodiazepines are most frequently used anxiolytics that enhance the effect of the neurotransmitter gamma-aminobutyric acid (GABA), resulting in sedative, anxiolytic, and muscle-relaxant properties. They have a rapid onset of anxiolytic action. However, people may develop drug tolerance or substance dependence (Singewald et al., 2015).

- Beta-blockers

Beta-blockers, which are predominantly used to control arrhythmia and high blood pressure, are another medication used to treat SAD. They can help control some of the physical symptoms of social anxiety, such as increased heart rate, sweating, and tremors, by blocking the blocking the receptor sites for the stress hormones adrenaline and noradrenaline, which slows down the heart rate. Beta-blockers are commonly used to treat the "performance anxiety" type of SAD. However, they may cause potential side effects, such as erectile dysfunction, memory loss, and difficulty sleeping (Stein, 2022).

While only a minority actively seeks assistance, about half of the patients experience symptom remission after several years of treatment (Figure 2) (Feske and Chambless, 1995). Despite the existence of diverse pharmacological and psychotherapeutic interventions, a significant portion of patients fails to attain full remission, and symptoms frequently recur over time. Moreover, a considerable number of individuals exhibit a general unresponsiveness to these treatments (Stein, 2022). Consequently, there is a pressing need for in-depth exploration of underlying mechanisms and enhancements in therapeutic alternatives. However, understanding the underlying neuronal mechanisms of psychological diseases, such as social anxiety disorder (SAD), is a complex challenge. With functional neuroimaging studies, SAD patients can be confronted with social situations and local brain activation can be measured. Using functional magnetic resonance imaging (fMRI) the

changes in blood flow and oxygen consumption that occur with neuronal activity can be measured (Glover, 2011). Studies with SAD patients revealed for example an increased activity of the AMY in response to social threat in SAD patients (Stein et al., 2002). Even so fMRI studies have a relatively high spatial resolution, they lack temporal resolution and also detailed mechanistic insight within an activated region (Glover, 2011). Furthermore, human studies face ethical constraints and limitations in the available neurobiological manipulation options. Animal models offer a controlled environment to study the underlying mechanisms of these disorders, providing insights that can be translated to human conditions. Rodents, in particular, are commonly used due to their genetic similarities. Therefore, animal models are essential to examine brain-behavior relationships and the contribution of specific neuronal networks to a given abnormal behavior under controlled laboratory conditions.

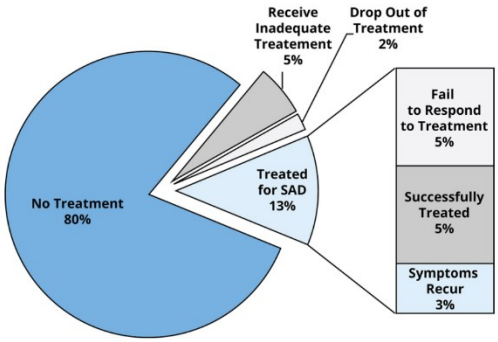

Figure 2: Treatment response of social anxiety disorder (SAD).Treatment rate of adults with SAD based on data from (Feske and Chambless, 1995; Kessler et al., 2005; Ruscio et al., 2008). Image: T. Kashdan, http://noba.to/vz2qug96.

1.2.2 Animal Models for Social Fear - The Social Fear Conditioning Paradigm

Establishing a valid animal model necessitates closely replicating various aspects of a psychiatric disease, a task fraught with challenges. To attain the utmost similarity, criteria have been proposed for assessing the validity of animal models. McKinney and Bunney first outlined validity criteria in 1969, albeit in a loosely defined manner (McKinney and Bunney, 1969). Subsequent years witnessed adaptations and modifications by researchers, with the most widely embraced criteria in animal research proposed by Willner in 1984, encompassing predictive, face, and construct validity (Willner, 1984):

1. **Predictive validity:** This dimension gauges the capacity of an animal model to foresee the outcome of a specific manipulation. For instance, if a drug proves effective in treating a disease within an animal model, predictive validity implies that the drug will likely exhibit efficacy in humans and vice versa. This emphasizes the similarity of treatment outcomes.
2. **Face validity:** Examining the behavioral or physiological alterations induced by exposing experimental animals to a model, face validity assesses the analogy between the model-induced changes and the pathological behavior observed in patients suffering from the human disease being modeled. In essence, it evaluates how closely the animal model mirrors the human disease in terms of symptoms and progression.
3. **Construct validity:** This dimension pertains to the ability of an animal model to recruit the same neurobiological substrates as the respective disorder in humans. While these criteria persist, researchers continually engage in discussions about their relevance and often introduce additional considerations. For instance, some groups introduce etiological validity, addressing early environmental/developmental factors or external triggers, thereby contributing more to construct validity. Despite its ongoing use, construct validity remains a broadly defined term, particularly challenging when attempting to align with the biological nature of a specific disease due to limited knowledge.

In efforts to refine these criteria, researchers have made conceptual strides (Belzung and Lemoine, 2011). Additionally, improvements in animal models involve the application of genetic approaches, where knowledge of the target is essential, and the ongoing integration of human findings (Cryan and Slattery, 2007). Certain criteria, such as thoughts of suicide, resist remodeling due to their inherently complex nature. The difficulty in fully understanding the causative factors of the disease in humans underscores the challenges of mimicking these aspects in animal models.

A significant portion of our understanding of neuronal processes related to fear and anxiety is derived from animal studies, primarily involving rodents and employing fear conditioning models. Fear conditioning, an associative learning task, involves animals associating a previously non-aversive conditioned stimulus (CS), often a tone, with a simultaneously presented aversive unconditioned stimulus (US), typically a mild foot shock. Through repeated pairings, the CS alone eventually triggers the conditioned fear response, a phenomenon known as operant conditioning (LeDoux, 2000).

In the social fear conditioning (SFC) paradigm (Toth et al., 2012) operant conditioning is utilized to generate social fear and avoidance in male mice, which can be considered the core symptom of SAD. During SFC, mice are placed in a conditioning chamber where social fear-conditioned animals

(SFC^+) receive a foot shock (US) each time they make direct contact with a conspecific. Control mice (SFC^-) undergo the same conditions without receiving a foot shock when investigating the conspecific. Following this procedure, SFC^+ animals display social avoidance of conspecifics, evidenced by reduced time spent investigating the conspecific. On the subsequent day, the animals are repeatedly exposed to novel unfamiliar conspecifics without punishment, mirroring exposure therapy in SAD patients. Here, the animals gradually overcome the previously induced social fear, reflected in increased social interaction over time. From a translational perspective, understanding the mechanisms mediating this so-called extinction of social fear is crucial, as these identified mechanisms could serve as targets for new drug development to support the treatment of SAD. Unlike many other protocols, the SFC does not induce unspecific symptoms such as anhedonia, general anxiety, or impairment of locomotor activity (Alfieri et al., 2022). This makes it currently the preferred option for studying the mechanisms of SAD. Notably, just one more protocol is currently used to investigate specific social impairment, which is the classical social defeat protocol, where experimental animals are defeated by an aggressive conspecific. If repeated for several days, these animals also exhibit specific social impairments without the manifestation of unspecific side effects (Franklin et al., 2017).

A neuropeptide that has been repeatedly associated already with the SFC is OXT, which is an important messenger in the regulation of emotion, but plays a clear role in the modulation of social behaviors (Masis-Calvo et al., 2018). Consequently, the next chapter will delve into more detailed information about the neuropeptide OXT and the corresponding signaling cascades via oxytocin receptor (OXTR) binding.

1.3 The Brain Oxytocin System

OXT is a peptide composed of nine amino acids with a chemical structure represented as H-Cys-Tyr-Ile-Gln-Asn-Cys-Pro-Leu-Gly-NH2. Its production is stimulated by a variety of physiological and psychological factors, reflecting its effects on the body and brain (Jurek and Neumann, 2018). Therefore, physiological functions such as milk ejection, uterine contractions, sexual arousal and penile erection, but also effects several aspects of social interactions (Althammer and Grinevich, 2017).

The main sources of OXT production are the paraventricular nucleus (PVN) and supraoptic nucleus (SON) of the hypothalamus, which contain two types of neurons differing in size and function: magnocellular and parvocellular neurons (Jurek and Neumann, 2018; Mohr et al., 1988).

Magnocellular neurons are found in the PVN and SON and synthesize either OXT or arginine vasopressin (AVP), which is a closely related nonapeptide (Gainer et al., 2002). These neurons project directly to the posterior pituitary gland (neurohypophysis) for release of the peptides in the bloodstream (Mohr et al., 1988). The magnocellular OXT producing neurons however can also from bifurcations and send axonal projections to several brain regions for OXT release in the central nervous system (CNS) (Althammer and Grinevich, 2017). Parvocellular neurons are mainly located in the PVN, on the other hand, are smaller in size and produce various other neuropeptides beside OXT, which are released into the hypophyseal portal system, for example CRH (Bondy et al., 1989). The parvocellular neurons in the PVN are thought to be the main source for centrally released OXT. For example, very well established are OXT projections to the spinal cord and brain stem to control several physiological functions, i.e. cardiovascular reactions or erection (Althammer and Grinevich, 2017). Interestingly, other regions, such as the BNST and accessory nuclei of the hypothalamus, have also been found to produce OXT (Rhodes et al., 1981).

Within the CNS, OXT can be released from the soma and dendrites coordinating OXT neurons within the hypothalamus, or reach distant brain regions via axonal projections and terminal release (Landgraf and Neumann, 2004; Ludwig et al., 1994; Morris and Pow, 1991). Long-range projections of OXT neurons in mammals and reptiles include the PFC, anterior olfactory nucleus, nucleus accumbens (NAC), septum, HIP, and medial and central AMY (Grinevich et al., 2016).

A well described transportation mechanism is the packaging and exocytosis of OXT from dense-core vesicles, which does not only occur at axon terminals, but also all other parts of the neuron (Brownstein et al., 1980). Another, possibly faster way is the local synthesis of mRNA, which apparently happens in dendrites of magnocelluar neurons, but not in axonal compartments (Mohr and Richter, 2003).

Beside temporal aspects, also the half-life time of OXT might influence its effects. OXT's half-life in the blood is estimated to be around 3-6 minutes, with primary degradation by the enzyme oxytocinase produced in the liver and kidneys. However, metabolization and clearance of OXT in the CNS are not fully understood. OXT might have a longer half-life in the brain, of about 20 minutes and be degraded by peptidases (Mens et al., 1983; Rydén and Sjöholm, 1969). Finally, receptor density and affinity also play an important role in OXT's effects, which will be discussed in the next chapter.

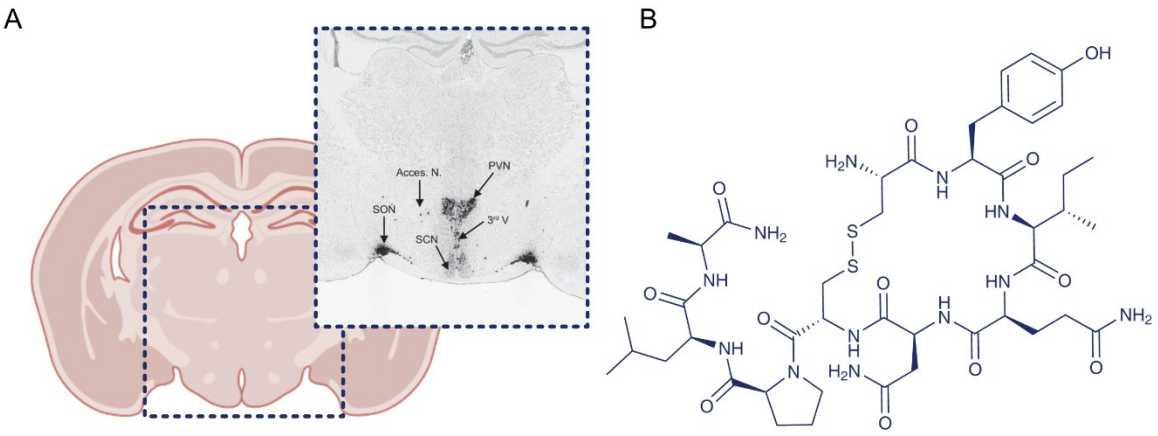

Figure 3: Oxytocin (OXT) expression and structure. A) Brain regions in the mouse that express OXT mRNA in the hypothalamic paraventricular nucleus (PVN) and supraoptic nucleus (SON), and weaker expression along the walls of the third ventricle and the accessory nuclei, as revealed by in situ hybridization. B) Chemical structure of OXT. Image adapted from (Jurek and Neumann, 2018).

1.3.1 The Oxytocin Receptor

The effects of OXT are mediated by binding to the OXTR. The OXTR is a GPCR that is composed of 389 amino acids, with seven transmembrane domains, an extracellular NH2-terminal binding region and an intracellular carboxyl terminus (Gimpl and Fahrenholz, 2001) (Figure 4, B). Beside the binding of OXT it can also bind the structurally related hormone AVP, although with lower affinity vice versa OXT also binds to the AVP receptor subtypes vasopressin receptor 1a (V1a), 1b (V1b) and 2 (V2) (Busnelli et al., 2013).

The receptor is expressed in the CNS on neurons in synapses, as well as on axons and glial processes (Mitre et al., 2016). Additionally, recent studies have shown that OXTRs are also expressed on astrocytes in various brain regions (Wahis et al., 2021). In the brain, highest expression levels are found in the central, medial, and basolateral AMY, NAC, bed nucleus of the stria terminalis (BNST), PVN, medial preoptic area, ventromedial nucleus of the HYP, HIP, ventral pallidum, periaqueductal gray (PAG), striatum (Str), LS, ventral tegmental area (VTA), and olfactory bulb (OB) (Figure 4, A), a comprehensive list of brain areas that have been identified to express the OXTR in rodents can be found in Jurek et al (Jurek and Neumann, 2018).

In peripheral tissue, the receptor is mainly expressed in reproductive organs such as the uterus and mammary glands, but can also be found in other organs (Gutkowska and Jankowski, 2012; Halbach et al., 2015; Moreno-López et al., 2013; Ostrowski et al., 1995; Taylor et al., 1989). However, this chapter focusses on OXTR in the CNS.

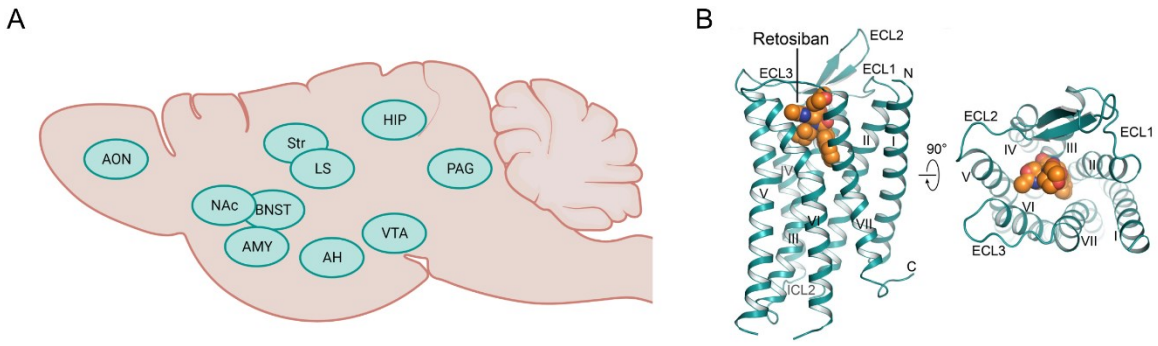

Figure 4: Oxytocin receptor (OXTR) expression and structure. Spatial distribution of OXTR that receives OXT axons in the rodent brain. AH, anterior hypothalamus; AON, anterior olfactory nucleus; AMY, amygdala; BNST, bed nucleus of the stria terminalis; HIP, hippocampus; LS, lateral septum; NAc, nucleus accumbens; PAG, periaqueductal gray; Str, striatum; VTA, ventral tegmental area (adapted from (Grinevich et al., 2016)). B) Overall structure of retosiban-bound OXTR. Left viewed parallel to the membrane plane, Right, viewed from the extracellular space (Image from (Waltenspühl et al., 2020))

When OXT is released in the brain and binds to its receptor, a cascade of intracellular signaling events is triggered, leading to changes in cell function and behavior. In general, in G protein-coupled receptors (GPCR) the β/γ subunit of the G-protein separates from the α-subunit, upon ligand binding. There are 4 subtypes of the Gα protein, Gαs, Gαi/o, Gαq/11 and Gα12/13, which further lead to different downstream signaling pathways and consequently to gene transcription. For the OXTR, promiscuous coupling to Gαi/o and Gαq/11 subtypes have been described so far (Busnelli and Chini, 2018). Coupling to Gαq/11 protein leads to increase of intracellular Ca^{2+} and activation of second messenger systems, such as the phospholipase C ß (PLCß), modulating synaptic transmission and plasticity. In contrast activation of the Gi/o subsequently decreases levels of the second messenger cyclic adenosine monophosphate (cAMP) witch then further results in decreased neuronal excitability (Eliava et al., 2016). This effects could be shown by application of specific ligands that selectively activates the Gαi-protein-coupled OXTR (eg atosiban) in cell cultures (Reversi et al., 2005). To what extent neurons express either OXTR-Gαq or -Gαi proteins, or even both simultaneously, is not clear yet. Like many other GPCR, the OXTR has been shown to form homomers (Cottet et al., 2010) as well as heterodimers with other GPCRs, which include for example the dopamine 2 receptor and the highly related V1a and V1b receptors (La Mora et al., 2016; Terrillon et al., 2003). Furthermore, the expression and integration of OXTRs depends on the availability of OXT. Secretion of OXT over a prolonged period can result in desensitization and internalization of the receptors (Busnelli and Chini, 2018). It has been shown that internalized

OXTRs are not degraded, but recycled back to the cell membrane, but the exact mechanism and function is not clear yet (Conti et al., 2009).

In summary, the OXTR can adopt multiple conformations in the CNS, and ligand binding has the potential to initiate a diverse range of downstream signaling cascades, many of which are still not fully elucidated. This diversity may yield entirely different effects on cells and might result in distinct behavioral outcomes. The field of OXTR-mediated signaling is largely unexplored territory with many open questions. A more comprehensive understanding of the distribution of specific receptor conformations and their associated downstream signaling pathways could significantly contribute to unraveling OXTR-mediated effects in certain behaviors, particularly those related to social fear.

1.3.2 Implications of Brain OXT Signaling in Social Behavior

OXT signaling within CNS plays a pivotal role in modulating various aspects of behavior, especially social behavior. Extensive research has highlighted its involvement in diverse contexts, ranging from pair bonding to anxiolysis, and from pro-social behaviors to memory enhancement (Jurek and Neumann, 2018).

The involvement of OXT in pair bonding has been demonstrated particularly in prairie voles (Microtus ochrogaster). Studies involving intracerebroventricular (icv) infusion of OXT have shown its ability to induce partner preference, emphasizing its crucial role in fostering social bonds (Bosch and Young, 2018; Carter et al., 1992). Moreover, OXT is identified as a key player in nurturing the bond between mothers and their offspring, as evidenced by studies showcasing its essential role in maternal behaviors (Demarchi et al., 2021; Neumann, 2003; Slattery and Neumann, 2008). In male rats, the local infusion of synthetic OXT into specific brain regions, including the PVN, AMY, or PFC, exerts robust anxiolytic effects (Bale et al., 2001). However, the intricate nature of OXT signaling is exemplified by contradictory findings, such as OXT infusion into the basolateral amygdala (BLA) impairing fear extinction in rats (Lahoud and Maroun, 2013). This underscores that OXT signaling is finely tuned, influenced by factors such as the site of action, dosage, timing, sex, species, and strain. OXT's impact extends to cognitive functions, as it has been found to enhance spatial memory during motherhood and is essential for social memory in both males and females (Rilling and Young, 2014). Binding of OXT in LS has been linked to improved social discrimination abilities (Popik et al., 1992; Tomizawa et al., 2003). Moreover, OXT has demonstrated its ability to facilitate pro-social behavior and prevent social avoidance in both rats and mice (Lukas et al., 2013)

Overall OXT signaling emerges as a multifaceted player in social behavior and anxiolysis. These functions, as well as reproductive and homeostatic mechanisms of OXT signaling, are extensively explored. However, implications of OXT specifically in social fear are more sparse and further investigation is urgently needed.

1.4 Neuronal Circuits of Social Fear

The behavioral and physiological response to a threatening stimulus arises from the coordinated communication of interconnected neurons in various brain regions. These networks, also known as neuronal circuits or assemblies, can exist within the same region, forming microcircuits, or can connect distant areas of the brain through long-range axonal projections. Thus, neuronal networks can be viewed as both functional and anatomical entities (Bargmann and Marder, 2013; Purves et al., op. 2012). While a large amount of research has dissected the neuronal substrates of fear and anxiety, very sparse studies focus specifically on social fear. Not surprisingly, some regions involved in social fear overlap with regions and circuits found in general fear and anxiety processing.

A major and complex processing station that modulates memory encoding and consolidation by evaluating the emotional relevance of perceived stimuli is the amygdala (AMY) (Richardson et al., 2004). Neuroimaging studies suggested amygdala-hyper-responsivity in SAD patients confronted with pictures of angry faces compared with healthy controls (Evans et al., 2008). Interestingly, acute intranasal administration of Oxytocin (OXT) attenuated the heightened AMY reactivity to fearful faces in SAD patients, suggesting an involvement of OXT in modulating exaggerated processing of social signals of threat in patients with SAD (Labuschagne et al., 2010). However, more detailed insights in the neuronal structures and mechanisms involved in social fear arises from rodent studies. Employing an innovative technology known as CANE (capturing activated neuronal ensembles), scientists successfully labeled neurons selectively activated during encounters with fearful social stimuli in the ventromedial hypothalamus (VMH). In the experimental setup, mice underwent aggression from a dominant resident before participating in a social interaction test with a non-aggressive conspecific. Remarkably, optogenetic stimulation of the identified neurons induced social avoidance during the subsequent social interaction test, even in the absence of a prior aggressive encounter with a resident (Sakurai et al., 2016). In a quite similar experimental setup using *in vivo* calcium imaging, a separate research group observed a reorganization of neuronal activity in the VMH of mice during social encounter following social defeat. The findings suggest that dynamic alterations in the activity of specific neurons may play a crucial role in mediating adaptations in social behavior after experiencing social trauma. (Krzywkowski et al.,

2020). Utilizing the SFC paradigm, an elevation in c-fos positive cells in the prefrontal cortex (PFC) was observed following exposure to a conspecific mouse in social fear conditioned mice. Additionally, pharmacological inhibition of the PFC with muscimol resulted in a reduction of social avoidance in SFC^{+} mice, implying the involvement of GABAergic neurons in the PFC in mediating the expression of social fear. (Xu et al., 2019). In a subsequent study, the same research group demonstrated through chemogenetic inhibition that the reduction of social fear expression is specifically regulated by somatostatin (SSt) expressing interneurons in the PFC (Wang et al., 2020). Possibly this behavioral alterations are further mediated by inhibitory inputs from the PFC to the PAG (Franklin et al., 2017).

Beside the brain regions and neuronal mechanisms that mediate the expression of social fear another question is how a fear memory can also be eradicated, referred to as fear extinction. Fear extinction is a crucial process in psychological therapy and the most important component of the whole picture of fear circuits regarding clinical relevance. To what extent fear extinction relies on the formation of a fear extinction memory, the modulation of the existing fear circuit, or a combination of both mechanisms, is not fully understood yet. Since fear responses can recover spontaneously, extinction surely not erase the original fear memory trace completely. Given the great overlap between regions associated with fear learning and extinction learning, the possibility exists, that these mechanisms are closely related. Most likely, the original fear circuit is modified and a closely related formed extinction circuit leads to a competition between this two networks (Bouton, 2004). Regarding specifically the extinction of social fear, studies have indicated that the infusion of synthetic OXT into the dorsal part of the lateral septum (LSd) before social fear extinction training in mice conditioned against a conspecific resulted in elevated levels of social investigation. These levels were comparable to those observed in unconditioned animals (Zoicas et al., 2014). This implies that the lateral septum (LS) is not only implicated in the circuits of social fear but specifically plays a role in the aspect of social fear extinction. Notably, the LS is a region that exhibits extensive interconnections with all the aforementioned regions.

1.4.1 Implications of the Lateral Septum

The LS is a subcortical region located between the lateral ventricles, the corpus callosum, and the decussation of the anterior commissure and has been implicated in several aspects of motivated behaviors. In the mouse brain, the LS spans along the rostral-caudal axis from bregma: +1.1 to -0.1. Along the dorsal-ventral axis, the LS can be divided into three layers: the dorsal, intermediate and ventral part (Risold and Swanson, 1997)(Figure 5, A). A small proportion of LS neurons express

glutamate (Lin et al., 2003), however, the majority, i.e., over 90%, express the inhibitory neurotransmitter GABA (Zhao et al., 2013). GABAergic neurons are heterogeneous in morphology and often co-expression of other peptides (Melzer and Monyer, 2020). In the LS it has been shown that specifically in the rostral part of the LS (LSr), a subgroup of GABAergic neurons express neurotensin (Nts) (Chen et al., 2022), whereas in more caudal regions, SSt expressing GABAergic neurons predominate as the primary subtype (Köhler and Eriksson, 1984). Furthermore, neurons in the LS differ based in their receptor expression. So far, LS neurons are described to possess neuropeptide receptors for OXT, serotonin (5-HT), AVP, dopamine (DA), corticotropin-releasing factor (CRF) and estrogen (ER). Neurons expressing these different receptors seem to be distributed in a specific spatial pattern, partially overlapping with each other (Menon et al., 2022; Sheehan and Numan, 2000). The innervation of the LS shows a topographic organization. While the LSr receives information from the hippocampus (HIP), cortical regions and AMY, the LSc is predominantly targeted by the HIP solely. Moreover, it has been shown, that neurons of the LS form local microcircuits within the LS region, which may serve an autoinhibitory function, controlling its output and hence the downstream signaling, but they also send long range projections, other subcortical regions, especially different sub-nuclei of the hypothalamus (HYP) (Sheehan et al., 2004)(Figure 5, B).

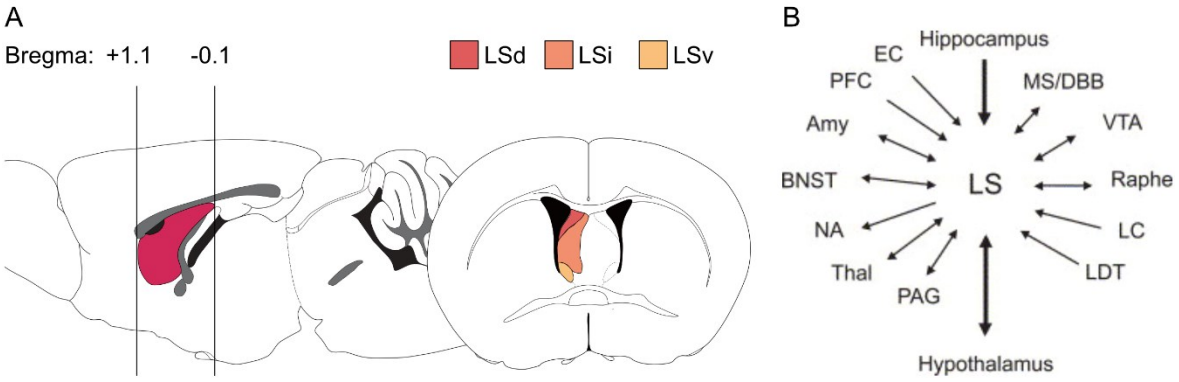

Figure 5: Structure and connectivity of the lateral septum (LS). Left: Showing the extension of the LS along the rostral-caudal axis, right: showing the subdivision within the LS along the dorsal-ventral axis, LSd= dorsal part of the LS, LSi= intermediate part of the LS, LSv= ventral part of the LS. B) Schematic illustration of the afferent and efferent connections of the LS, EC= entorhinal cortex, PFC= prefrontal cortex, Amy= amygdala, BNST= bed nucleus of the stria terminalis, NA= nucleus accumbens, Thal= thalamus, PAG= periaqueductal gray, MS/DBB= medial septum/diagonal band of broca, VTA= ventral tegmental area, LC= locus ceruleus, LDT= laterodorsal tementum (Image from (Sheehan et al., 2004)).

Functionally, the LS is considered as an integration station responsible for adjusting and evaluating perceived information, which it then conveys to downstream targets to elicit appropriate

behavioral and physiological responses (Besnard and Leroy, 2022; Rizzi-Wise and Wang, 2021). Due to its highly heterogeneous nature, different subregions with distinct connectivity patterns may regulate a wide range of functions like aggression (Brady and Nauta, 1953; Oliveira, Vinícius Elias de Moura et al., 2021), reward processing (Olds and Milner, 1954; Vega-Quiroga et al., 2018), but also innate physiological needs such as eating (Carus-Cadavieco et al., 2017). Several aspects of fear behavior have also been linked to LS activity and in the regulation of fear (Rizzi-Wise and Wang, 2021). Activation of the LS via glutamatergic input from the HIP decreases anxiety-like behavior, while inhibition has the opposite effect (Parfitt et al., 2017). Additionally, activation of a specific subpopulation of SSt expressing neurons in the LSd predicts freezing after contextual fear conditioning (Besnard et al., 2019). On the contrary, activation of type 2 CRF receptor expressing neurons in the LS promotes persistent anxious behavior (Anthony et al., 2014).

However, less studies have associated the LS specifically with social fear. OXT administration in the LSd has been shown to facilitate extinction success when administered before extinction training (Zoicas et al., 2014). The same effect has also been shown in virgin female mice (Menon et al., 2018). Another study found that oxytocin receptor expressing ($OXTR^+$) neurons from the hippocampal cornu ammonis region 1 (CA1), and 2 (CA2) that project to the LS control discrimination of social stimuli, supporting the important role of OXT and the LS in social contexts (Raam et al., 2017). Contrary, activation of $OXTR^+$ neurons in the LS have also been shown to enhance contextual fear conditioning (Guzmán et al., 2013). Magel2 deficient mice (Magel2KO) show deficits in pro-social behavior and cannot extinguish social fear in the SFC. Using this mouse line, it could be shown, that photoinhibiton of SSt expressing neurons in the LS promoted social fear extinction. Further the author suggest that in wild type (WT) animals, the SSt neurons in the LS are inhibited by OXT release from the SON, which promotes successful extinction (Dromard et al., 2023). Furhtermore, infusion of neuropeptide Y into the dorsal part of the LS reduced the expression of SFC-induced social fear (Kornhuber and Zoicas, 2021)

Even though the precise mechanisms underlying extinction are not fully understood, it is evident that active changes in the brain, likely involving learning-associated mechanisms, are necessary. One crucial mechanism in this context is the acetylation of histones by class I histone deacetylases (HDACs). Interestingly, the inhibition of HDAC activity in the LS resulted in an increased expression of local GABA-A receptors, further facilitating social fear extinction learning in the SFC paradigm (Bludau et al., 2023). Additionally, the regulation of specific long non-coding RNAs has been linked to the success of social fear extinction (Royer et al., 2022). It has been demonstrated that the knockdown of specific isoforms of the long non-coding RNA Meg3 delayed social fear extinction. This suggests

that, in addition to region-specific signaling, downstream molecular mechanisms also play a crucial role in the overall neuronal network of social fear.

In summary, the LS is implicated in a broad spectrum of motivated behaviors, encompassing fear and anxiety-related behaviors, but also particular aspects of social fear. However, a comprehensive understanding of the LS's involvement and the precise mechanisms through which it regulates specific aspects of social fear requires detailed investigations into distinct neuronal subpopulations within the LS.

1.5 Recent Technologies to Correlate Activity of Septal $OXTR^+$ Neurons with Social Fear Related Behavior in Mice *in vivo*

Understanding the intricate relationship between the activity of $OXTR^+$ neurons in the LS and social interaction pre- and post-socially traumatic events is a crucial aspect in understanding the involvement of these neurons in social fear. Recent progress in electrophysiological and optical recording methodologies has empowered researchers to observe neuronal activity *in vivo*. These advancements have significantly enhanced our insight into the dynamic interactions among neurons within circuits, shedding light on how neuronal activity patterns contribute to cognitive and behavioral processes (Cui et al., 2014).

The most direct and temporally precise measurement of neuronal activity involves electrophysiological recordings. By utilizing implanted electrodes in the brain, voltage changes can be recorded in freely moving or head-fixed animals. Nonetheless, assigning these records to individual neurons requires an additional computational spike sorting step. The primary challenges associated with this technique include the challenge of long-term tracking of individual neurons and the inherent difficulty in defining cell identity (Roth and Ding, 2020). A more cell type specific approach involves employing genetically encoded voltage-sensitive dyes, enabling the direct visualization of membrane depolarization. Despite offering high temporal and spatial resolution, thereby providing valuable insights into cellular activity, voltage imaging often encounters challenges such as limited signal strength and constraints in longitudinal recording when compared to alternative methods (Grinvald and Hildesheim, 2004). The third alternative is calcium (Ca^{2+}) imaging, akin to voltage imaging, involving the expression of a fluorescent indicator. Here, genetically encoded Ca^{2+} indicators (GECIs), typically delivered through viral injection into specific brain regions. GECIs are constructed by fusions of fluorescent proteins and Ca^{2+} buffer proteins, such as calmodulin, undergoing a conformational change in response to Ca^{2+} binding. Intracellular

calcium signaling plays a pivotal role in a diverse array of cellular processes, and neuronal activity triggers a brief influx of calcium (Roth and Ding, 2020). Thus, calcium serves as a more indirect measure of neuronal activity but acts as a reliable proxy for such measurements. While voltage-sensitive dyes can also be genetically encoded to enable cell type-specific expression, the significant advantage of GECIs lies in the longitudinal recording of neuronal activity, extending over several days.

Visualizing fluorescent dyes within the brain requires suitable optical imaging techniques. One approach involves two-photon confocal microscopy implemented on fixed-stage microscopes, achieving optimal resolution. However, in most cases, this method requires immobilizing the animal, exposing the imaged region to an objective (Russell, 2011). Another, more accessible method is the use of fiber-optic-based microendoscopes. These devices are small enough to be head-mounted and utilize optic fibers to deliver the excitation beam and collect the emitted light from the targeted neurons in awake animals (Helmchen et al., 2001).

When combined with cre-dependent selective expression of genetically encoded fluorescent indicators, Ca^{2+} imaging becomes a tool for measuring the neuronal activity of specific cell populations in mice (Russell, 2011). The bacteriophage recombinase Cre, facilitating recombination between two loxP sites, has found widespread application in mice (Luo et al., 2008). Various transgenic mice expressing Cre recombinase with distinct expression patterns have been generated, including the OXTR-Cre mouse line, where the Cre recombinase is specifically expressed in cells expressing OXTR (Harris et al., 2014). Viral vectors can be employed to target transgene expression, delivering genetic material in transgenic Cre animals. Several recombinant vectors, such as the adeno-associated virus (AAV), allow long-term gene expression without significant toxicity (Luo et al., 2008). By using site-specific infusion of a calcium indicator flanked with loxP sites, the calcium indicator can be selectively expressed in Cre-expressing cells.

Therefore, utilizing the transgenic OXTR-Cre mouse line in combination with a Cre-dependent recombinant virus expressing a GECI and delivered into the LS, this approach enables specific measurement of the activity of $OXTR^{+}$ neurons in the LS throughout the SFC paradigm.

1.6 Aims and Outline of the Present Study

SAD is a debilitating mental health disorder, that can immensely impair an individual´s ability to function in various areas of life, leading to isolation and overall a decreased quality of live. The lack of effective treatment options and the high relapse rates, emphasize the urgency of understanding

the neuronal mechanisms that mediate this disease and especially its extinction. A key aspect of social fear extinction is the restoration of social functioning after a socially traumatic event. Since the OXT system is highly implicated in the overall regulation of social behavior and anxiolysis, $OXTR^+$ neurons in the brain are a promising candidate for involvement. The LS, a brain region that comprises $OXTR^+$ cells, has been shown already to mediate an extinction facilitating effect in the SFC paradigm.

However, the mechanism how $OXTR^+$ neurons in the LS mediate this effect remains elusive. Therefore, in this thesis I aimed to, A) characterize the subpopulation of $OXTR^+$ cells in the LS in more detail, and B) shed light on the detailed functional involvement of this neurons during social fear extinction and C) Characterize the activity of $OXTR^+$ in the LS in response to social interaction before and after SFC-induced social trauma.

A) Characterization of $OXTR^+$ neurons in the LS regarding distribution, connectivity and co expression

Given the high heterogeneity of anatomical and molecular aspects of LS neuronal subpopulations, I aimed to detect a possible distribution pattern of $OXTR^+$ neurons within the LS using receptor autoradiography, uncover downstream target of this neurons with viral tracing techniques, and reveal possible subtypes regarding molecular composition of this neurons using in situ hybridization techniques.

B) Functional involvement of $OXTR^+$ neurons in the LS in SFC paradigm

Based on the hypothesis that $OXTR^+$ expressing cells are not uniformly distributed within the LS, I further aimed to investigate the role of OXTR mediated signaling in different subregions of the LS on social fear extinction. Since OXTR can couple to different Gα subunits, I also aimed to generate a more detailed picture of the downstream effects by using subtype specific OXTR ligands.

C) Activity dependent characterization of LS - $OXTR^+$ neurons during social interaction before and after SFC-induced social fear

I further hypothesized, the effect of OXT in the LS on social fear extinction is mediated by a altered activation of $OXTR^+$ neurons after experience of a social trauma. Therefore, I aimed to resolve the specific temporal involvement of this neurons during different stages of SFC paradigm, i.e. during social interaction before induction of social fear and throughout the extinction.

Overall in this study I aimed to provide a deeper understanding about the nature of the $OXTR^+$ neurons in the LS and their role in social interaction and social fear extinction. Furthermore, I aimed

to integrate the findings in the large-scale picture of the neuronal circuit that underlies social fear extinction.

2 MATERIAL AND METHODS

2.1 Animal and Husbandry

All studies were conducted according to the Guide for the Care and Use of Laboratory Animals of the National Institute of Health and where approved by Government of Oberpfalz and the ARRIVE guidelines for animal research (Kilkenny and Altman, 2010). Wildtype CD1 mice were purchased from Charles River Laboratories (Sulzfeld, Germany). Transgenic mice (CD1 background) expressing Cre recombinase in neurons containing OXTR (OXTR-Cre), as described elsewhere (Harris et al., 2014), were obtained from the Max-Planck-Institut in Munic (research group Dr. Jan Deussing). Details are available on a public database (http://www.gensat.org/) under the name: Tg(Oxtr-cre)ON66Gsat/Mmucd. The animals were further bred in the animal facilities of the University of Regensburg (Germany). All Cre-transgenic mice were bred using heterozygous female and wildtype male mice of CD1 background and were maintained as heterozygous. All animals were housed under standard laboratory conditions (12/12 hrs light/dark cycle, lights on at 07:00 a.m., 21 - 23 °C, 55-60 % humidity, food, and water ad libitum) in in polycarbonate cages (16 x 22 x 14 cm) until described otherwise. Mouse cages were changed weekly. All experiments were performed between 08:00 and 13:00 and between 8-18 weeks of age.

2.2 Behavioral Assays

2.2.1 Social Fear Conditioning

The Social Fear Conditioning (SFC) paradigm creates robust and specific fear of conspecifics in mice. The paradigm consists of three experimental phases performed on consecutive days and was carried out as previously described by (Toth et al., 2012) (Figure 6).

Day 1 – Social Fear Acquisition

Mice were placed in a conditioning chamber (45 x 22 x 40 cm), and after a 30 seconds habituation period a non-social stimulus, represented by an empty mesh wire cage (7 x 7 x 6 cm) was introduced. After 3 min the non-social stimulus was replaced by a similar cage containing an unfamiliar male mouse as a social stimulus. Unconditioned mice (SFC^-) were allowed to freely investigate the stimulus for 3 minutes, while conditioned mice (SFC^+) received between an electric foot shock (0.7 mA) when they made direct contact with the stimulus animal. Conditioned animals were shocked until they moved to the opposite side of the chamber (≈ 1 s shock duration), and

received between 1-5 shocks in total. Animals were considered as successfully conditioned and returned to the home cage, when no more contact was made for 6 min after the first shock, or 2 min after ≤ 2 shocks.

Day 2 – Social Fear Extinction

On the following day, mice underwent social fear extinction. Here the animals were exposed to three non-social stimuli (empty wire mesh cages) and six different unfamiliar social stimuli (male mice in wire mesh cages) in their home cage. Investigation level of the non-social stimuli indicates non-social fear, while the investigation level of the social stimuli reflects social fear. Each stimulus is presented for 3 minutes, with a 3-minute inter-exposure interval.

Day 3 – Recall of Social Fear Extinction

One day after extinction recall of the prior induced and extinguished social fear is conducted by exposing the mice to six different unfamiliar social stimuli in their home cage for 3 minutes, with a 3-minute inter-exposure interval, to assess extinction success. Again, social investigation level was used as readout parameter of social fear.

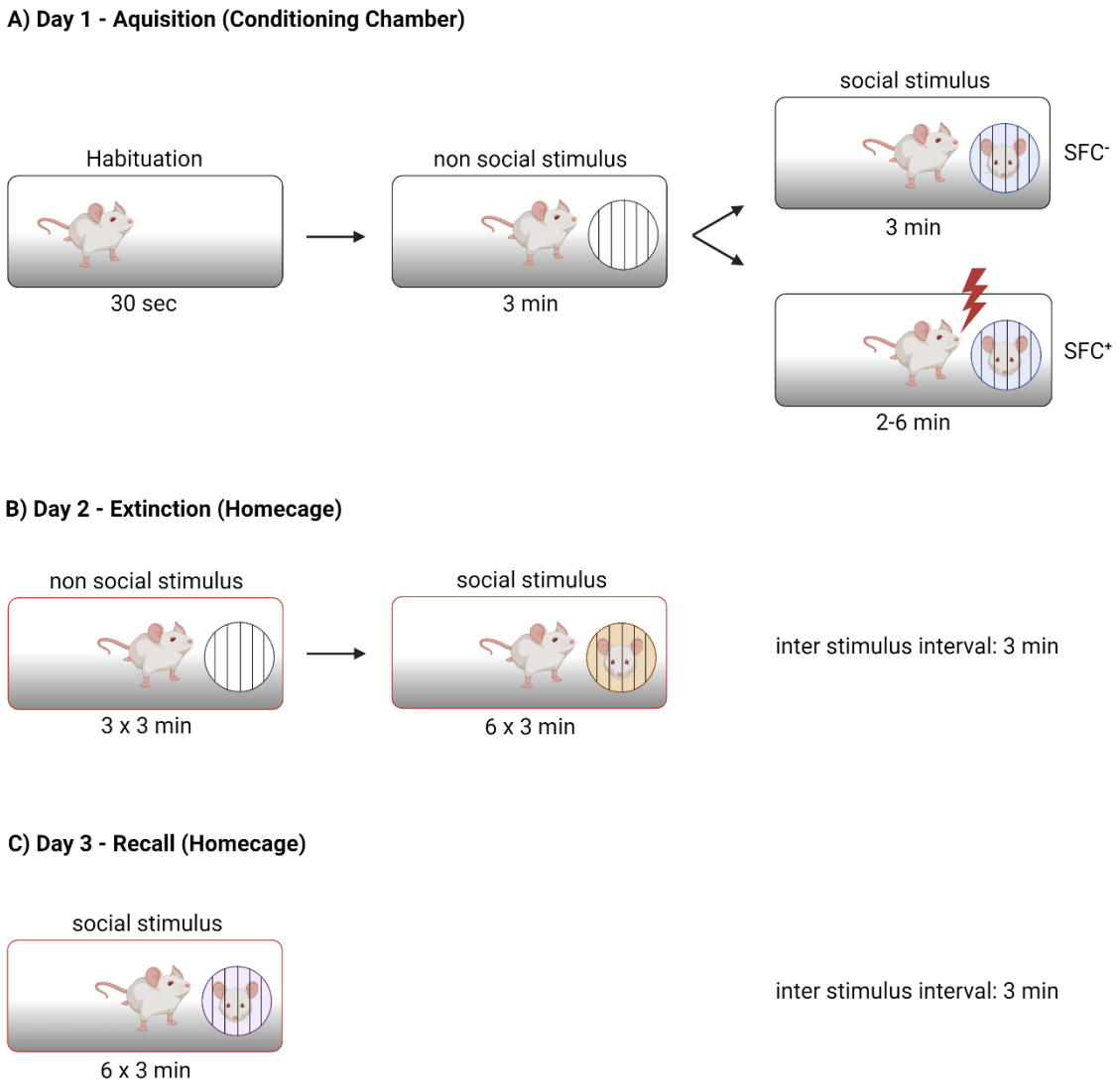

Figure 6: Schematic representation of the three phases of the social fear conditioning (SFC) paradigm. A) On day 1 during acquisition of social fear mice were habituated to the conditioning chamber for 30 seconds. Subsequently a non-social stimulus was presented for 3 min each. Unconditioned mice (SFC^-) were allowed to explore the social stimulus freely, whereas conditioned mice (SFC^+) received a foot shock when investigating the social stimulus. B) On day 2 during social fear extinction, mice are exposed to 3 non-social and 6 social stimuli leading to a gradual loss of social fear. C) During social fear recall on day 3 mice are again exposed to 6 social stimuli to evaluate whether extinction of social fear was successful (adapted from (Menon et al., 2018)).

2.2.2 Elevated Plus Maze

The Elevated Plus Maze (EPM) generates a natural conflict between the exploratory drive and the innate fear of open and exposed areas in rodents. The open arms (OA) are normally considered to be dangerous by rodents and they tend to spent more time in the closed arms (CA) of the maze. Therefore, increased exploration of the OA is typically interpreted as a low level of anxiety. The test

was conducted as previously described (Reber and Neumann, 2008). The arena consists of two open (6 x30 x 0.3 cm, 140 lux) and two closed arms (6 x 30 x 16 cm, 25 lux) radiating from a central platform (6 x 6 cm). The maze is elevated 35 cm above the floor. Animals were placed on the central platform facing a closed arm and allowed to freely explore the EPM for 15 minutes. The maze was cleaned before each test and the whole experiment was video recorded. Subsequently, the time animals spent in the center, CA, OA (forelimbs have entered the OA) and full OA (all paws have entered the OA) was calculated.

2.3 Surgical Procedures

After arrival, animals were habituated to the new environment for at least one week, before surgeries were conducted. Mice received a subcutaneous injection of the analgesic Buprenorhine (0.05 mg/kg, Buprenovet, Bayer, Germany) 30 min before the start of the surgery. Animals were anesthetized with Isoflurane (4% Isoflurane, Abbott GmbH, Germany) and mounted in a stereotactic frame (Kopf Instruments, Canada). Anesthesia was maintained with Isoflurane throughout surgical procedure. Eyes were covered with ophthalmic ointment (Bepanthen, Bayer, Germany) to avoid drying. Before cutting the skin on top of the skull, a local anesthetic (2% Lidocainhydrochlorid; Bela-pharm, Germany) was injected subcutaneously. Further steps were performed under constant and carefully observed Isoflurane anesthesia. All coordinates used are based on the mouse brain atlas (Paxinos and Franklin, 2019).

2.3.1 Viral Infusions

Virus suspension was infused with a 30 -gauge (G) needle (Hamilton, USA) in a stereotactic mounted micro pump (UMP3T, Word Precision Instruments, UK) with a flow rate of 100 nL/min. After infusion, the needle was kept in place for 10 min and then slowly removed. The drill hole in the skull was closed using bone wax (Ethicon, USA) and the incision was sutured using sterile nylon material and treated with Lidocaine (2% Lidocainhydrochlorid; Bela-pharm, Germany). Viral constructs were obtained from UNC Gene Therapy Center Vector Core (University of North Carolina at Chapel Hill, USA) or MIT Vector Core (provided by Simon Chang). For Ca^{2+} imaging, AAV-DJ-EF1a-DIO-GCaMP6m (UNC, 5 x 10^{12} GC/mL) with a dilution of 1:1.5 in saline and a volume of 250nL per injection level was used. The LSc was targeted unilateral at anterior-posterior (AP) +0.15, medio-lateral (ML) -0.5 and dorso-ventral (DV) -3.35 and -3.0 from the bregma. For anterograde tracing AAV_9-CMV-DIO-Syn-mCherry (MIT, 1 x 10^{13} GC/µL) with a volume of 100nL per hemisphere was used. The LSc was

targeted bilaterally at anterior-posterior (AP) +0.15, medio-lateral (ML) ±0.5 and dorso-ventral (DV) -3.2 from the bregma.

2.3.2 Guide Cannula Implantation

For icv infusions, an 8 mm long 21 G guide cannula was stereotaxically placed 2 mm above the lateral ventricle. For local infusion, 8 mm long 23 G guide cannulas were implanted bilaterally 2 mm above different subregions of the LS (Table 1). The cannulas were fixed to two stainless steel screws using dental cement (Kallocryl, Speiko-Dr. Speier GmbH, Germany). Mice were single housed after surgery and allowed to recover for at least 5 day. Animals were handled daily to habituate them to the infusion procedures and to minimize non-specific stress response at the day of experiment. All guide cannulas were closed using a stylet, which was cleaned daily during the handling procedure with 70% ethanol.

Target	AP	ML	DV	Angle
Icv	+0.2	+1.0	-1.4	0°
LSr	+0.85	+/-0.5	-1.6	0°
LSm	+0.5	+/-0.5	-1.6	0°
LSc	+0.15	+/-0.5	-1.6	0°

Table 1: Stereotaxic coordinates for guide cannula implantation. AP= anterior-posterior, ML= medio-lateral, DV= dorso-ventral. All measures in [mm] according to bregma. Icv= intracerebroventricular, LSr= rostral part of the lateral septum, LSm= medial part of the lateral septum, LSc= caudal part of the lateral septum.

2.3.3 GRIN Lens Implantation

For Ca^{2+} imaging, the Gradient Refractive Index (GRIN) lens was implanted, after viral injection. ProView™ integrated lenses were used (Inscopix, USA), in which the lens (0.5 NA, 1.5 pitch, 0.5 x 6.1 mm) is attached to a baseplate. The craniotomy drilled for the virus was extended for the lens implantation with a trephine bit (1.8 diameter tip, Fine Science Tools, USA). The integrated lens was attached to an nVista dummy microscope integrated into a Pro-View stereotax rod (Inscopix, USA) and slowly lowered at a rate of 100 µm/min from DV 0 to -3.1 mm. The skull was thoroughly dried, and the lens was secured to the skull with Metabond (Parkell, USA). After the cement was dry, the skin was sutured tightly and the baseplate was covered with a protective cover (Inscopix, USA).

2.4 Deep Brain Single-Cell Imaging

2.4.1 Ca^{2+} Imaging in Freely Behaving Mice

To attach the microendoscope (2 g, 650 x 1050 µm field of view (FOV), single-channel epifluorescence: 475 nm blue LED excitation, 535 nm green LED collection, Inscopix, Palo Alto, CA, USA), the animal was gently fixed by hand, the protective cover removed and the microendoscope secured to the baseplate with a fixation screw. Animals were then allowed to adapt for 5 min before the start of the experiment. To determine the optimal focus and LED Power, the microendoscope was attached one day prior to start of experiment and settings were kept consistent in all animals over different days of recording.

2.4.2 Data Acquisition and Processing

Greyscale tiff images were acquired using the Inscopix Data Acquisition Software v2.0.0 (Inscopix, Palo Alto, CA) at 10 frames/s with an exposure time of 100 ms. Video streams from Ca^{2+} and behavioral imaging were triggered via TTL pulses delivered by an AMi interface (Stoelting, Wood Dale, IL, USA) and controlled by ANY-maze (Stoelting, Wood Dale, IL, USA). All Ca^{2+} imaging recordings were initially pre-processed in batch using the Inscopix Data Processing Software v1.6 Python API (Inscopix, USA). All frames collected for a single mouse over the course of a session were initially concatenated and cropped to remove empty parts of the FOV, such as the rim of the lens, and spatially downsampled in the X and Y dimensions by a factor of two. A band-pass spatial filter was then applied to reduce noise and remove artifacts. The resulting videos were exported to identify individual regions of interest (ROI) and extract their Ca^{2+} traces using Constrained Nonnegative Matrix Factorization for microEndoscopic data in MATLAB (https://github.com/zhoupc/CNMF_E, (Zhou et al., 2018)). To ensure high quality segmentation, all extracted components were manually refined to exclude components with traces that contained motion artifacts, high noise levels or whose ROIs lacked a round, soma-like shape. For the EPM recordings, individual Ca^{2+} traces were normalized to ΔF/F (also called z-score) across each recorded trial, i.e. the change of a cell´s fluorescence normalized to the mean fluorescence across the entire recording. SFC traces were instead z-scored using the break intervals around each recording as baseline, i.e. the change of a cell´s fluorescence normalized to the mean fluorescence across the break interval.

2.4.3 Longitudinal Registration Across Experimental Sessions

To ensure consistent identity preservation of all ROIs throughout distinct recording sessions, a dual strategy was employed. Initially, the spatial footprints of individual neurons were used with the CellReg tool in MATLAB (https://github.com/zivlab/CellReg) to automatically detect potential positional variations (translations + rotations) with a high degree of confidence across consecutive days (Sheintuch et al., 2017). Subsequently, the outcomes of this automated matching were meticulously cross-referenced with the corresponding recording videos from each session. This manual verification step was conducted to ensure a heightened level of accuracy and to rectify any discrepancies, establishing robust alignment across sessions.

2.4.4 Linear Model for Modulated Neurons

To identify neurons whose activity was significantly correlated to the timing of the contact behavior, we created a linear model using the statistical package "statspackage" in R. For each individual ROI, we correlated the scored social contact, a period of 3s before the start of every social interaction ('before contact') and after the end ('after contact') with the calcium imaging activity for each stage of the paradigm. Neurons that were significantly correlated ($p < 0.05$) for one of the three behaviors were categorized as modulated against the non-responsive not significant neurons. Modulated neurons were then classified as excited or inhibited if the regression coefficients were positive or negative, respectively. Cells were categorized as "modulated" by a significant predictor if the independent variables (predictors) within the linear model fitted to the cell's activity were deemed significant ($p < 0.05$). Conversely, cells were classified as "non-responsive" if the significance threshold was not met ($p > 0.05$). In instances where predictors were significant, positive regression coefficients designated cells as "excited", while negative coefficients identified cells as "inhibited". To handle the issue of multiple comparisons, we utilized the Benjamin-Hochberg procedure, which effectively corrected for statistical considerations.

2.5 In vivo Pharmacology

All substances were freshly diluted from concentrated stock solutions on the day of the experiment in sterile Ringer´s solution (B. Braun, Melsungen AG, Germany). For both, icv and intra-LS infusion, the stylet was removed and replaced by the infusion cannula (27 G, 10 mm). A total volume of 2 µL was manually infused icv, while for local LS infusions a volume of 0.2 µL/hemisphere was applied (Table 2). As control (vehicle; Veh) sterile Ringer´s solution was applied.

Substance	Target	Concentration	Source	Identifier
OXT	icv	0.1 µg/ 2 µL	Sigma Aldrich	O6379
OXT	local	5 ng/ 0.2 µL	Sigmal Aldrich	O6379
Atosiban	local	20 ng/ 0.2 µL	Tocris	Cat#6332
Carbetocin	local	0.4 µg/ 0.2 µL	Tocris	Cat#4852

Table 2: Concentrations of substances either infused intracerebroventricular (icv), or locally in the lateral septum (LS). OXT= oxytocin, atosiban= oxytocin receptor G_i-agonist, carbetocin= oxytocin receptor G_q-agonist. All substances were infused via guide cannulas.

After infusions, the cannula was kept in place for 10 s to guarantee appropriate local substance diffusion. The animals where carefully observed when returned to the homecage. None of them showed convulsions, or tremor behavior after injection. For visualization and validation of the corresponding infusion site, mice were injected with ink postmortem.

2.6 Tissue Collection and Slice Preparation

2.6.1 Snap Frozen Tissue

Brains were rapidly removed, flash frozen in pre-chilled N-methylbutane on dry ice and stored at -80°C. Tissue was then equilibriated to -20°C and sliced in coronal sections using a Cryostat (CM3000, Leica, Germany). For RNAscope, 10 µm sections were mounted on Superfrost Plus slides (AB00000112E01MNZ50, Thermo Fisher Scientific, Germany). For Receptor Autoradiography, 16 µm sections were mounted of Superfrost slides (J1800AMNZ, Thermo Fisher Scientific, Germany) and for tissue punches of the septum brains were sliced in 200 µm sections. The tissue was then stored at -80°C again until further processing.

2.6.2 Perfused Tissue

For visualization of the anterograde tracing, brains were fixed by intracardial perfusion of paraformaldehyde (PFA). Animals were anesthetized using a mixture of ketamine (10%, 1 mL/kg, Medistar Arzneimitter GmbH, Germany) and Xylazine (2%, 0.5 mL/kg, Serumwerk Bernburg AG, Germany), intraperitoneally (i.p.) administered. Transcardial perfusion was then performed using ice-cold 0.01 M phosphate buffered saline (1 x PBS) and 1 x PBS supplemented with 4% PFA (Sigma Aldrich, Germany, pH 7.4) at a speed of 19 mL/min for 3 min. Afterwards, brains were removed and

postfixed for 24 h at 4 °C in 4% PFA solution, and cryoprotected in 30% sucrose in 1 x PBS for 48 h. Afterwards, brains were rapidly frozen in N-methylbutane cooled on dry ice and stored at -80°C. For microscopy, tissue was then equilibriated to -20°C and cut in 40 µm coronal sections and mounted on Superfrost slides, covered with ROTI DAPI mount.

2.7 Molecular Method

2.7.1 RNAscope

Visualization of single RNA molecules was carried out using RNAscope. This in situ hybridization technique was performed according to the manufacturer´s protocol (RNAscope Multiplex Fluorescent V2 Assay, Advanced Cell Diagnostics). Briefly, fresh frozen brain slices were stored at -80°C until further processing. Sections were post-fixed in 4% PFA in 0.1 M PBS cooled to 4°C for 30 min. Sections were then dehydrated in 50%, 70% and two times in 100% ethanol. After drying hydrogen peroxidase was applied for 10 min in order to remove blood residues. Cells were then permeabilized by 10 min protease III treatment and washed with 0.1 M PBS. Tissue was then covered with RNAscope probes targeting OXTR (412171-C1), SSt (404631-C3) and Nts (420441-C3) at 40°C for 2 h. After hybridization of the probe, sections were washed twice for 2 min in RNAscope wash buffer and sequentially incubated with RNAscope Amp-I and Amp-II for 30 min and Amp-III solution for 15 min, with two washing steps with Wash buffer in between each treatment. Signal was developed using the TSA Plus fluorophore Cy5 (1:1000), Cy3 (1:1000) and Flp (1:1000) (FP1168, FP1170, FP1171, perkin Elmer). Sections were covered with Roti-Mount FlurCare DAPI. Images were obtained with a confocal microscope (SP8, Leica Microsystems, Germany) at 65x magnification at different subregions of the LS. Images were analyzed using a custom Cell Profiler Pipeline, adapted from (Erben and Buonanno, 2019).

2.7.2 Receptor Autoradiography (RAR)

Mice were euthanized with CO_2 and brain were removed and snap frozen on dry ice and stored at -20°C until cryosectioned coronally at 16µm targeting the whole LS (Bregma (+)1.1 – (-)0.1 mm) and mounted on superfrost microscope slides. Slides were stored at -20°C until the receptor-binding study was performed according to (Lukas et al., 2010) using a linear OXTR antagonist [125I]-d(CH2)5[Tyr(Me)2-Tyr-Nh2]9-OVT (NEX254010UC, Perkin Elmer, USA). In brief, the slides were thawed and dried at room temperature, followed by fixation in paraformaldehyde (PFA, 0.1%). Then slides were washed two times in 50 mM Tris (pH 7.4), exposed to tracer buffer (50 mM tracer,

50 mM Tris, 10 mM MgCl2, 0.1% bovine serum albumin (BSA)) for 60 min, and washed three times in Tris buffer 10 mM MgCl2. The slides were then shortly dipped in water and dried at room temperature overnight. On the following day, slides were exposed to Biomax MR films for 5 days (Kodak, France). The films were scanned at high resolution (1200 dpi at 8-bit) using a flatbed scanner (EPSON Perfection V800, Epson Corporation, Germany). Quantification of grey value was performed in IMAGE J (NIH, Bethesda, MD, USA) with taking the mean of 3 sections per region of interest (ROI). For quantification, no adjustments were made to the images. ROIs were selected by comparison to an atlas (Paxinos and Franklin, 2019). Specific binding was determined by substraction of tissue background sampled from a control region for each slide. Left and right regions were scored separately and pooled if no significant hemispheric difference was found.

2.7.3 Genotyping

The Cre-LoxP system uses the bacteriophage P1 Cre recombinase to catalyze the excision of selected DNA sequences flanked by LoxP sequences, and therefore allows cell type specific modification in genetically modified mouse lines (Orban et al., 1992). The OXTR-Cre mouse line expresses Cre integrase specifically in $OXTR^+$ cells, as described previously (Harris et al., 2014) OXTR-Cre females were bred with WT males and offspring was genotyped using the KAPA mouse genotyping kit to select for Cre positive (Cre^+) mice (KR0385_S-v1.17, KAPAbiosystems, Germany). Briefly, tissue was collected as ear punches and kept on -20°C until further processing. Tissue was lysed at 75°C for 10 min (KAPA express extract buffer), followed by enzyme inactivation at 95°C for 5 min (KAPA Express Extract Enzyme). Template DNA was then mixed with a genotyping mix containing DNA polymerase, dye and the corresponding primers targeting Cre and Control DNA (Metabion, Germany)(Table 3).

Primer	Sequence (5´-3´)	Size amplicon (bp)	Identifier
Cre-F2	CCACCAGCCAGCTATCAACT	249	200730B001A06
Cre-R2	CAGCTTGCATGATCTCCGGT	249	200730B001F05
Thy1-F1	TCTGAGTGGCAAAGGACCTTAGG	372	200730B001C05
Thy1-R1	CCACTGGTGAGGTTGAGG	372	200730B001B05

Table 3: Identification number, sequence, and amplicon size of primers used for genotyping.

PCR was performed with the following cycling steps (Table 4):

Step	Temperature	Duration	Cycles
Initial denaturation	95°C	3 min	1
Denaturation	95°C	15 sec	35-40
Annealing	60°C	15 sec	
Extension	72°C	15 sec/kb	
Final extension	72°C	1 min/kb	1

Table 4: Polymerase chain reaction (PCR) protocol used for genotyping.

For southern analysis PCR product was mixed with RotiStain (Carl Roth, Germany) and loaded on 1% agarose gel (pore size 200-500 nm) and then electrophoresed for 1 h at 140 V and 80 mA. Gel was imaged under UV light using ChemicDoc XRS system (Bio-Rad, Germany).

2.8 Statistical Analysis and Figures

Data was analyzed using SPSS, Version 26.0 (IBM Corp., USA) and depicted using GraphPad Prism version 8.0 (GraphPad Software, USA, www.graphpad.com).

For data analysis with one factor and two groups, independent T-Test or Mann-Whitney-U Test was used. Analysis of variance (ANOVA) has been used, when more than two groups were compared, either with one factor (One-way ANOVA) or two factors (Two-way ANOVA) or a Kruskall-Wallis test. For analysis over different time points mixed model ANOVA was applied. All tests were followed by a Bonferroni *post hoc* test, whenever appropriate. For microendoscopy experiments, all test where followed by a Dunn post hoc test. Values of the post hoc tests are stated in the body text, while values of the general test are stated in a separate table for each experiment. Statistical significance was accepted at $p \leq 0.05$, a trend was accepted at $p \leq 0.07$. All values are represented as the mean ± standard error of the mean (SEM).

Main figures and other illustrations were created using BioRender (BioRender.com) and Affinity Designer (https://affinity.serif.com/en-us/designer/).

2.9 Experimental Design

The following section contains a short outline of each experiment of this thesis, including a graphical illustration.

2.9.1 Characterization of OXTR$^+$ Cells within the LS

To study the rostro-caudal distribution of OXTR within the LS, OXTR-autoradiography was used. Brains of 4 adult male and 4 female mice were cryocut coronally at 16 µm targeting the whole LS (Bregma (+)1.1 – (-)0.1 mm). LSr was defined as Bregma: (+)1.1 – (+)0.5 and LSc was defined as Bregma (+)0.5-(-)0.1 (Figure 7, A). Grey value was measured using Image J, including the Fiji distribution (Schindelin et al., 2012). To determine the binding specificity, tissue background was sampled from the Str was subtracted for each slide (Figure 7, B).

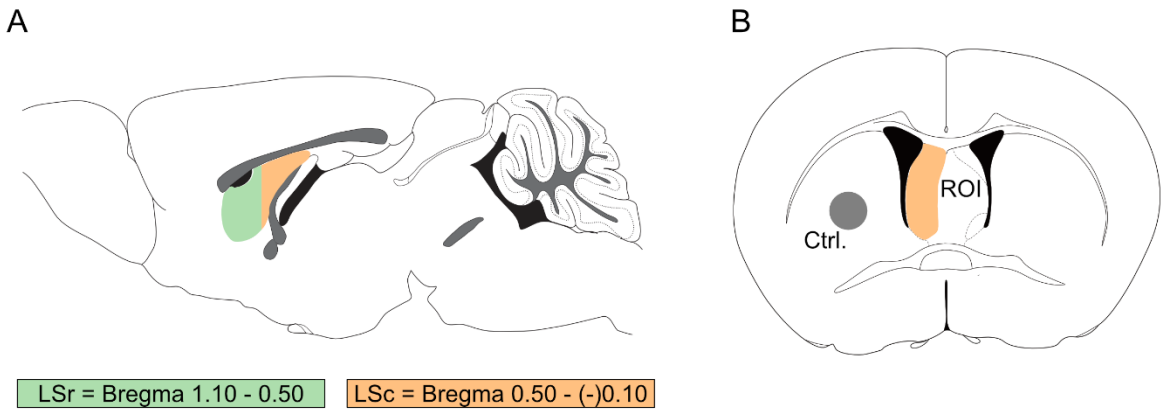

Figure 7: Experimental design to evaluated the rostro-caudal distribution of oxytocin receptor- (OXTR) binding with the lateral septum (LS) in male and female mice. A) represents the whole extension of the sampled area, with green representing the rostral part of the LS (LSr) and orange representing the caudal part of the LS (LSc) according to bregma in [mm]. B) representative image of the selected and measured regions. Orange represents the region of interest (ROI), and gray the control region (Ctrl.) measured in the striatum.

To characterize the molecular identity of OXTR$^+$ neurons in the LS more closely, OXTR mRNA together with SSt and Nts mRNA levels along in different parts of the LS were assessed in different parts of the LS using RNAscope. Brains of 3 adult males were sliced coronally at 10 µm collecting three equally distributed targets along the rostral and caudal part respectively (Figure 8, A). For each slice three images where taken along the dorsal-ventral axis of the LS, representing the dorsal (LSd), intermediate (LSi) and ventral part (LSv) respectively (Figure 8, B). Images where acquired at

65x magnification using a confocal laser scanning microscope (SP8, Leica Microsystems, Germany). Co-localization was automatically analyzed with a custom written CellProfiler pipeline (*www.cellprofiler.org*). Briefly, extended nuclei (accepted as cells) with more than 3 OXTR mRNA dots were counted as $OXTR^+$, while cells with more than 10 SSt, or Nts mRNA dots were counted as SSt, or Nts expressing cells.

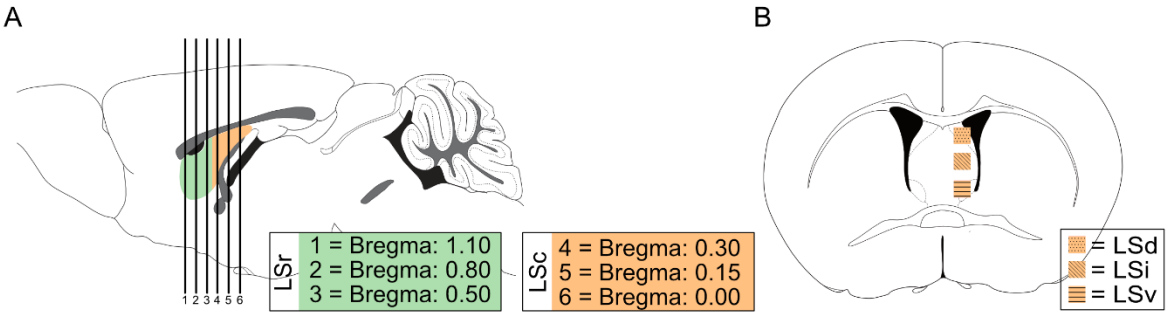

Figure 8: Experimental design to evaluate oxytocin receptor (OXTR) mRNA distribution within the lateral septum (LS). In order to represent the overall distribution of OXTR, somatostatin (SSt) and neurotensin (Nts) mRNA distribution in within the LS slices and images where collected and stained at different subdivisions of the whole region. A) Slice collection along the rostral-caudal extension of the LS. B) Image collection along the dorsal-ventral axis of each single slice.

To determine possible downstream targets of $OXTR^+$ neurons in the LSc, four adult male OXTR-Cre mice were injected bilaterally with an anterogradely transducing virus (Figure 9, A) expressing synaptophysin in the axon terminal of OXTR expressing neurons. After 3 weeks of transfection, 40 µm brain slices taken between the olfactory bulb and the cerebellum were collected (Figure 9, B). Slices were directly mounted on glass slides and covered with DAPI stain. Images where acquired with a fluorescence microscope (Leica THUNDER, Leica Microsystems, Germany) with 10 – 20x magnification. Projection areas were manually detected, based on red fluorescent signal.

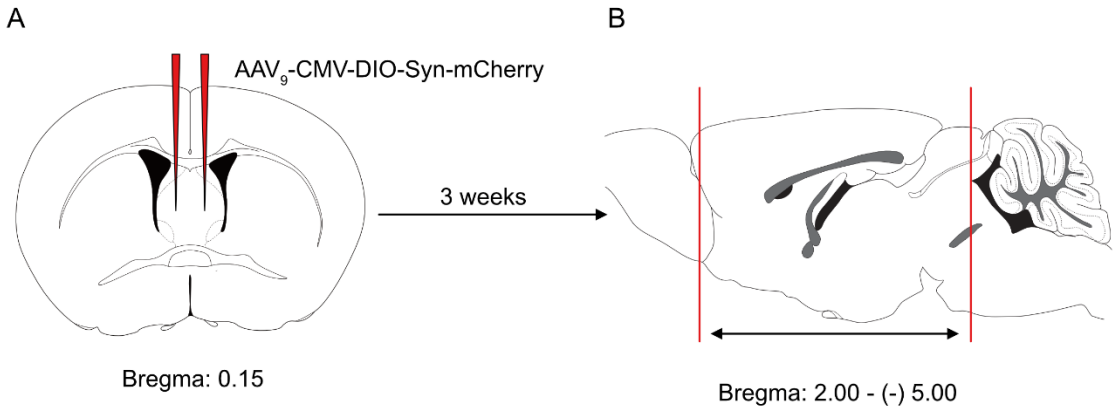

Figure 9: Experimental design to evaluate the downstream targets of oxytocin receptor expressing (OXTR$^+$) cells in the caudal part of the lateral septum (LSc). A) Injection site of the anterogradely transducing virus: AAV$_9$-CMV-DIO-Syn-mCherry, targeting the LSc. B) Slice collection after 3 weeks transfection time along the rostral caudal extension of the LS according to bregma in [mm].

2.9.2 Pharmacological Manipulation of OXTR Signaling within the LS

To examine the involvement of OXT signaling in social fear extinction, either OXT, carbetocin or atosiban were applied icv or bilaterally in the LS in male mice prior to extinction training (Figure 10, A, C). The effect of OXT on social fear extinction was evaluated by either icv or intra-LS injection 10 min prior to extinction training. Doses and timing were selected based on earlier experiments (Zoicas et al., 2014). In order to analyze if different G-protein coupled effector signaling cascades differentially effect social fear extinction, either carbetocin (=Gαq coupled signaling) or atosiban (=Gαi coupled signaling) was applied prior to extinction training. Timing and doses were selected on the basis of earlier experiments (Busnelli et al., 2013). Lastly, the effect of OXT in different subregions of the LS along the rostral-caudal axis of the LS was examined. In each experiment, an equal volume of sterile Ringer´s solution (Veh) was infused as control.

All behavioral experiments were video recorded (Figure 10, B). The correct cannula placement was verified by ink injection postmortem and visual inspection (Figure 10, D). Investigation time was scored manually using JWatcher program (V 1.0, Macquarie University and UCLA).

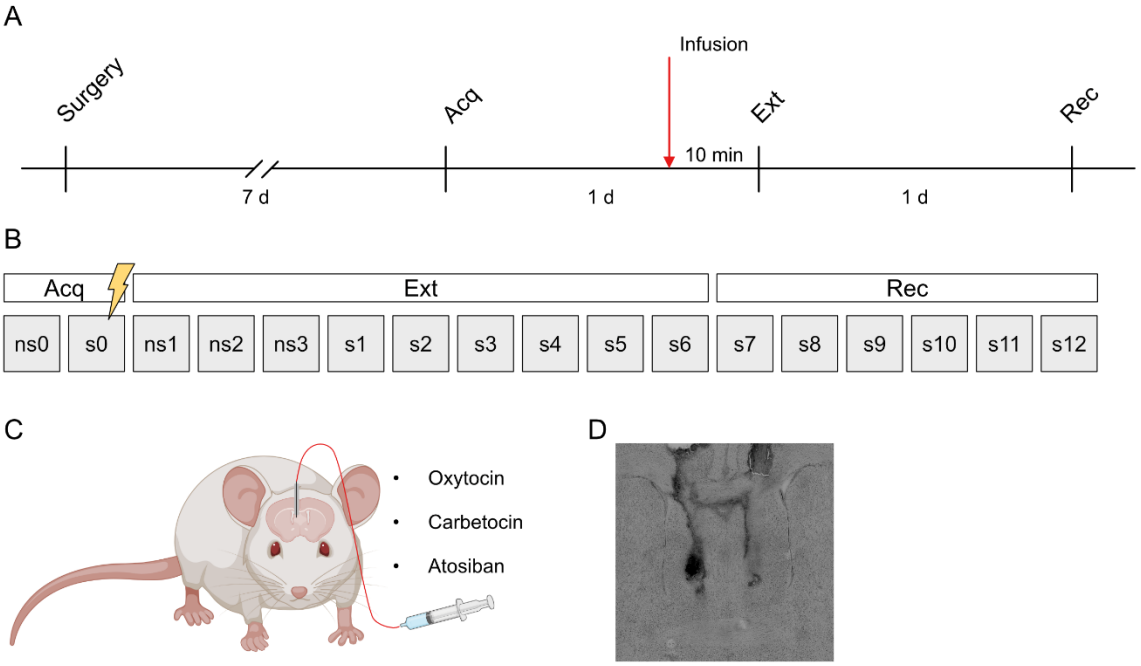

Figure 10: Experimental design to evaluate the effects of oxytocin receptor mediated signaling by either intracerebroventricular (icv) or intra-septal infusion on social fear extinction. A) Experimental timeline. Animals recovered from surgery for 7 days before animals went through the social fear conditioning (SFC) paradigm. 10 min prior to extinction (Ext) of social fear substances were administered. B) detailed experimental setup shows the presentation of the different non-social (ns 0-3) and social (s 0-12) stimuli during the experimental phases. C) Animals were infused with either oxytocin (OXT), carbetocin or atosiban through a guide cannula. D) Postmortem, animals were infused with ink to verify the infusion site.

2.9.3 Temporal characterization of OXTR^{+} Neurons within the LS

Declaration: The in vivo calcium imaging experiment described in this chapter was performed in collaboration with Prof. Dr. Tatiana Korotkova (University of Köln, Germany), providing the Insopix system and calcium imaging expertise, and Prof. Dr. Inga Neumann (University of Regensburg, Germany) providing experimental materials and behavioral expertise for this project. Experiments were carried out by Francisco de los Santos (Doctoral thesis, University of Köln, Germany) and Theresa Schäfer (Doctoral thesis, University of Regensburg, Germany). Detailed contributions are stated below.

Contributions to the project by Theresa Schäfer:

- *TVA adaptations*
- *Experimental Design*
- *Animal Breeding, genotyping and handling*
- *Validation experiments (behavior and virus validation)*

- *Experiment: controlling animals*
- *Analysis of behavioral data*
- *Data pre-processing: execution*
- *Final figures and data interpretation of all results shown in this thesis*

Contributions to the project by Francisco de los Santos:

- *Virus injection and GRIN lens implantation*
- *Experiment: controlling Inscopix system*
- *Data pre-processing: teaching and support*
- *Analysis of Calcium imaging data: including coding and generation of individual plots and written explanation in this thesis*
- *Final figures and data interpretation of all results shown in Francisco de los Santos thesis*

In vivo calcium imaging in freely behaving mice was used to correlate the activity of $OXTR^+$ neurons in the LSc with behavior. In neurons, Ca^{2+} signaling is precisely controlled and related to important functions such as membrane excitability, neurotransmitter release, and synaptic plasticity (Brini et al., 2014). Therefore, in this study a Cre-dependent genetically encoded calcium indicator (GECI) was unilaterally injected in the LSc of nine male OXTR-Cre mice. By implantation of a Gradient Index (GRIN) lens above the injection site, the light can be transferred to a head-mounted miniaturized microendoscope (miniscope). This setup allows not only cell type-specific activity recording, but also tagging of responsive cell over several days of experiment in freely moving animals. In order to examine, if $OXTR^+$ neurons respond differently to social interaction before, during and after a socially traumatic event, but also during natural anxiety-like behavior, the SFC paradigm was slightly extended, hereinafter referred to as adapted SFC (aSFC) (Figure 11, A). The experimental design started with exposure of the mice to the EPM to correlate activity of $OXTR^+$ neurons in the LSc with generalized anxiety-like behavior. Subsequently, the animals were exposed to a slightly modified SFC paradigm (aSFC), which starts with a 3 min social interaction (SE) in the homecage to monitor the activity of $OXTR^+$ neurons in the LSc during natural social investigation. On the next day social fear was aquired (Acq) by operant conditioning in a conditioning chamber and on the following days extinction (Ext) and recall (Rec) of social fear were performed as described in chapter 2.2.1 and again in the homecage. During each experimental different social stimuli (s1-s14) or non-social stimuli (ns1-ns4) where presented to the experimental mouse, referred to as different conditions (Figure 11, B). To avoid bleaching of the GECI, selected conditions were recorded (indicated in

orange or green) and Ca2+ signal was either evaluated throughout the recorded condition, or during contact behavior (for detailed information see 2.4)

Prior to each experimental day (EPM, SE, Acq, Ext, Rec) the miniscope was attached to the baseplate and a pre-recording revealed approximately 15 healthy and responding neurons in all nine experimental animals (Figure 11, D).

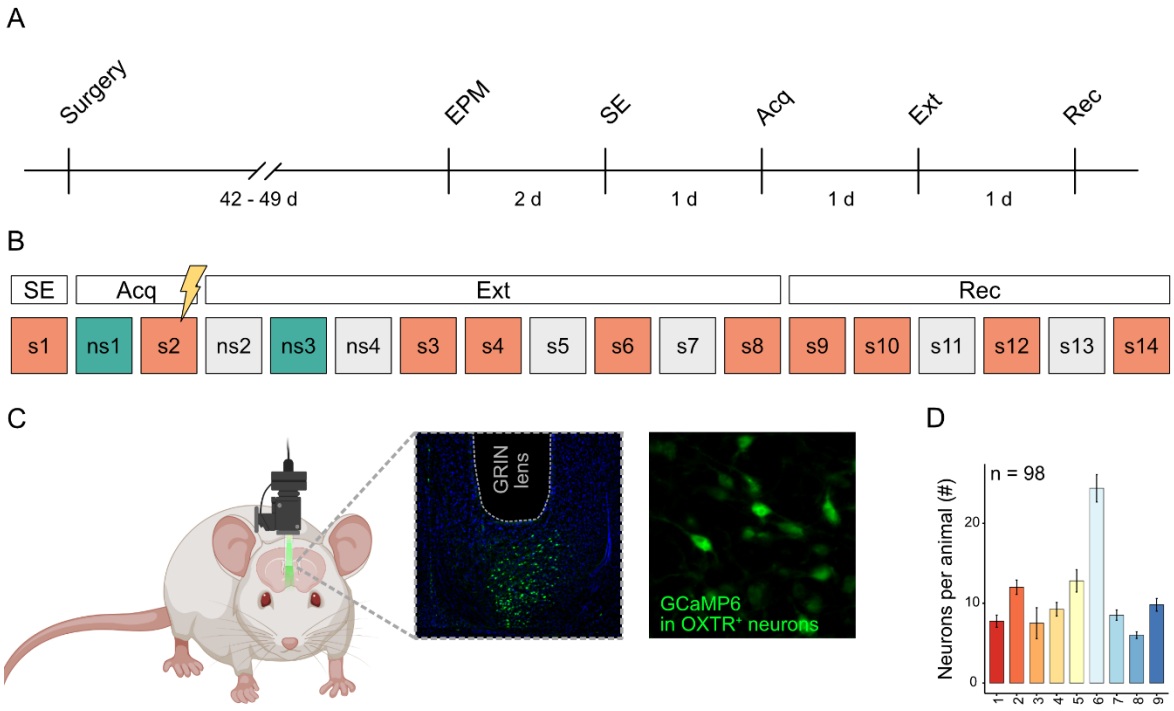

Figure 11: Experimental design to correlate the activity of oxytocin receptor expressing (OXTR$^+$) neurons in the caudal part of the lateral septum (LSc) with behavior during the elevated plus maze (EPM) and the adapted social fear conditioning (aSFC) paradigm. A) Shows the overall experimental timeline. After a transfection time of 42-49 days (d), animals were exposed to the EPM. 2 days later, animals underwent a modified SFC paradigm, referred to as aSFC, which starts with a social exposure (SE) prior to induction of social fear. On the following days, the SFC paradigm was performed as described previously. B) Detailed experimental setup of the aSFC paradigm and presentation of the different social stimuli (s 1-14) and non-social stimuli (ns 1-4) during the different experimental phases. C) Representative illustration of recording and transfected neurons (green) and placement of the gradient refractive index (GRIN) lens. D) recorded neurons during test recording in all 9 experimental mice, n indicates total number of recorded neurons.

After termination of the whole experiment, animals where perfused with PFA (see chapter 2.6.2), brains removed, cryocut and visualized using a fluorescence microscope to determine proper virus and lens placement (Figure 11, C). Behavior was manually scored using the BORIS software (Friard and Gamba, 2016), in order to compare activity during contact behavior (Table 5).

Scored behavior	Description
	EPM
center	The behavior starts when the forelimbs have entered the center and ends when the forelimbs have entered another zone
CA	The behavior starts when the forelimbs have entered the CA and ends when the forelimbs have entered another zone
OA	The behavior starts when the forelimbs have entered the OA and ends when the forelimbs have entered another zone
fullOA	The behavior starts when all four paws have entered the OA and ends when the forelimbs enter the center
	aSFC
Eating	The total amount of time the animal spent eating
Drinking	The total amount of time the animal spent drinking
Grooming	The total amount of time the animal spent grooming
Exploration	Summarizes all remaining activities of the animal during the recorded time
Contact	The total amount of time the animal spent exploring the stimuli (non-social or social) with direct nose contact. Undirect sniffing and stretch-approach postures were not considered as investigation of the stimuli

Table 5: Ethogram of experimental behaviors.

For separate analysis of of mice with successful and unsuccessful social fear extinction, a threshold of 45% of contact level during s7 and s8 was assigned, as previous reported by (Royer et al., 2022). Animals with a mean contact level < 45% during s7/s8 were considered as successful extinction animals and referred to as fast extinction animals (FEA), while animals with a mean contact level > 45% during s7/s8 were considered as successful extinction animals and referred to as slow extinction animals (SEA)

3 RESULTS

3.1 Characterization of OXTR$^+$ Cells in the LS

The presence of OXTR expression in the LS has been consistently confirmed. Moreover, validated evidence supports projections from OXTR-producing regions to the LS (Grinevich et al., 2016). Nonetheless, a more precise characterization of OXTR+ cells within the LS is needed, specifically in terms of their spatial distribution, downstream targets, and the array of neurotransmitters and receptors they express. This information remains elusive at present.

3.1.1 OXTR Binding within the LS

OXTR binding was abundantly found in all subregions of the LS. To determine whether OXTR binding differs along the rostral to caudal extension of the LS in male and female mice, I performed receptor autoradiography (RAR) (see 2.7.2) and compared the OXTR binding density in the LSr and LSc (Figure 12,A) (see 2.9.1). Independent of sex a higher OXTR binding in the LSc could be observed ($p < 0.001$). Furthermore, male and female mice showed similar OXTR binding density in the rostral and caudal part of the LS, which indicates that the distribution pattern is region specific, but sex independent (Table 6, Figure 12, B).

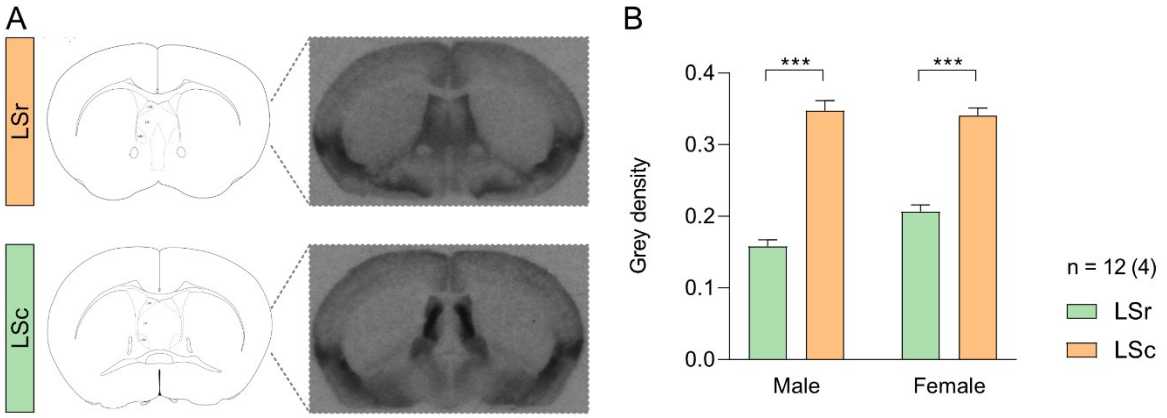

*Figure 12: Oxytocin receptor (OXTR) binding density differs within the lateral septum (LS) in male and female mice. A) Schematic views and representative images of OXTR binding in the rostral part of the lateral septum (LSr) and the caudal part of the lateral septum (LSc). B) OXTR binding in the LSr and LSc in males and females. Data represents means ± SEM. *** p<0.001, n = image number over (animal number)/ group, for detailed statistics see Table 6.*

OXTR binding	Two-way ANOVA	Figure 12
Grey density	(Region) $F_{1,12} = 74.5$	$p < 0.001$
	(Sex) $F_{1,12} = 1.26$	$p = 0.285$
	(Region x Sex) $F_{1,12} = 2.15$	$p = 0.168$

Table 6: Statistics – Oxytocin receptor (OXTR) distribution based on OXTR-autoradiography. Factor region represents LSr vs LSc effects and factor sex represents male vs female mice effects.

3.1.2 OXTR mRNA Expression within the LS

To quantify the total amount of $OXTR^+$ cells in the LS and the proportion of $OXTR^+$ cells that co-express for either SSt, Nts or both, I used RNA-scope, an *in-situ* hybridization technique (Figure 13, A). In total 21% of the evaluated cells in the LS express OXTR (Figure 13, B left)(see 2.7.1). Within that population of OXTR expressing cells, the majority (60,18 %) does not co-express mRNA for Nts (8,27 %), SSt (15,47 %), or a combination of both (16,08 %) (Figure 13, B right).

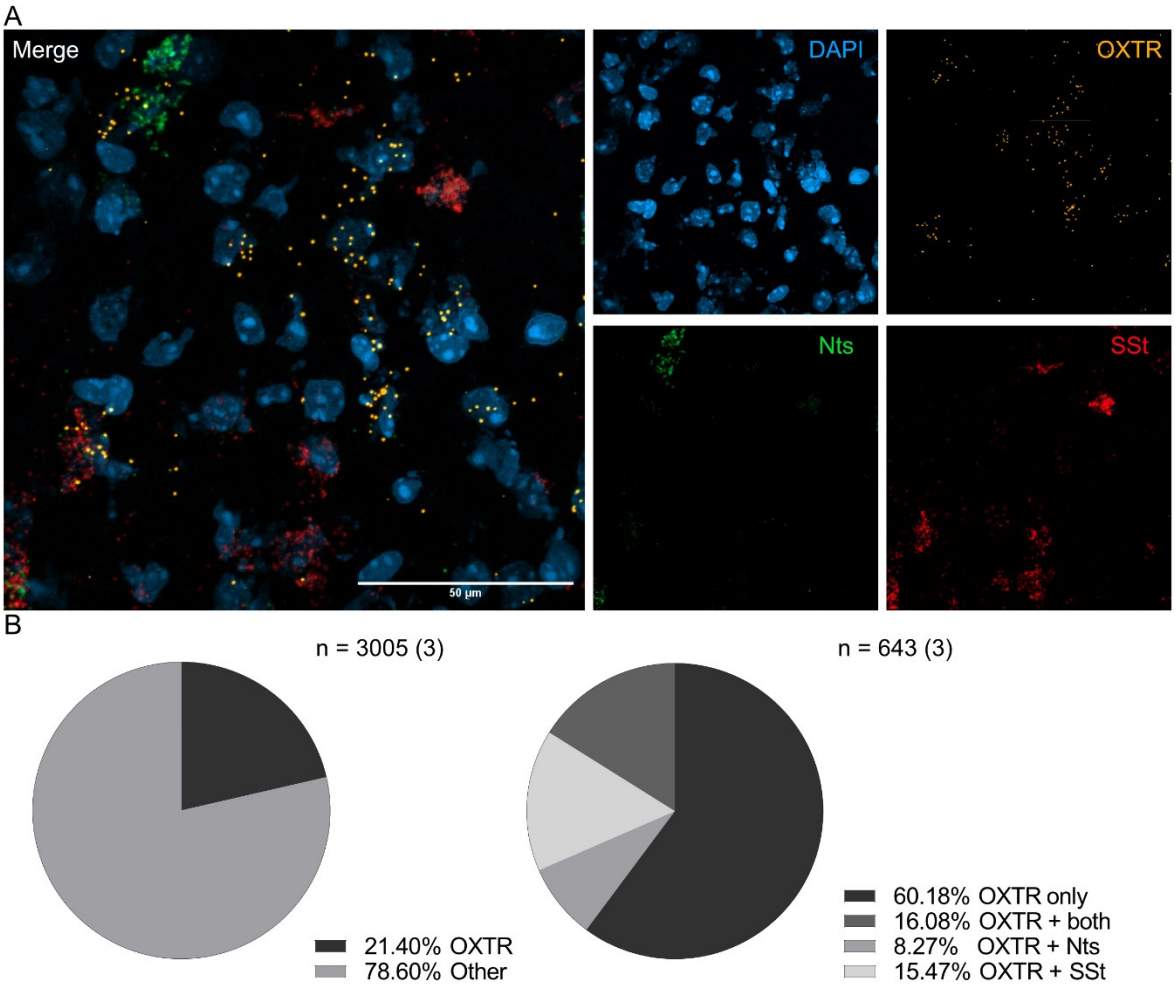

Figure 13: Proportion of oxytocin receptor expressing (OXTR⁺) cells in the lateral septum (LS) and co-expression with neurotensin (Nts) and somatostatin (SSt). A) Representative image from the LS showing triple in situ hybridization of mRNA encoding OXTR (yellow), SSt (red), Nts (green), and a DAPI nuclear counterstain. Scale bar, 50 µm. B) Left: Percentage of OXTR⁺ cells in the LS. Right: Percentage of OXTR which co-express Nts, SSt, or a combination of both. n = cell number over (mouse number).

In order to assess whether OXTR mRNA exhibits a specific distribution pattern, as seen in OXTR binding, I conducted an analysis of OXTR mRNA transcript levels along both the rostral-caudal and dorsal-ventral axes in the LS. This approach was employed to gain a more detailed understanding of the spatial distribution of OXTR within the LS.

While the amount of OXTR mRNA expression is uniform across the rostral-caudal extension of the LS (Figure 14, A), a higher OXTR mRNA was found in the intermediate part compared to the dorsal ($p < 0.001$) and the ventral parts ($p = 0.006$) of the LSr (Figure 14, B). Similarly, in the LSc the intermediate part shows a higher OXTR mRNA expression compared to the dorsal ($p = 0.017$), but not the ventral, part (Figure 14, C). The distribution pattern found on OXTR mRNA level is also

reflected in the regional proportion of $OXTR^+$ cells within the total cell population, here a cell was counted as $OXTR^+$ if 3 or more mRNA dots were visible on the respective cell (see 2.9.1). Therefore, $OXTR^+$ cells do not differ across the rostral-caudal extension of the LS (Figure 14, D), but in the LSr is a significant increase of $OXTR^+$ cell in the intermediate part compared to the dorsal ($p < 0.001$) and ventral part ($p = 0.004$)(Figure 14, E). However, in the LSc the intermediate part just differs with a trend compared to the ventral part ($p = 0.07$, Figure 14, F). In order to compare the individual OXTR transcript level of the cells, scores were assigned to separate high (21-58 dots/cell), medium (10-20 dots/cell), and low OXTR expressing cells (3-9 dots/cell). In both subregions (LSr and LSc) the majority of $OXTR^+$ cells express 3-9 dots/ cell. Even though the high expressing cells are a minor part of the OXTR expressing cells, the proportion in the LSc is higher compared to the LSr, 11 % vs 3 % respectively (Figure 14, H – I).

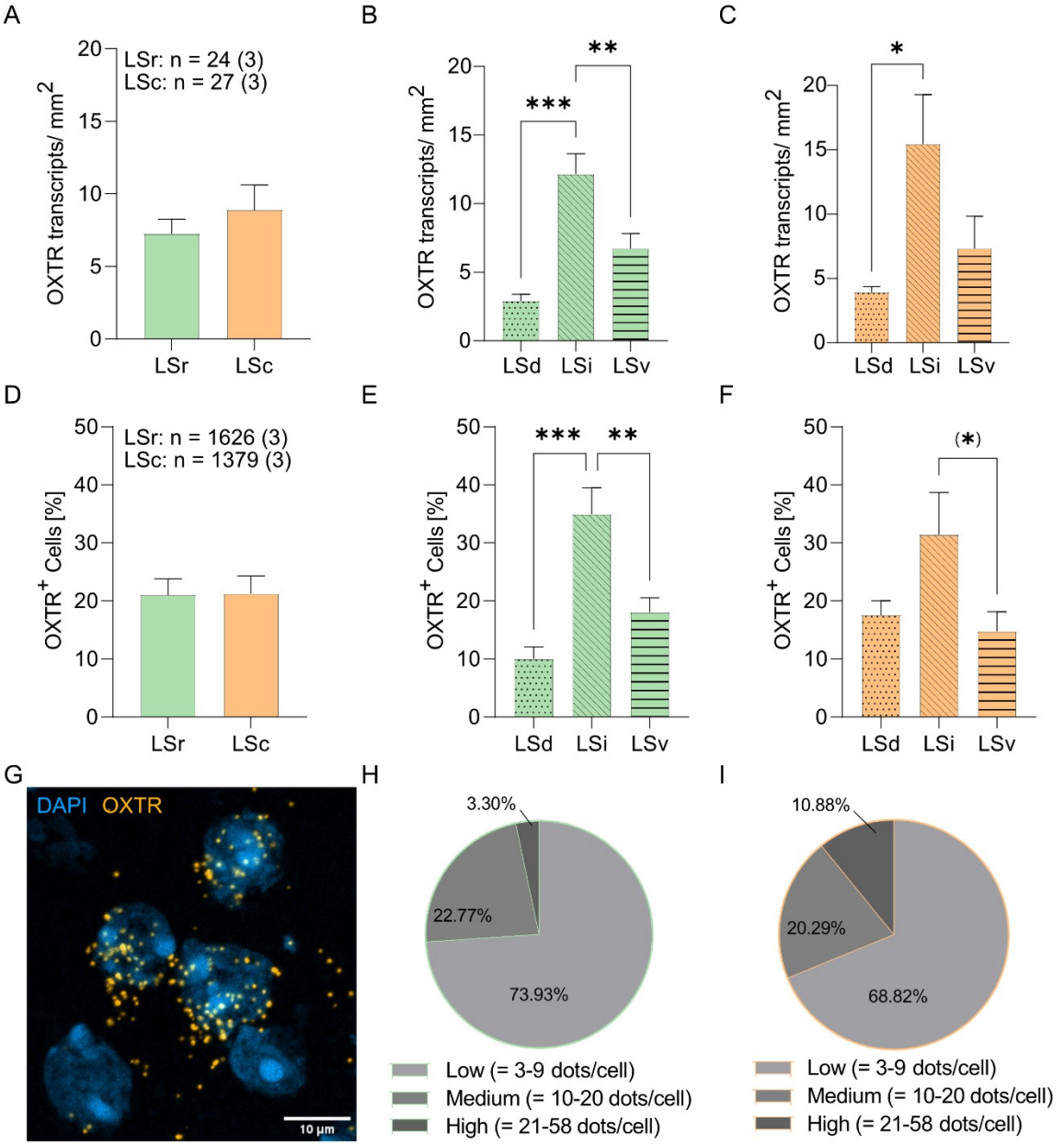

*Figure 14: Subregion specific quantification of oxytocin receptor (OXTR) mRNA expression and OXTR expressing (OXTR⁺) cells within the lateral septum (LS). A-C) Transcript expression level analyzed per area. Images were taken at 63x magnification (135x135 µm image size), n = image number over (animal number). D-F) Percentage of positive cells relative to all cells, n = absolute cell number over (animal number). G) Representative image of cells expressing OXTR mRNA (orange) and a DAPI nuclear counterstain. Scale bar, 10 µm. H-I) Proportion of individual OXTR⁺ cells with different transcription level in the LSr (green, left) and LSc (orange, right) respectively. Data represents means ± SEM. *** p < 0.001, ** p < 0.01, * p < 0.05, (*) p < 0.07. For detailed statistics see (Table 7).*

OXTR Transcripts	Mann-Whitney-U Test (Region), One-way ANOVA	Figure 14 A-C
Region	$U_{38.1} = -0.981$	$p = 0.333$
Subregion – LSr	$F_{2,21} = 17.9$	$p < 0.001$
Subregion – LSc	$F_{2,24} = 3.91$	$p = 0.016$
OXTR Cells	Mann- Whitney-U Test (Region), One-way ANOVA	Figure 14 D-F
Region	$U_{40.7} = -0.807$	$p = 0.424$
Subregion – LSr	$F_{2,21} = 15.5$	$p < 0.001$
Subregion – LSc	$F_{2,24} = 3.40$	$p = 0.050$

Table 7: Statistics – Oxytocin receptor (OXTR) distribution, based on RNAscope. Factor region represents LSr vs LSc effects and factor subregion represents LSd vs LSi vs LSv.

3.1.3 Downstream Targets of OXTR$^+$ Neurons in the LSc

As shown above 21,4% of the cells in the LS express OXTR mRNA, and local OXTR binding is abundant. The LS receives projections from OXT producing regions, such as the PVN or SON (Grinevich et al., 2016). However, the downstream targets of OXTR$^+$ neurons in the LS remains elusive. As shown above, the OXTR density increases towards the LSc, therefore, I aimed to determine the downstream targets of OXTR$^+$ neurons specifically of the LSc, to further clarify the communication route of this neuronal subtype in the LSc. To determine where OXTR$^+$ neurons project to, I injected an AAV expressing a Cre-dependent synaptophysin-mCherry (Syp-mCherry) fusion protein into the LSc of OXTR-ires-Cre mice (Figure 15, A). Presynaptic Syp-mCherry puncta in the medial habenula (Mhb), demonstrated the presence of Mhb-innervating OXTR$^+$ neurons from the LSc (Figure 15, B). In addition, to the Mhb, I detected, synaptophysin-mCherry signal in the CA2/3 regions of the dorsal HIP and the ventral diagonal band of broca (VDB).

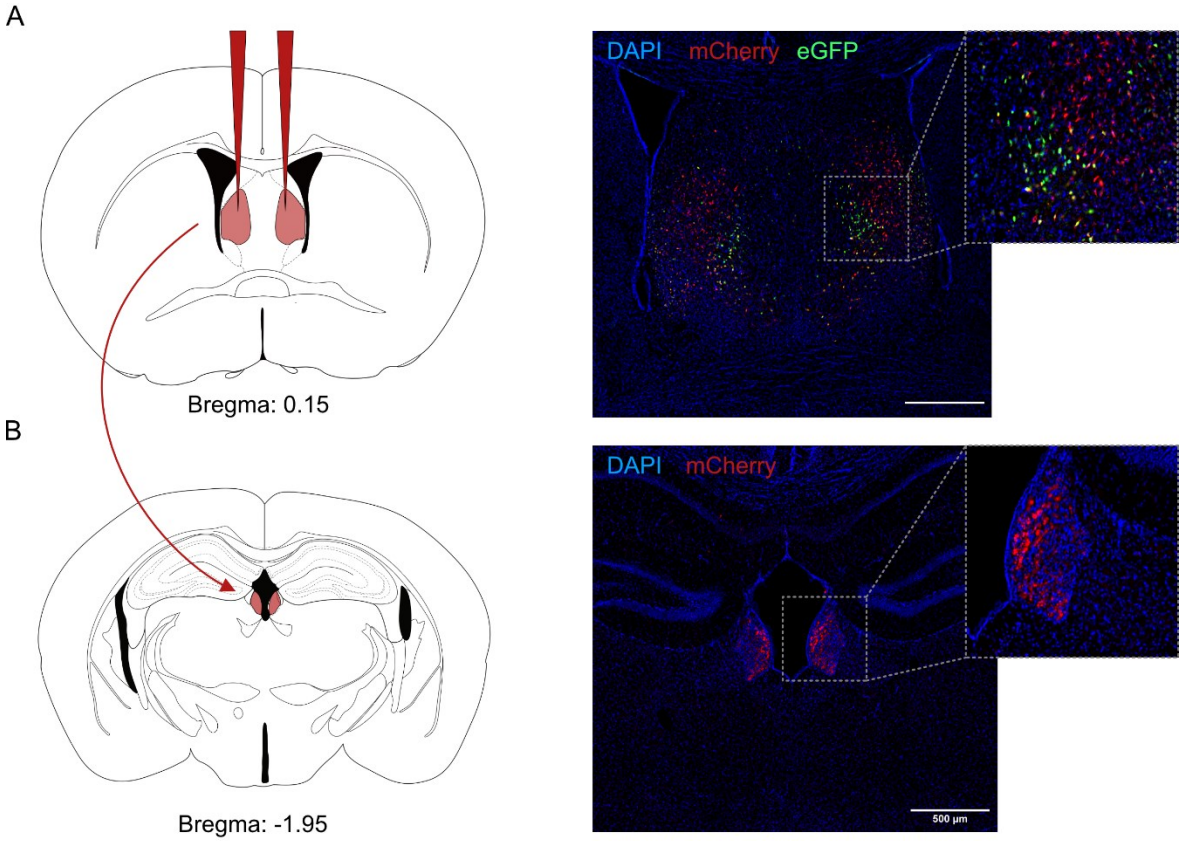

Figure 15: Oxytocin receptor expressing (OXTR$^+$) neurons in the caudal part of the lateral septum (LSc) project to the medial habenula (Mhb). AAV expressing a Cre-dpendent Synaptophysin (Syp)-mCherry fusion protein (AAV9-CMV::DIO-Syp-mCherry) was bilaterally injected into the LSc of OXTR-ires-Cre mice. Presynaptic Syp-mCherry puncta are shown in red. The anterogradely labeled presynaptic terminals (Syp-mCherry puncta) represent direct projection sties of LSc OXTR+ neurons. Prominent Syp-mCherry labeling was observed in the Mhb. Accuracy of the tracing approach was verified by co-injecting AAV9-hSyn::DIO-eGFP, which helped to identify correctly targeted neurons at the injection site, since most Syp-mCherry is transported to presynaptic terminals and thus often not visible in the cell soma. The highest Syp-mCherry puncta density originating from the LSc was observed in the Mhb. Scale bars represent 500 µm.

3.2 Pharmacological Manipulation of the Septal OXT System

Previous research has already suggested that OXT administration, either icv or into the dorsal part of the LS, can enhance the process of social fear extinction (Zoicas et al., 2014). Given that the studies conducted in this thesis with RNAscope and RAR for OXTR have shown a heterogenous distribution of OXTR$^+$ cell in the LS, here I aimed to investigate specifically the role of OXTR$^+$ cells in the LSc, the region with the highest expression level.

3.2.1 Effects of OXT Infusion in the LSc on Social Fear Extinction

To investigate, whether OXT binding in the LSc affects social fear extinction as well as social behavior in general, I infused SFC^+ and SFC^- mice (n = 43/ 2 cohorts) with either Veh or OXT 10 min before extinction training (Figure 16, A). During acquisition, SFC^+ animals that were treated with OXT later on received significantly less foot shocks ($p = 0.039$) (Figure 16, B), which could lead to a decreased social avoidance behavior. Typically, animals receive 1-3 foot shock to establish complete social avoidance, with subsequent grouping ensuring an equal distribution of foot shock between treatment and veh groups. However, rare instances may disrupt this even distribution, such as the exclusion of animals due to issues like improper cannula placement or other abnormalities, which occurred in this particular case. The next day, and prior to social fear extinction training, all mice displayed similar investigation of the non-social stimuli (Figure 16, C), which indicates, that acquisition does not alter general exploratory or anxiety-related behaviors in the mice. During extinction training, SFC^+/Veh animals showed reduced social investigation in the beginning (s1-s3: $p < 0.01$, s4: $p = 0.021$, s5 $p = 0.037$), but similar social investigation during the last social stimulus presentation compared to the SFC^-/Veh group. This indicates successful induction of social fear, which could be extinguished by repeated social stimulus presentation. Furthermore, SFC^-/OXT treated animals did not differ in social investigation time compared to SFC^-/Veh treated animals, indicating that administration of OXT in the LSc does not alter social stimulus investigation per se. SFC^+/OXT treated animals displayed increased social investigation in the beginning of extinction training (s1: $p = 0.066$, s2: $p = 0.011$), reflecting a partial reversal of social fear and a facilitated social fear extinction compared to SFC^+/Veh animals. Even though, SFC^+/OXT animals showed increased social investigation with progressing stimuli presentation, they still significantly differ from SFC^-/OXT animals during the last stimulus presentation (s6: $p = 0.042$), indicating an unsuccessful social fear extinction (Figure 16, D). During recall, SFC^+/Veh animals only showed reduced investigation time during the first social stimulus (s7: $p = 0.020$) compared to SFC^-/Veh, whereas SFC^+/OXT animals showed reduced social investigation time during the second and third presentation during recall (s8: $p = 0.039$, s9: $p = 0.048$) compared to SFC^-/OXT (Figure 16,E). Nevertheless, stable investigation during the last social stimuli presented, indicates a successful and stable extinction of social fear in both conditioned groups.

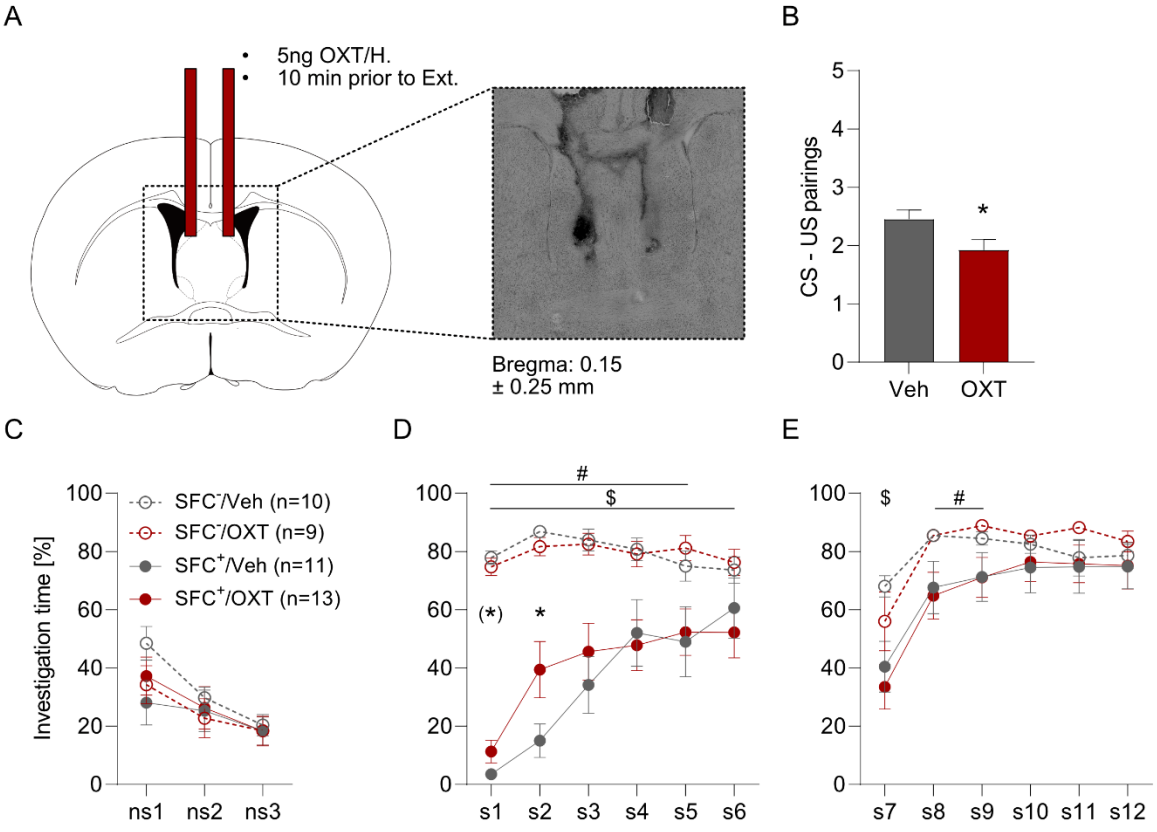

Figure 16: Oxytocin (OXT) infusion in the caudal part of the lateral septum (LSc) facilitates social fear extinction. A) Schematic representation indicating the site of bilateral OXT infusion (5ng/ 0.2µL/ hemisphere) into the LSc, with a representative image of the infusion site. Accepted diffusion range within the LS was set on Bregma 0.4 – (-)0.1 mm. B) Number of CS-US pairings presented to social fear conditioned mice (SFC⁺) during acquisition of social fear (day 1). C) Percentage of time investigating the non-social stimuli (ns1-ns3) presented prior to social fear extinction training of all treatment groups (SFC⁻/Veh; SFC⁻/OXT, SFC⁺/Veh; SFC⁺/OXT). D) Percentage of time investigating the social stimulus presented during social fear extinction. E) Percentage of time investigating the social stimulus presented during social fear extinction recall. Data represents mean ± SEM. p ≤ 0.05 or (*) p ≤ 0.07 SFC+/OXT vs SFC⁺/Veh, $ p ≤ 0.05 SFC⁺/Veh vs SFC⁻/Veh, # p ≤ 0.05 SFC⁺/OXT vs SFC⁻/OXT. For detailed statistics see Table 8.*

Acquisition	Independent T-Test	Figure 16, B
CS-US pairings	$T_{22} = 2.20$	P = 0.039
Extinction ns 1-3	Mixed Model ANOVA	Figure 16, C
Investigation Time	(Time) $F_{2,78} = 27.1$	P < 0.001
	(Conditioning) $F_{1,39} = 0.390$	P = 0.536
	(Treatment) $F_{1,39} = 0.159$	P = 0.692
	(Time x Conditioning) $F_{2,78} = 1.71$	P = 0.187
	(Time x Treatment) $F_{2,78} = 0.089$	P = 0.915
	(Conditioning x Treatment) $F_{1,39} = 1.03$	P = 0.317
	(Time x Conditioning x Treatment) $F_{2,78} = 2.47$	P = 0.091
Extinction s 1-6	Mixed Model ANOVA	Figure 16, D
Investigation Time	(Time) $F_{5,101} = 11.7$	P < 0.001
	(Conditioning) $F_{1,39} = 53.2$	P < 0.001
	(Treatment) $F_{1,39} = 0.226$	P = 0.637
	(Time x Conditioning) $F_{5,101} = 12.9$	P < 0.001
	(Time x Treatment) $F_{5,101} = 0.832$	P = 0.464
	(Conditioning x Treatment) $F_{1,39} = 0.299$	P = 0.588
	(Time x Conditioning x Treatment) $F_{5,101} = 1.89$	P = 0.150
Recall s 7-12	Mixed Model ANOVA	Figure 16, E
Investigation Time	(Time) $F_{5,93} = 25.4$	P < 0.001
	(Conditioning) $F_{1,39} = 6.55$	P = 0.014
	(Treatment) $F_{1,39} = 0.003$	P = 0.955
	(Time x Conditioning) $F_{5,93} = 2.56$	P = 0.073
	(Time x Treatment) $F_{5,93} = 1.27$	P = 0.288
	(Conditioning x Treatment) $F_{1,39} = 0.071$	P = 0.792
	(Time x Conditioning x Treatment) $F_{5,93} = 0.256$	P = 0.811

Table 8: Statistics – Effects of Oxytocin (OXT) infusion into the caudal part of the lateral septum (LSc) prior to social fear extinction. Factor Time represents stimulus presentation during SFC, factor Conditioning represents SFC^+ vs SFC^- effects, factor Treatment represents OXT vs Veh effects.

3.2.2 Effects of Atosiban Infusion in the LSc on Social Fear Extinction

To evaluate whether the effects of OXT are mediated by Gαi-coupled signaling pathways, the selective OXTR-Gαi agonist Atosiban was administered bilaterally into the LSc 10 minutes prior to

social fear extinction training in two cohorts of animals consisting of a total of 43 mice (Figure 17,A). SFC^+ animals that were treated with Atosiban later on received significantly less foot shocks during acquisition ($p = 0.022$) (Figure 17, B), potentially resulting in a decrease in social avoidance behavior. All groups displayed similar levels of investigation toward non-social stimuli (Figure 17, C), suggesting that acquisition did not affect general exploratory behavior in the animals. During extinction training, SFC^+/Veh animals exhibited an overall reduction in social investigation (s1: $p < 0.01$, s2: $p = 0.002$, s3 $p = 0.007$, s4 $p = 0.040$, s5 $p = 0.020$, s6 $p = 0.040$) compared to SFC^-/Veh animals. This indicates the successful induction of social fear but an unsuccessful elimination of social fear upon repeated presentation of social stimuli during extinction training. SFC^-/Atosiban animals did not differ in their investigation time of social stimuli compared to SFC^-/Veh treated animals, suggesting that Atosiban binding in the LSc does not inherently alter the investigation of social stimuli. SFC^+/Atosiban animals exhibited increased social investigation during the first presentation of a social stimulus (s1: $p = 0.024$) compared to SFC^+/Veh animals. Moreover, from the third stimulus onward, SFC^+/Atosiban animals displayed similar levels of social investigation (s1: $p < 0.001$, s2: $p = 0.021$) compared to SFC^-/Atosiban treated animals, indicating a rapid extinction success. However, during the final presentation of a social stimulus, they once again exhibited decreased social investigation compared to SFC^-/Atosiban treated animals (s6: $p = 0.038$), suggesting a resurgence of social fear (Figure 17, D). During recall SFC^+/Veh animals generally showed reduced investigation time, except for the fifth presentation during recall (s7: $p = 0.062$, s8: $p = 0.001$, s9 $p = 0.001$, s10 $p = 0.01$, s12 $p = 0.002$). In contrast, SFC^+/Atosiban treated animals did not differ in their investigation time during recall compared to SFC^-/Veh throughout the session. However, they exhibited significantly increased investigation time compared to SFC^+/Veh animals starting from the second stimulus presentation during recall (s8: $p = 0.030$, s9: $p = 0.004$, s10 $p = 0.002$, s11 $p = 0.067$, s12 $p < 0.001$), which indicates that SFC^+/Atosiban treated animals successfully overcame social fear in contrast to SFC^-/Veh animals (Figure 17,E).

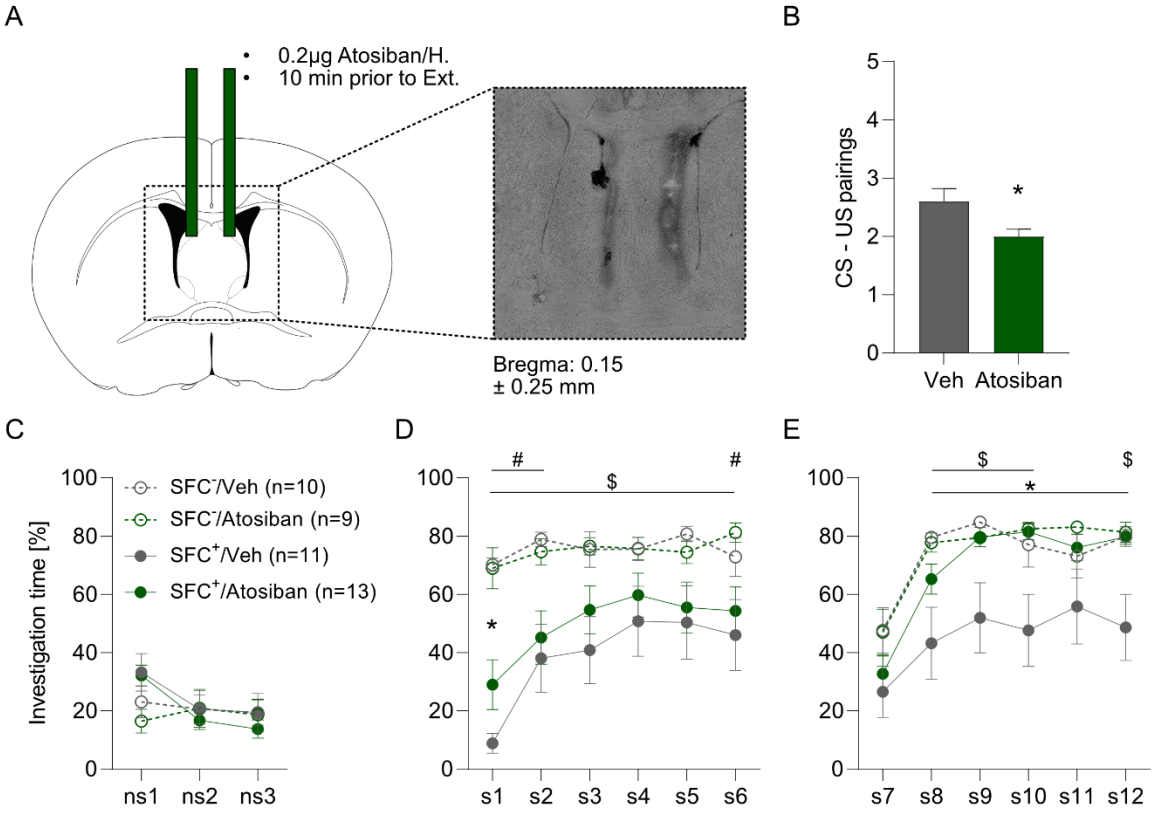

Figure 17: Atosiban infusion in the caudal part of the lateral septum (LSc) facilitates social fear extinction. A) Schematic representation of bilateral atosiban infusion (0.2µg/ 0.2µL/ hemisphere) in the LSc, with a representative image of the injection site. Accepted diffusion range within the LS was set on Bregma 0.4 – (-)0.1 mm. B) Number of CS-US pairings presented to conditioned mice (SFC⁺) during acquisition of social fear. C) Percentage of time investigating the non-social stimuli presented during social fear extinction of all treatment groups (SFC⁻/Veh; SFC⁻/Atosiban, SFC⁺/Veh; SFC⁺/Atosiban). D) Percentage of time investigating the social stimulus presented during social fear extinction of all treatment groups. E) Percentage of time investigating the social stimulus presented during social fear extinction recall. Data represents mean ± SEM. p ≤ 0.05 or (*) p ≤ 0.07 SFC⁺/OXT vs SFC⁺/Veh, $ p ≤ 0.05 SFC⁺/Veh vs SFC⁻/Veh, # p ≤ 0.05 SFC⁺/OXT vs SFC⁻/OXT. For detailed statistics see Table 9.*

Acquisition	Independent T-Test	Figure 17, B
CS-US pairings	$T_{20} = 2.48$	P = 0.022
Extinction ns 1-3	Mixed Model ANOVA	Figure 17, C
Investigation Time	(Time) $F_{2,70} = 9.66$	P < 0.001
	(Conditioning) $F_{1,35} = 0.396$	P = 0.533
	(Treatment) $F_{1,35} = 0.436$	P = 0.513
	(Time x Conditioning) $F_{2,70} = 9.46$	P < 0.001
	(Time x Treatment) $F_{2,70} = 0.138$	P = 0.871
	(Conditioning x Treatment) $F_{1,35} = 0.900$	P = 0.900
	(Time x Conditioning x Treatment) $F_{2,70} = 1.06$	P = 0.351
Extinction s 1-6	Mixed Model ANOVA	Figure 17, D
Investigation Time	(Time) $F_{2.7,96} = 9.38$	P < 0.001
	(Conditioning) $F_{1,35} = 21.0$	P < 0.001
	(Treatment) $F_{1,35} = 0.573$	P = 0.454
	(Time x Conditioning) $F_{2.7,96} = 4.21$	P = 0.010
	(Time x Treatment) $F_{2.7,96} = 0.580$	P = 0.614
	(Conditioning x Treatment) $F_{1,35} = 0.653$	P = 0.425
	(Time x Conditioning x Treatment) $F_{2.7,96} = 0.430$	P = 0.714
Recall s 7-12	Mixed Model ANOVA	Figure 17, E
Investigation Time	(Time) $F_{3,105} = 28.3$	P < 0.001
	(Conditioning) $F_{1,35} = 6.55$	P = 0.005
	(Treatment) $F_{1,35} = 0.003$	P = 0.034
	(Time x Conditioning) $F_{3,105} = 0.627$	P = 0.600
	(Time x Treatment) $F_{3,105} = 1.31$	P = 0.275
	(Conditioning x Treatment) $F_{1,35} = 0.071$	P = 0.060
	(Time x Conditioning x Treatment) $F_{3,105} = 1.12$	P = 0.346

Table 9: Statistics – Effects of atosiban infusion in the caudla part of the lateral septum (LSc) prior to social fear extinction. Factor Time represents stimulus presentation during SFC, factor Conditioning represents SFC^+ vs SFC^- effects, factor Treatment represents atosiban vs vehicle effects.

3.2.3 Effects of Carbetocin Infusion in the LSc on Social Fear Extinction

To evaluate whether the effects of OXT are mediated by Gαq-coupled signaling pathways, the selective OXTR-Gαq agonist Carbetocin was administered bilaterally in the LSc 10 minutes prior to

social fear extinction training in two cohorts of animals consisting of a total of 41 mice (Figure 18,A). All animals received a similar number of foot shocks during Acquisition (Figure 18, B). All groups displayed similar levels of investigation toward non-social stimuli (Figure 18, C), suggesting that acquisition did not affect general exploratory behavior in the animals. During extinction training, SFC^+/Veh animals exhibited significantly reduced social investigation at the beginning (s1: $p < 0.01$, s2: $p < 0.01$, s3 $p = 0.002$, s4 $p = 0.024$, s5 $p = 0.068$), but demonstrated comparable levels of social investigation during the final presentation of a social stimulus compared to SFC^-/Veh animals. This suggests the successful establishment of social fear, which could be diminished through repeated presentations of the social stimulus. SFC^-/Carbetocin treated animals did not differ in their investigation time of social stimuli compared to SFC^-/Veh treated animals, suggesting that Carbetocin binding in the LSc does not inherently alter the investigation of social stimuli. SFC^+/Carbetocin treated animals displayed similar levels of social investigation compared to SFC^-/Carbetocin treated animals (s1: $p < 0.001$, s2: $p < 0.001$, s3: $p = 0.033$), indicating a rapid extinction success, but investigation time did not differ compared to SFC^+/Veh (Figure 18, D). During recall, SFC^+/Veh animals again exhibited reduced investigation time during the first two stimulus presentations (s7: $p = 0.002$, s8: $p < 0.001$) and still differed with a trend in the following two presentations (s9: $p = 0.054$, s10: $p = 0.067$) compared to SFC^-/Veh. SFC^+/Carbetocin treated animals also showed reduced social investigation during the first two stimuli presentations (s7: $p < 0.001$, s8: $p = 0.001$) compared to SFC^-/Carbetocin animals. Therefore, both groups showed a reinstatement of social fear, which could be extinguished from the second and fourth stimulus presentation during recall, respectively (Figure 18,E).

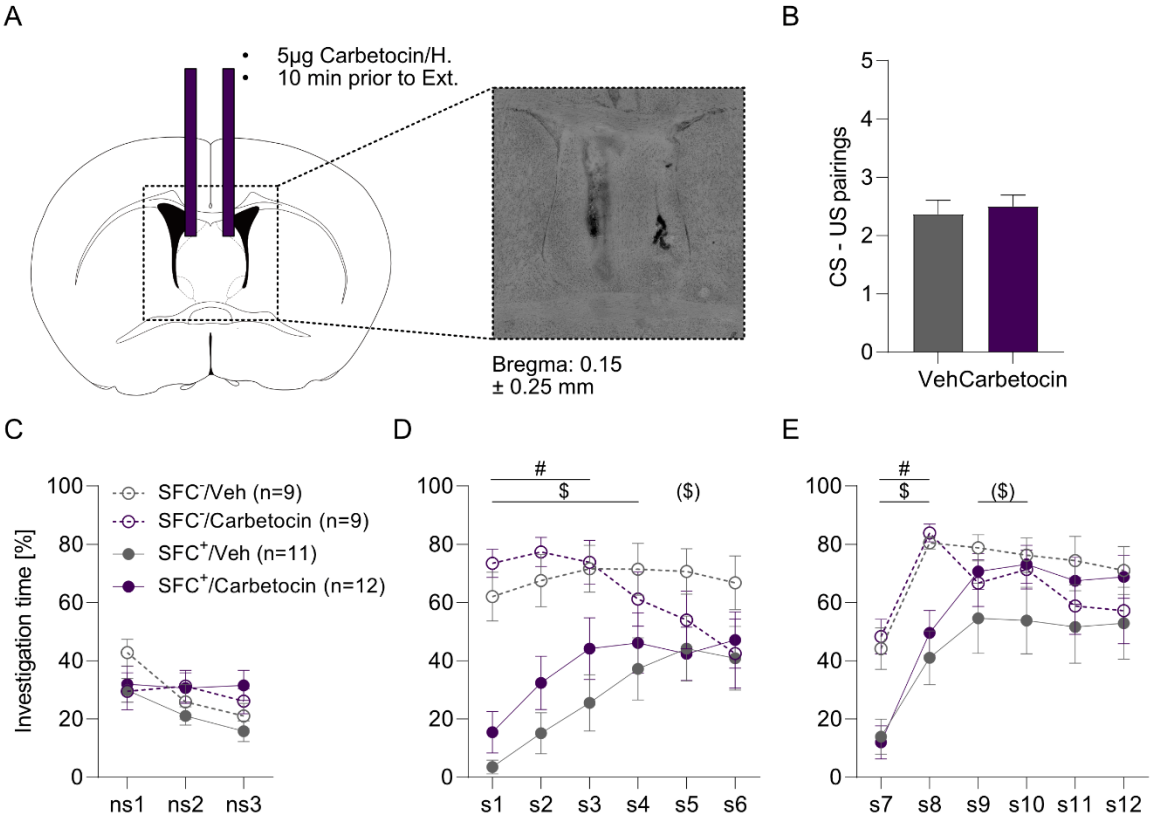

Figure 18: Carbetocin infusion in the caudal part of the lateral septum (LSc) does not influence social fear extinction. A) Schematic representation of bilateral carbetocin infusion (5µg/ 0.2µL/ hemisphere) in the LSc, with a representative image of the injection site. Accepted diffusion range within the LS was set on Bregma 0.4 – (-) 0.1 mm. B) Number of CS-US pairings presented to conditioned mice (SFC⁺) during acquisition of social fear. C) Percentage of time investigating the non-social stimuli presented during social fear extinction of all treatment groups (SFC⁻/Veh; SFC⁻/Carbetocin, SFC⁺/Veh; SFC⁺/Carbetocin). D) Percentage of time investigating the social stimulus presented during social fear extinction of all treatment groups. E) Percentage of time investigating the social stimulus presented during social fear extinction recall. Data represents mean ± SEM. $ p ≤ 0.05 or ($) p ≤ 0.07 SFC⁺/Veh vs SFC⁻/Veh, # p ≤ 0.05 SFC⁺/OXT vs SFC⁻/OXT. For detailed statistics see Table 10.

Acquisition	Independent T-Test	Figure 18, B
CS-US pairings	$T_{21} = 0.157$	P = 0.664
Extinction ns 1-3	Mixed Model ANOVA	Figure 18, C
Investigation Time	(Time) $F_{2,74} = 4.83$	P = 0.011
	(Conditioning) $F_{1,37} = 0.602$	P = 0.443
	(Treatment) $F_{1,37} = 0.235$	P = 0.235
	(Time x Conditioning) $F_{2,74} = 0.331$	P = 0.715
	(Time x Treatment) $F_{2,74} = 3.50$	P = 0.035
	(Conditioning x Treatment) $F_{1,37} = 0.148$	P = 0.148
	(Time x Conditioning x Treatment) $F_{2,74} = 0.383$	P = 0.683
Extinction s 1-6	Mixed Model ANOVA	Figure 18, D
Investigation Time	(Time) $F_{2.4,89} = 4.43$	P = 0.010
	(Conditioning) $F_{1,37} = 18.7$	P < 0.001
	(Treatment) $F_{1,37} = 0.132$	P = 0.719
	(Time x Conditioning) $F_{2.4,89} = 10.9$	P < 0.001
	(Time x Treatment) $F_{2.4,89} = 3.57$	P = 0.025
	(Conditioning x Treatment) $F_{1,37} = 0.930$	P = 0.341
	(Time x Conditioning x Treatment) $F_{2.4,89} = 0.863$	P = 0.443
Recall s 7-12	Mixed Model ANOVA	Figure 18, E
Investigation Time	(Time) $F_{3,110} = 33.1$	P < 0.001
	(Conditioning) $F_{1,37} = 6.55$	P = 0.023
	(Treatment) $F_{1,37} = 0.003$	P = 0.686
	(Time x Conditioning) $F_{3,110} = 7.95$	P < 0.001
	(Time x Treatment) $F_{3,110} = 0.330$	P = 0.802
	(Conditioning x Treatment) $F_{1,37} = 0.071$	P = 0.194
	(Time x Conditioning x Treatment) $F_{3,110} = 2.30$	P = 0.082

Table 10: Statistics - Effects of carbetocin infusion in the caudl part of the lateral septum (LSc) prior to social fear extinction. Factor Time represents stimulus presentation during SFC, factor Conditioning represents SFC^+ vs SFC^- effects, factor Treatment represents Atosiban vs vehicle effects.

3.2.4 Effects of OXT Infusion in Different Subregions of the LS

In light of the less pronounced effects observed in the above-mentioned results, which differ from earlier findings showing complete suppression of social fear expression with OXT administration in

the dorsal part of the LS (Zoicas et al., 2014), I conducted OXT infusions across various subregions along the rostral-caudal axis of the LS to investigate the region-specific impact of OXT signaling on social fear extinction (Figure 19, A-C). Either OXT or Veh was administered 10 minutes prior to social fear extinction training in a cohort consisting of a total of 33 mice. All groups received similar number of foot shocks during acquisition (Figure 19, D). Since the control animals from all groups (SFC^+/Veh) did not differ from each other during extinction training (Figure 19, E), the animals were pooled to one group for further comparisons (Figure 20).

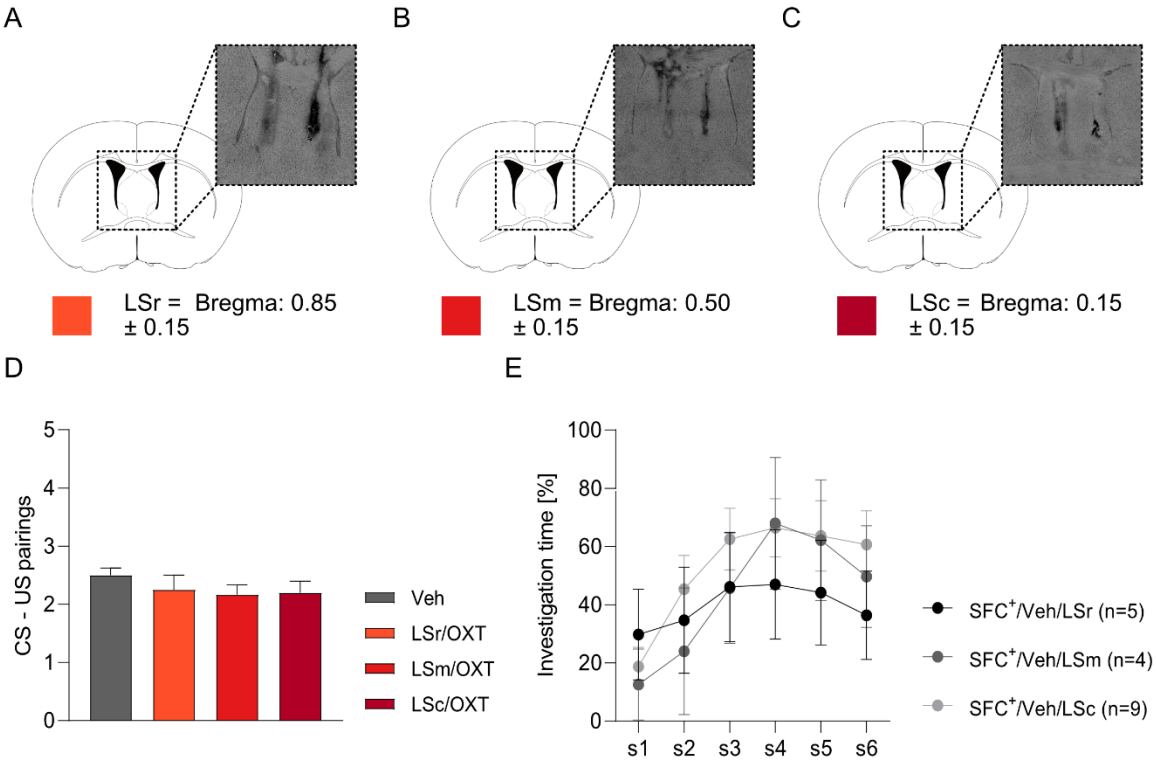

Figure 19: Oxytocin (OXT) infusion in different subregions of the lateral septum (LS) - part 1. A-C) Schematic representation of OXT infusion (OXT; 5ng/ 0.2µL/ hemisphere) in the rostral (LSr), medial (LSm) or caudal part of the LS (LSc), with a representative image of each injection site. Accepted diffusion range within the LS was set on ± 0.15 mm for each injection point. D) Number of CS-US pairings presented to conditioned mice (SFC^+) during acquisition of social fear. E) Percentage of time investigating the social stimulus presented during social fear extinction of all Veh treated groups (SFC^+/Veh/LSr; SFC^+/Veh/LSm, SFC^+/Veh/LSc). For detailed statistics see Table 11

Acquisition	One way ANOVA	Figure 19, D
CS-US pairings	(Region) F3,33 = 1.06	P = 0.382
Extinction s 1-6	Mixed Model ANOVA	Figure 19, E
Investigation Time	(Time) F2.4,36 = 10.2	P < 0.001
	(Region) F2,15 = 0.330	P = 0.724
	(Time x Region) F4.8,36 = 1.17	P = 0.345

Table 11: Statistics - Effects of vehicle infusion in different subregions of the lateral septum (LS) prior to social fear extinction. Factor Time represents stimulus presentation during SFC, factor Region represents LSr vs LSm vs LSc effects.

Both groups, SFC^+/Veh and SFC^+/OXT exhibited similar investigation time of the non-social stimulus in all targeted subregions (Figure 20, A, D, G). During extinction both treatment groups showed increased social interaction over the repeated presentation of the social stimuli, indicating an extinction progress over time. However, both groups did not differ from each other, indicating that OXT binding in the LSr does not influence social fear extinction in none of the subregions (Figure 20, B, E, H). During recall both groups showed reduced social investigation, which again increased over the stimuli presentation (Figure 20, C, F, I).

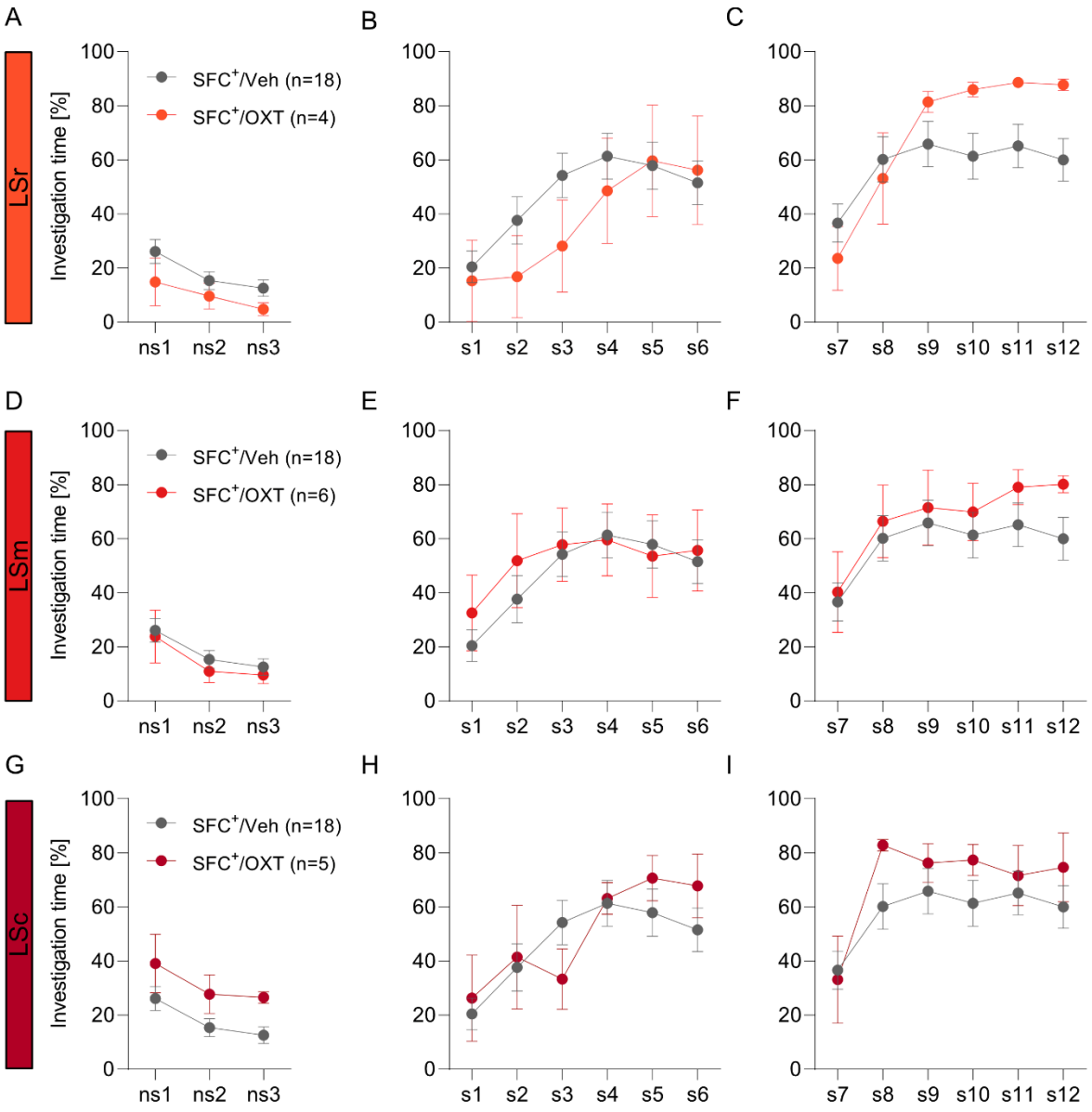

Figure 20: Oxytocin (OXT) infusion in different subregions of the lateral septum (LS) – part 2. A-C) Percentage of time investigating the presented stimuli (non-social and social) during extinction and recall. Animals were injected in the LSr with OXT, or Veh 10 min prior to extinction training. D-F) Percentage of time investigating the presented stimuli (non-social and social) during extinction and recall. Animals were injected in the LSm with OXT, or Veh 10 min prior to extinction training. G-I) Percentage of time investigating the presented stimuli (non-social and social) during extinction and recall. Animals were injected in the LSc with OXT, or Veh 10 min prior to extinction training. For detailed statistics see Table 12.

LSr		
Extinction ns 1-3	Mixed Model ANOVA	Figure 22, A
Investigation Time	(Time) $F_{1.3,27} = 6.30$	P = 0.012
	(Treatment) $F_{1,20} = 1.27$	P = 0.272
	(Time x Treatment) $F_{1.3,27} = 0.334$	P = 0.635
Extinction s 1-6	Mixed Model ANOVA	Figure 22, B
Investigation Time	(Time) $F_{2.3,45} = 8.82$	P < 0.001
	(Treatment) $F_{1,20} = 0.364$	P = 0.553
	(Time x Treatment) $F_{2.3,45} = 1.21$	P = 0.312
Recall s 7-12	Mixed Model ANOVA	Figure 22, C
Investigation Time	(Time) $F_{2.8,55} = 14.2$	P < 0.001
	(Treatment) $F_{1,20} = 0.583$	P = 0.454
	(Time x Treatment) $F_{2.8,55} = 3.34$	P = 0.028
LSm		
Extinction ns 1-3	Mixed Model ANOVA	Figure 22, D
Investigation Time	(Time) $F_{1.3,28} = 12.1$	P < 0.001
	(Treatment) $F_{1,22} = 0.251$	P = 0.621
	(Time x Treatment) $F_{1.3,28} = 0.850$	P = 0.850
Extinction s 1-6	Mixed Model ANOVA	Figure 22, E
Investigation Time	(Time) $F_{2.2,49} = 6.68$	P < 0.001
	(Treatment) $F_{1,37} = 0.544$	P = 0.740
	(Time x Treatment) $F_{2.2,49} = 0.589$	P = 0.577
Recall s 7-12	Mixed Model ANOVA	Figure 22, F
Investigation Time	(Time) $F_{2.7,60} = 7.60$	P < 0.001
	(Treatment) $F_{1,37} = 0.602$	P = 0.469
	(Time x Treatment) $F_{2.7,60} = 0.684$	P = 0.684
LSc		
Extinction ns 1-3	Mixed Model ANOVA	Figure 22, G
Investigation Time	(Time) $F_{1.3,28} = 7.63$	P = 0.001
	(Treatment) $F_{1,21} = 3.68$	P = 0.069
	(Time x Treatment) $F_{1.3,28} = 0.025$	P = 0.926
Extinction s 1-6	Mixed Model ANOVA	Figure 22, H
Investigation Time	(Time) $F_{2.2,46} = 8.70$	P < 0.001

	(Treatment) $F_{1,21}$ = 0.058	P = 0.812
	(Time x Treatment) $F_{2.2,46}$ = 1.43	P = 0.249
Recall s 7-12	Mixed Model ANOVA	Figure 22, I
Investigation Time	(Time) $F_{2.5,53}$ = 9.70	P < 0.001
	(Treatment) $F_{1,21}$ = 0.620	P = 0.440
	(Time x Treatment) $F_{2.5,53}$ = 0.969	P = 0.403

Table 12: Statistics - Effects of oxytocin (OXT) infusion in different subregions of the lateral septum (LS) prior to social fear extinction. Factor Time represents stimulus presentation during SFC, factor Treatment represents OXT vs Veh effects.

3.2.5 Effects of icv OXT Infusion on Social Fear Extinction in Mice from 2 Different Breeding Colonies – pilot study

Since the above presented results did not reveal striking effects, I repeated an original experiment from 2014, where OXT was administered intracerebroventricular (icv) (Zoicas et al., 2014), in order to verify the effect of OXT on social fear extinction. To account also for cohort effects, that might influence the overall behavior of animals, I used one cohort of animals from Charles River Laboratories (CR-Cohort, n = 11) and another cohort that was bred at the University of Regensburg in our own facilities (UR-Cohort, n = 9) and infused them with either Veh or OXT 10 min prior to extinction training (Figure 21,A). Both treatment groups in both cohorts received a similar number of foot shock during acquisition (Figure 21, B, C). Furthermore, both cohorts and treatment groups exhibited similar investigation of the non-social stimulus, which indicates, that acquisition does not alter general explorative behavior in the animals (Figure 21, D, G). During extinction, both treatment groups from CR-Cohort exhibited increased social interaction during repeated social stimulus presentation, indicating an extinction success over time. However, SFC^+/OXT and SFC^+/Veh animals did not differ from each other. Therefore, icv OXT had no effect on social fear extinction progress in the CR-cohort (Figure 21, E). Similarly, during recall both treatment groups did not differ from each other (Figure 21, F). The treatment groups from UR-Cohort also did not differ from other, neither during extinction nor during recall. However, none of the animals exhibited increased social interaction as a result of consecutive presentations of the social stimuli, indicating an increased manifestation of the traumatic event, that could not be eradicated. Also, during recall the animals from the UR-Cohort did not interact with the presented social stimuli, (Figure 21, I).

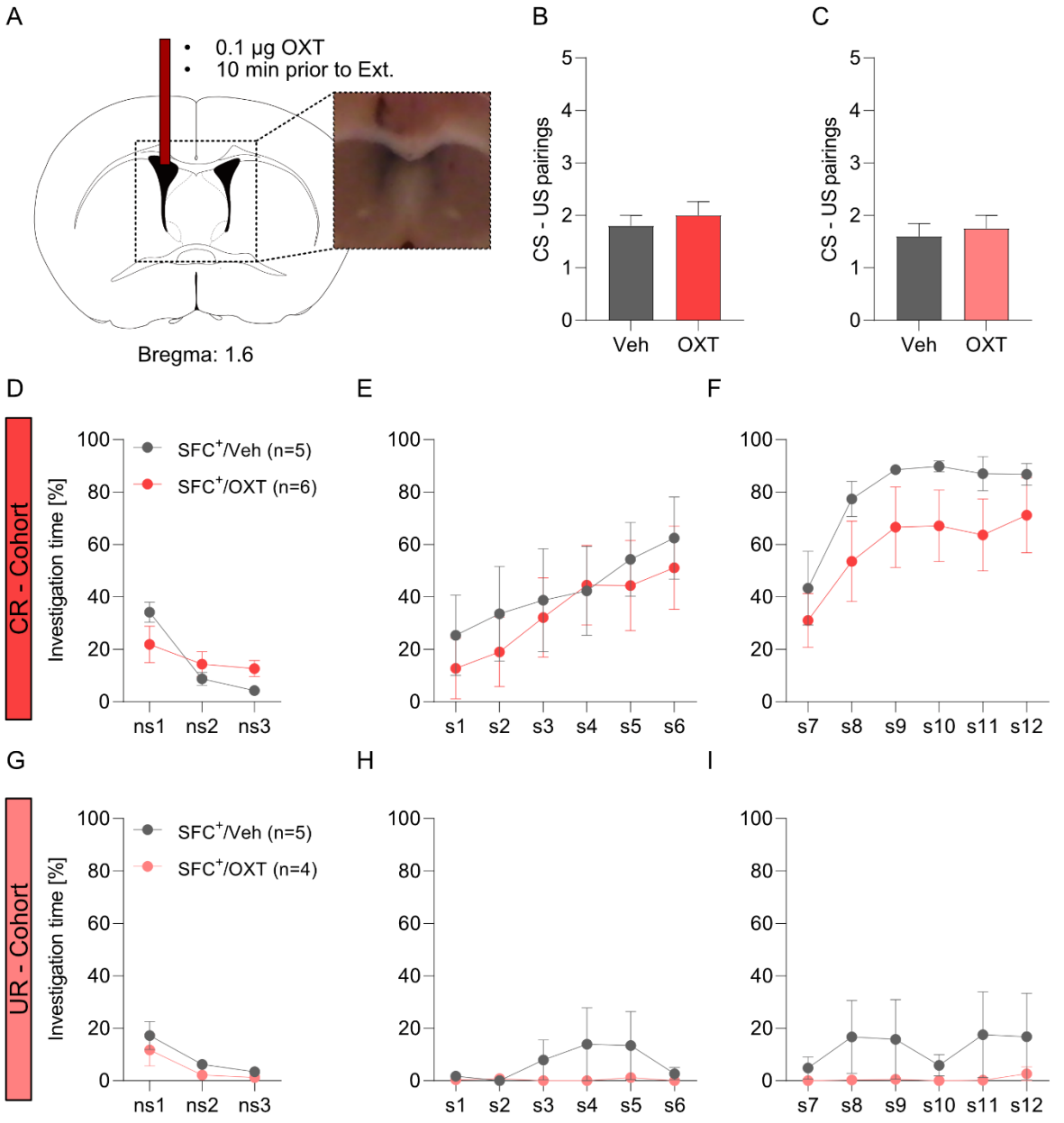

Figure 21: Intracerebroventricular (icv) administration of oxytocin (OXT) in mice from two different breeding cohorts has no effect on social fear extinction – pilot study. A) Schematic representation of OXT infusion (OXT; 0.5 µg/ 2 µL), with a representative image of the injection site. B-C) Number of CS-US pairings presented to conditioned mice (SFC⁺) during acquisition of social fear. D,G) Percentage of time investigating the non-social stimuli presented during social fear extinction of both cohorts and treatment groups (SFC⁺/Veh; SFC⁺/OXT). E,H) Percentage of time investigating the social stimulus presented during social fear extinction. F,I) Percentage of time investigating the social stimulus presented during social fear extinction recall. Data represents mean ± SEM. For detailed statistics seeTable 13.

Acquisition	Independent T-Test	Figure 23, B,C
CS-US pairings	(CR-Cohort) $T_9 = 0.592$	P = 0.568
	(UR-Cohort) $T_7 = 0.424$	P = 0.685
	CR-Cohort	
Extinction ns 1-3	Mixed Model ANOVA	Figure 23, D
Investigation Time	(Time) $F_{2,18} = 10.8$	P < 0.001
	(Treatment) $F_{1,9} = 0.024$	P = 0.880
	(Time x Treatment) $F_{2,18} = 3.06$	P = 0.072
Extinction s 1-6	Mixed Model ANOVA	Figure 23, E
Investigation Time	(Time) $F_{1.9,17} = 6.43$	P < 0.001
	(Treatment) $F_{1,9} = 1.98$	P = 0.667
	(Time x Treatment) $F_{1.9,17} = 0.289$	P = 0.736
Recall s 7-12	Mixed Model ANOVA	Figure 23, F
Investigation Time	(Time) $F_{2,18} = 13.0$	P < 0.001
	(Treatment) $F_{1,9} = 1.90$	P = 0.202
	(Time x Treatment) $F_{2,18} = 0.284$	P = 0.748
	UR-Cohort	
Extinction ns 1-3	Mixed Model ANOVA	Figure 23, G
Investigation Time	(Time) $F_{1,7} = 10.6$	P = 0.013
	(Treatment) $F_{1,7} = 1.18$	P = 0.313
	(Time x Treatment) $F_{1,7} = 0.158$	P = 0.706
Extinction s 1-6	Mixed Model ANOVA	Figure 23, H
Investigation Time	(Time) $F_{1,7} = 0.818$	P = 0.396
	(Treatment) $F_{1,7} = 0.721$	P = 0.424
	(Time x Treatment) $F_{1,7} = 0.158$	P = 0.405
Recall s 7-12	Mixed Model ANOVA	Figure 23, I
Investigation Time	(Time) $F_{1,7.5} = 0.860$	P = 0.390
	(Treatment) $F_{1,7} = 0.863$	P = 0.384
	(Time x Treatment) $F_{1,7.5} = 0.634$	P = 0.460

Table 13: Statistics - Effects of icv Oxytocin (OXT) infusion prior to social fear extinction. Factor Time represents stimulus presentation during SFC, factor Treatment represents OXT vs Veh effects.

3.3 Temporal Characterization of OXTR$^+$ Neurons in the LSc

Declaration: The following results are generated in collaboration with Francisco de los Santos (University of Köln). For detailed contributions see chapter 2.9.3.

Based on the cellular heterogeneity and the pharmacological effects mediated by OXT signaling we aimed to characterize OXTR$^+$ neurons in the LSc also on temporal level. Injection of an adeno-associated virus containing the genetically encoded calcium indicator GCaMP6f flanked by a double-floxed inverse open reading frame (DIO) into the LSc of OXTR-Cre mice, enabled direct tracking of individual OXTR$^+$ neurons in the LSc. The activity of these cells was then recorded during EPM and throughout the adapted SFC (aSFC) paradigm (see 2.9.3).

3.3.1 Activity of OXTR$^+$ neurons in the LSc during exposure to the EPM

On behavioral level, animals spent most time in the CA (62,73%) and less time in the center (15,24%), OA (11.28) and with full OA entries (10.75%), reflecting comparable levels of anxiety-related behavior in the EPM.

To quantify how OXTR$^+$ neurons respond to different environments, neuronal activity measured in fluorescence intensity was compared to mean activity over the whole trial (= ΔF/F), which served as a baseline (see 2.4.2). Hereby, CA is considered a safe and reassuring environment, while OA, or full OA is considered as a risky and, therefore, rather stressful environment. The activity of OXTR$^+$ neurons did not differ during the exploration of the CA vs OA or during full OA entries ($p = 0.18$), indicating that OXTR$^+$ neurons in the LSc are not responding to the exploration of different non-social environments. Furthermore, the overall activity of OXTR$^+$ neurons in the LSc is very low during EPM.

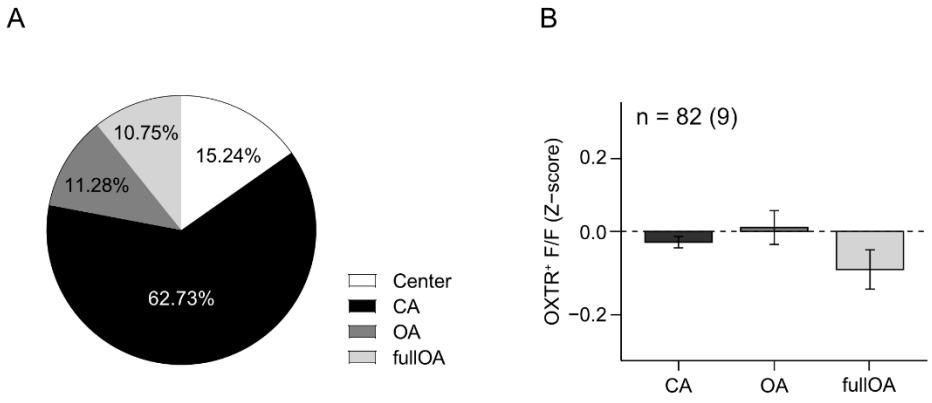

Figure 22: Activity of oxytocin receptor expressing (OXTR⁺) neurons does not change upon exploration of different sections in the elevated plus maze (EPM) test. A) Location of the animal in the center, closed arm (CA), open arm (OA), or fullOA represented in percentage of the total time spent in the EPM, i.e. 15 min. B) Ca^{2+} signal at different locations. n indicates number of cells recorded over (animal number). ΔF/F represents z-scored individual Ca^{2+} traces of OXTR⁺ neurons (see 2.4.2), data represents mean ± SEM. For detailed statistics see Table 14.

ΔF/F	Kruskal-Wallis	Figure 24, B
Location	$X^2(2) = 3.4$	p = 0.18

Table 14: Statistics – Elevated plus maze (EPM) Ca^{2+}- Imaging. Factor location represents fluorescent changes of OXTR⁺ neurons during CA vs OA vs fullOA.

3.3.2 Activity of OXTR⁺ Neurons in the LSc during SFC

Next, we analyzed neuronal activity under different conditions throughout the aSFC paradigm (see 2.9.3). Briefly, the aSFC starts with a 3 min social interaction (SE) in the home cage where the social stimulus 1 (s1) was presented to monitor the activity of OXTR⁺ neurons in the LSc during natural social investigation. On the next day social fear was aquired (Acq) by operant conditioning in a conditioning chamber, here a non-social stimulus 1 (ns1) and a social stimulus (s2) were presented and on the following days extinction (Ext, presentation of ns 2 – 4 and s 3 - 8) and recall (Rec, presentation of s 9 - 14) of social fear were performed again in the home cage. To quantify how LSc-OXTR⁺ neurons respond across the experimental days before and after induction of the social trauma (SE, Ext, Rec) and specifically during the different conditions (ns 1 – 4 and s 1 – 14), the neuronal activity under each condition was explicitly compared with the activity during the breaks, recorded before and after each condition, which served as a baseline. Therefore ΔF/F represents the change of a cell´s fluorescence normalized to the mean fluorescence across the break interval

The animals showed similar investigation of the non-social stimulus before (ns1) and after (ns3) acquisition, indicating that acquisition had no effect on general explorative behavior (Figure 23, A). Overall activity of $OXTR^+$ neurons was low during non-social stimuli conditions. Furthermore, activity did not change upon interaction with the empty cage, compared to other behaviors, which includes eating, drinking grooming and exploration of the home-cage, neither before (ns1), nor after (ns3) acquisition (Figure 23, B).

During SE animals showed a high social investigation time during the first social exposure, i.e. prior to acquisition (s1). In contrast, after acquisition social exploration was decreased during presentation of the first social stimulus during extinction training (s1 vs s3, p= 0.002), indicating a successful induction of social fear in all animals. This could be reversed by extinction training, as the animals showed again increased social interaction during presentation of the last social stimulus (s3 vs s8, p= 0.046) and did not differ anymore from contact levels found before acquisition (Figure 23, C).

Along the three abovementioned conditions, i.e. s1, s3 and s8, the neuronal activity differed during social contact behavior compared to other behaviors displayed (s1: $p = 0.004$, s3: $p = 0.012$, s8: $p = 0.050$), suggesting a specific response of $OXTR^+$ neurons upon social interaction (Figure 23, D). Direct comparison of the activity during social interaction revealed an increase of activity after acquisition (s1 vs s3: $p = 0.032$), which decreased after successful extinction training (s3 vs s8: $p < 0.001$). These results suggest that LSc-$OXTR^+$ neurons are modulated in an inverse manner compared to social interaction behavior (Figure 23, E).

Interestingly, detailed dissection of the behavioral raw data, revealed a subset of animals that successfully overcame the induced social fear during extinction training (for assignment of the groups see 2.9.3), as indicated by decreased social interaction in the beginning (s1 vs s3: $p = 0.016$) but increased contact during the end of extinction training (s1 vs s8: $p = 0.001$) which did no longer differ from levels found during SE (Figure 23, F). Those animals are referred to as Fast Extinction Animals (FEA, n = 5). These animals showed altered neuronal activity throughout the tree conditions compared to other behaviors as described above (s1: $p = 0.018$, s3: $p = 0.053$, s8: = $p = 0.001$, Figure 23, G), and also the direct comparison of the activity during social interaction revealed an increase of activity after acquisition (s1 vs s3: $p = 1.929e\text{-}2$), which decreased after successful extinction training (s3 vs s8: $p = 1.348e\text{-}5$, Figure 23, H).

Conversely another subset of animals was not able to extinguish prior induced social fear, as indicated by decreased social interaction in the beginning of extinction training (s1 vs s3: $p < 0.001$) which remained low until the last presentation of a social stimulus (s1 vs s8: $p < 0.001$, Figure 23,

I). Those animals are referred to as Slow Extinction Animals (SEA, n = 4). Within this group of animals, the activity during the different conditions did no longer differ compared to other behaviors, and also a direct comparison between the activity during social contact behavior did not differ from each other (Figure 23, J, K).

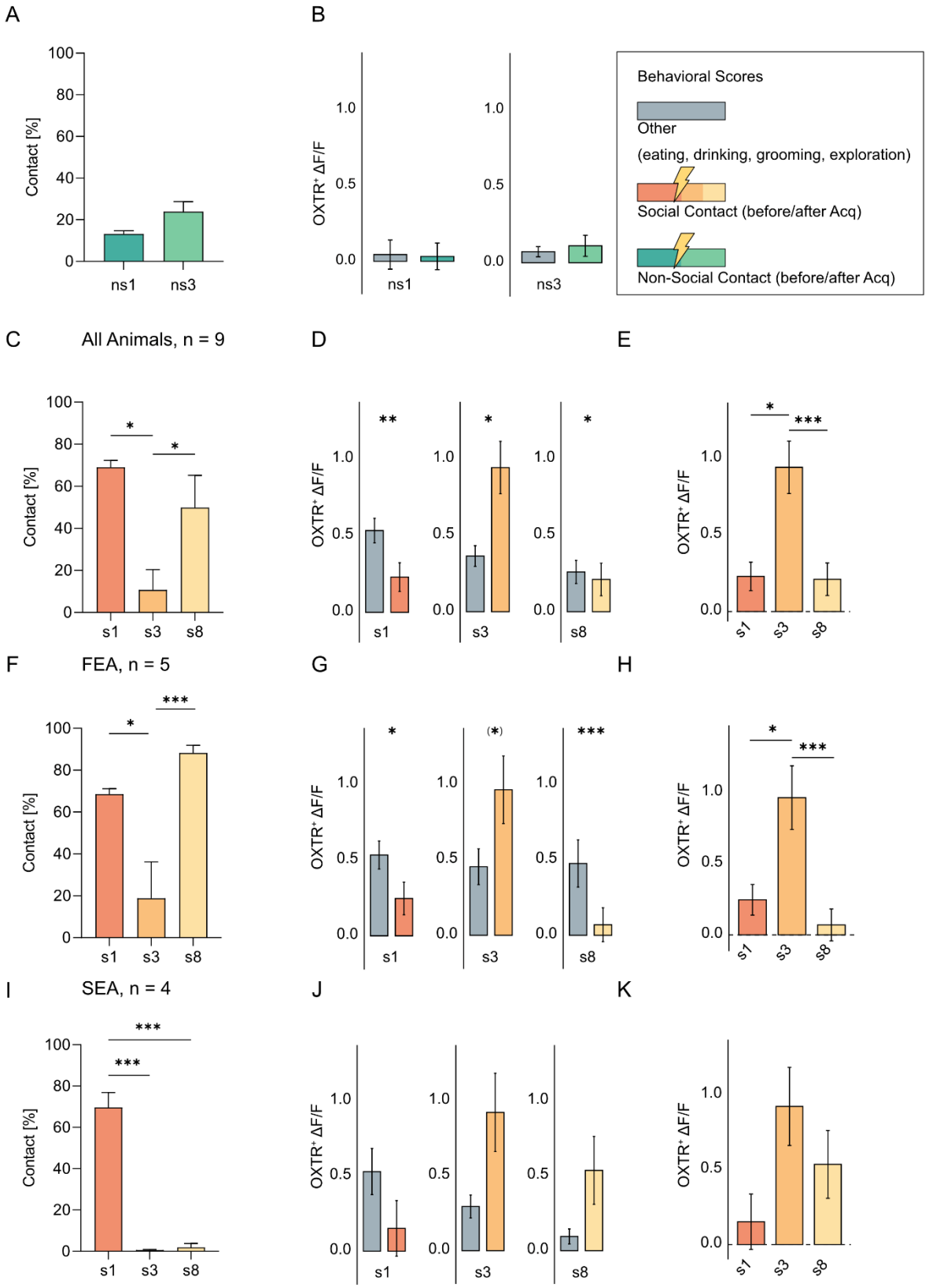

Figure 23: Activity of oxytocin receptor expressing (OXTR⁺) neurons in the caudal part of the lateral septum (LS) before and after acquisition of social fear. ns = non-social stimulus presentation, s = social stimulus presentation, numbers refers to different conditions within the adapted social fear conditioning (aSFC) paradigm. A) Contact level of all animals during presentation of the non-social stimuli. Continued on next page

*B) Behavior specific elicited Ca^{2+} signal during ns condition. C) Contact level of all animals during presentation of three social stimuli in all animals. D) Behavior specific elicited Ca^{2+} signal during s condition. E) Comparison of Ca^{2+} signal during in different social stimuli conditions. F) Contact level of all animals during presentation of three social stimuli in fast extinction animals (FEA). G) Behavior specific elicited Ca^{2+} signal during s condition. H) Comparison of Ca^{2+} signal during in different social stimuli conditions. I) Contact level of all animals during presentation of three social stimuli in slow extinction animals (SEA). J) Behavior specific elicited Ca^{2+} signal during s condition. K) Comparison of Ca^{2+} signal during different social stimuli conditions. Data represents mean ± SEM; (*) p ≤ 0.07, * p ≤ 0.05, ** p ≤ 0.01, *** p ≤ 0.001. For detailed statistics see Table 15*

Non-social interaction		
Behavior	T-test	Figure 25, A
Contact	$T_{9.6}$ = -2.124	P = 0.061
ΔF/F	Wilcoxon Rank test	Figure, B
ns1	W = 2647	P = 0.947
ns3	W = 4944	P = 0.661
Social interaction – all animals		
Behavior	One-way ANOVA	Figure 25, C
Contact	$F_{2,24}$ = 7.830	P = 0.002
ΔF/F	Wilcoxon Rank test	Figure, D
s1	W = 1045	P = 0.004
s3	W = 3240	P = 0.012
s8	W = 4119	P = 0.051
ΔF/F	Kruskal-Wallis	Figure, E
Stage	$X^2(2)$ = 15.65	P = 0.000401
Social interaction - FEA		
Behavior	One-way ANOVA	Figure 25, F
Contact	$F_{2,12}$ = 12.090	P = 0.001
ΔF/F	Wilcoxon Rank test	Figure, G
s1	W = 687	P = 0.018
s3	W = 659	P = 0.054
s8	W = 1470	P = 0.001
ΔF/F	Kruskal-Wallis	Figure 25, H
Stage	$X^2(2)$ = 21.09	P < 0.0001
Social interaction - SEA		
Behavior	One-way ANOVA	Figure 25, I

Contact	$F_{2,9}$ = 82.748	P < 0.001
ΔF/F	Wilcoxon Rank test	Figure 25, J
s1	W = 37	P = 0.128
s3	W = 1007	P = 0.176
s8	W = 508	P = 0.309
ΔF/F	Kruskal-Wallis	Figure 25, K
Stage	$X^2(2)$ = 0.88	P = 0.640

Table 15: Statistics – Ca^{2+}- Imaging in Oxytocin receptor expressing neurons in the caudal part of the lateral septum (LSc-$OXTR^+$) neurons before and after acquisition of social fear. Factor contact represents ns1 vs ns3, or s1 vs s3 vs s8 behavioral effects accordingly. Factor ns1/ns3, or s1/s3/s8 represents fluorescent changes of $OXTR^+$ neurons during other behavior (eating, drinking, grooming exploration) vs social contact/non-social contact. Factor Stage represents fluorescent changes of $OXTR^+$ neurons during social contact s1 vs s3 vs s8.

In support with the statement above, visualization of the stimulus investigation time throughout the whole aSFC paradigm, shows a continuous increase in social investigation during extinction training and a stable formation of an extinction memory (s3-s8), as indicated by high social investigation levels during recall (s9-s14, Figure 24, A). On the other side, the calcium signal during the recorded conditions throughout extinction training and recall decreases over time (Figure 24, B). These results indicate an opposite relationship of the activity of LSc-$OXTR^+$ neurons and extinction success.

More detailed investigation shows that this pattern is driven by the FEA, which show a fast eradication of social fear on a behavioral level (s3-s8, Figure 24, C) and corresponds to a fast decrease in neuronal activity over the recorded conditions throughout extinction training and recall (Figure 24, D).

On the other side, SEA exhibited increased social interaction just from the second social stimulus during recall on (s10-s14, Figure 24, E). In line with the general observation, that the activity of LSc-$OXTR^+$ neurons decreased with increased social interaction, the corresponding calcium signal throughout recorded conditions during extinction training and recall declines less and shows a higher variation (Figure 24, D).

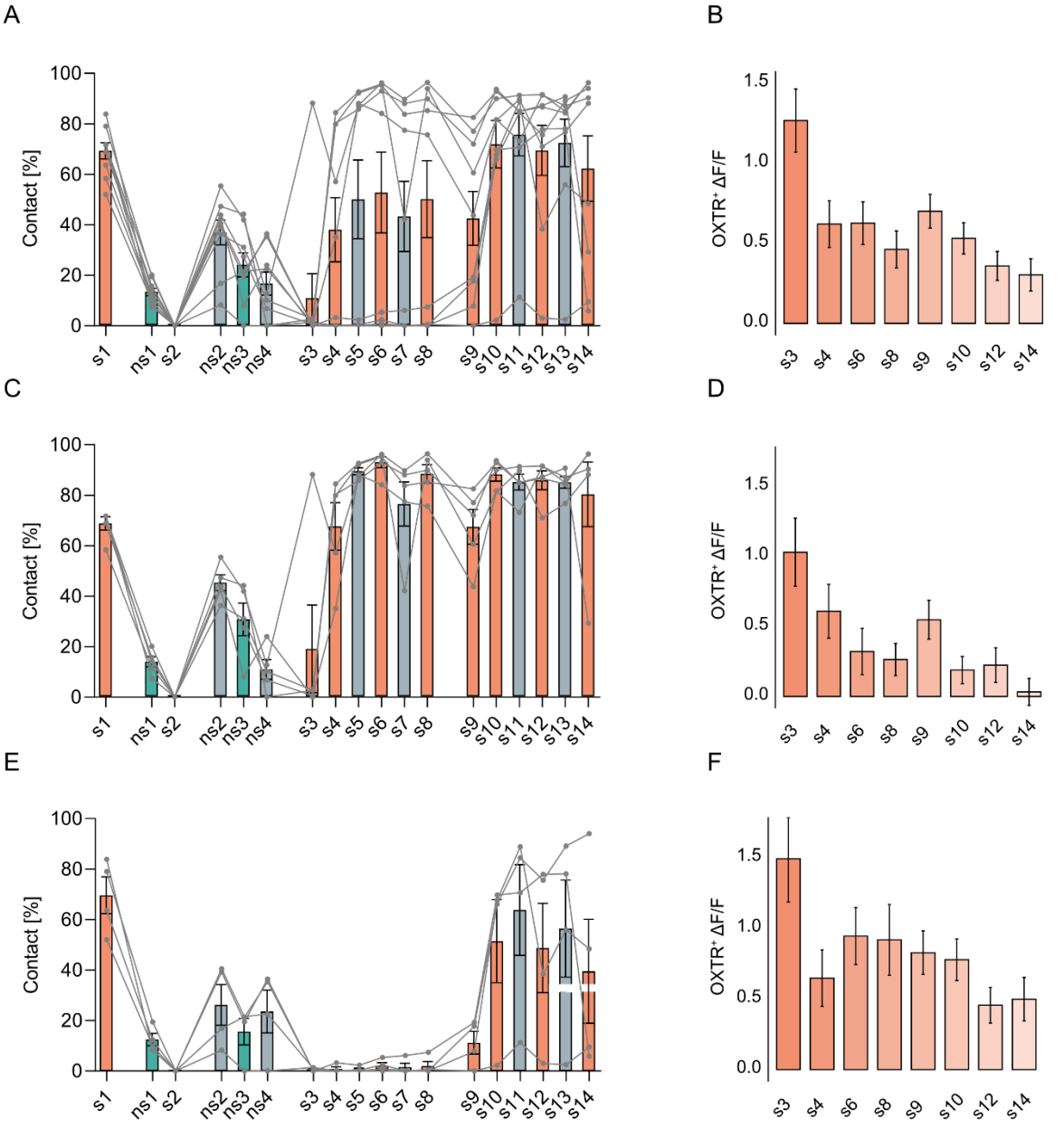

Figure 24: Contact behavior and Ca^{2+} signal of oxytocin receptor expressing ($OXTR^+$) neurons in the caudal part of the lateral septum (LSc) throughout the adapted social fear conditioning (aSFC) paradigm. A) Contact levels of all animals throughout the aSFC paradigm. Colored bars indicate recorded events, green = non-social stimuli, orange = social stimuli. B) Corresponding Ca^{2+} signal throughout extinction and recall of all animals. C) Contact levels of fast extinction animals (FEA) throughout the aSFC paradigm. D) Corresponding Ca^{2+} signal throughout extinction and recall of FEA. E) Contact levels of slow extinction animals (SEA) throughout the aSFC paradigm. F) Corresponding Ca^{2+} signal throughout extinction and recall of SEA.

We proceeded to assess the percentage of modulated LSc-$OXTR^+$ neurons related to contact behavior using a linear model (see 2.4.4). To achieve this, distinct sub-behaviors were defined: "during" (contact), "before" (three seconds preceding contact), and "after" (three seconds

following contact). Additionally, we analyzed the proportions under different conditions, specifically SE, Ext, and Rec, separately. This method allowed us to explore potential differences in activity before and after the acquisition of social fear, as well as after successful extinction of induced social fear. Neurons exhibiting increased activity were classified as excited, those with decreased activity as inhibited, and those with unchanged activity as non-responsive.

During SE, a relatively small proportion of neurons displayed modulation. Specifically, 22.2% were excited and 14.1% were inhibited before direct social contact occurred. This pattern shifted upon making social contact, with nearly half of the neurons (47.5%) being inhibited and a smaller percentage (12.1%) becoming excited. Following the contact event, the modulation reversed, evident by 42.4% of neurons being excited and 14.1% being inhibited (Figure 25, A).

In the context of extinction training, 30.2% of neurons were activated, whereas 23.6% were inhibited before social contact. During contact, approximately half of the neurons (51.9%) were inhibited, while 19.8% showed excitement. After the contact, a majority of cells (57.5%) were once again activated, with 20.8% being inhibited (Figure 25, B).

Upon successful extinction of social fear, specifically during recall, 33.3% of neurons were activated and 21.4% were inhibited before social contact. During contact, over half of the neurons (59.8%) were inhibited, while a smaller fraction exhibited excitement (23.1%). Post-contact, 51.3% of neurons were inhibited, contrasting with only 11.1% being activated (Figure 25, C).

Interestingly, the modulation of responsive neurons displayed a consistent pattern across diverse experimental conditions, encompassing SE, extinction, and recall. Notably, LSc-OXTR$^+$ neurons were predominantly inhibited during social contact, transitioning to a strong activation immediately following the contact event.

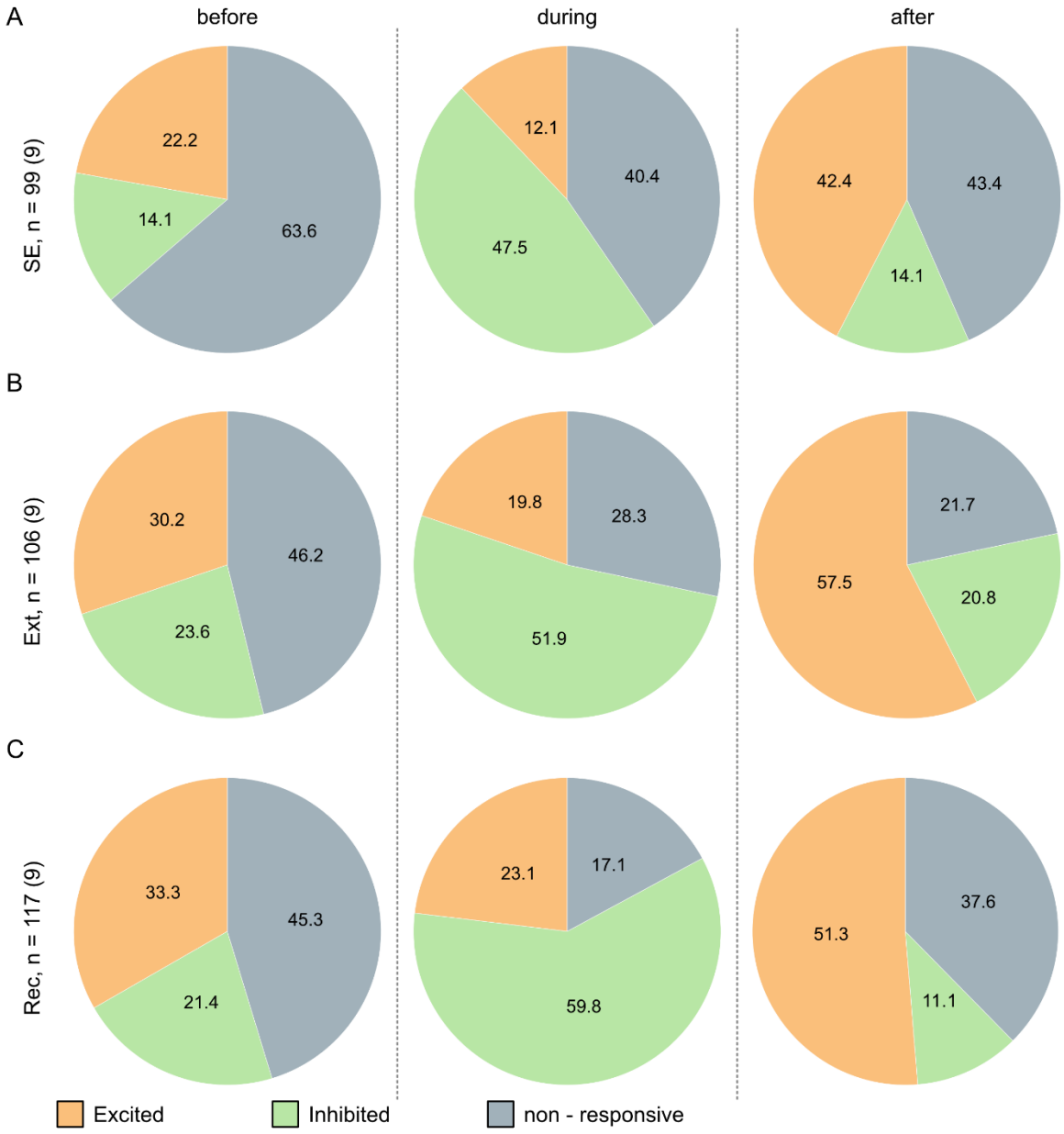

Figure 25: Proportion of modulated oxytocin receptor expressing (OXTR⁺) neurons in the caudal part of the lateral septum (LSc) before, during and after social contact during different experimental stages. Social contact is defined as direct nose contact with the cage of the social stimulus, before is defined as social contact -3 s and after is defined as social contact +3 s. A) Proportion of modulated neurons during social exposition (SE). B) Proportion of modulated neurons during extinction (Ext). C) Proportion of modulated neurons during recall (Rec). n = number of recorded neurons, number in brackets indicates animal number. Orange= exited-, green= inhibited- and gray= non-responsive neurons.

Despite the comprehensive perspective gained from examination of all animals, a separate analysis of the FAE and SEA revealed disparities in the percentage of modulated neurons between that groups. Those differences were particularly evident during the course of extinction training.

Within the FEA subgroup, a modest portion of neurons were modulation during SE. More specifically, 22.5% showed excitation, while 12.1% were inhibited prior to direct social contact. This

dynamic changed upon engaging in social contact, when half of the neurons (50%) were inhibited, and a smaller fraction (15%) excited. Subsequent to the contact event, the modulation pattern shifted, with 35% of neurons becoming excited and 20% being inhibited (Figure 26, A).

In the context of extinction training, 21.7% of neurons became more active, while an equal proportion of 21.7% had reduced activity before social contact. During the contact phase, the majority of neurons (87%) showed a decrease in activity, with a minor subset (6.5%) displaying increased activity. After the contact, a majority of cells demonstrated modulation, but with an equitable distribution, 37% became more active, and 39.1% exhibited decreased activity (Figure 26, B).

Upon the successful elimination of social fear, particularly during the recall phase, 44.9% of neurons displayed heightened activity, while 14.3% showed reduced activity before social contact. During contact, half of the neurons (51%) exhibited decreased activity, and a smaller portion displayed increased activity (22.4%). Following the contact period, 40.8% of neurons exhibited reduced activity, in contrast to 12.2% displayed heightened activity (Figure 26, C).

While the proportions of modulated neural responses prior to and after social contact are quite similar across various conditions (SE, Ext, Rec), a significant decrease in neural activity occurs during social contact in the context of extinction training, wherein animals learn to overcome fear. During recall, following the successful elimination of fear, this decreased activity level reverts to the modulated pattern observed during SE, prior to the induction of social fear. This observed inhibition of LSc-OXTR^{+} neurons could potentially contribute to the rapid extinction success within this specific group of animals.

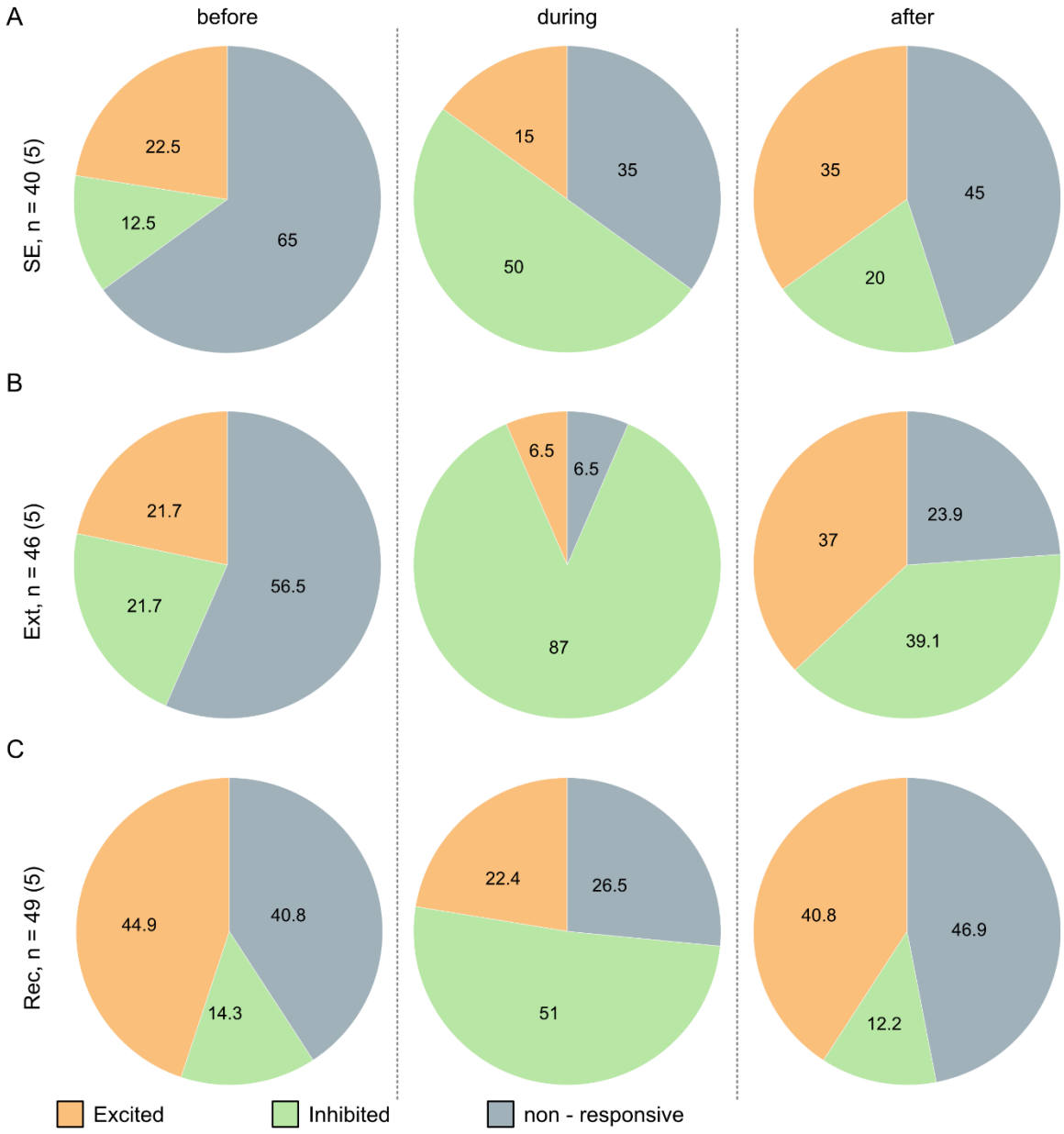

Figure 26: Proportion of modulated oxytocin receptor expressing (OXTR⁺) neurons in the caudal part of the lateral septum (LSc) before, during and after social contact during different experimental stages – fast extinction animals (FEA) only. Social contact is defined as direct nose contact with the cage of the social stimulus, before is defined as social contact -3 s and after is defined as social contact +3 s. A) Proportion of modulated neurons during social exposition (SE). B) Proportion of modulated neurons during extinction (Ext). C) Proportion of modulated neurons during recall (Rec). n = number of recorded neurons, number in brackets indicates animal number. Orange= exited-, green= inhibited- and gray= non-responsive neurons.

Within the SEA subgroup, 22% of the neurons showed heightened activity, and 15.3% were inhibited before direct social contact was established during SE. Upon social contact, nearly half of the neural responses (45.8%) indicated inhibition, while a smaller portion (10.2%) showed heightened activity. Subsequent to the contact event, the modulation pattern reversed, with 47.5%

of neural responses showing heightened activity and 10.2% displaying reduced activity (Figure 27, A).

During extinction training, 36.7% of neurons exhibited heightened activity, while 25% demonstrated reduced activity before social contact. During the contact phase, this proportion remained relatively stable, with 30% of neural responses indicating heightened activity and 25% showing reduced activity. Following the contact period, a majority of cells (73.3%) showed increased activity and only 6.7% displayed reduced activity (Figure 27, B).

During recall, half of the neural responses displayed modulation before contact, with 25% showing heightened activity and 26.5% indicating reduced activity. During contact, over half of the neural responses (66.2%) showed reduced activity, while 23.5% exhibited heightened activity. After the contact event, 58.8% of neural responses were heightened, contrasting with only 10.3% showing reduced activity (Figure 27, C).

Notably, in contrast to the FEA group, SEA animals showed substantial inhibition of LSc-OXTR$^+$ neurons upon social contact exclusively during recall. For the SEA subgroup, this condition coincided with achievement of successful social fear eradication, further reinforcing the notion that inhibition of LSc-OXTR$^+$ neurons, contributes to the extinction success. Additionally, unlike the FEA group, these animals showed a larger proportion of excited neural responses following the contact event across all conditions (SE, Ext, Rec), with the highest activation observed after the acquisition of social fear, specifically during extinction and recall. These findings, suggest, that variations in the modulation of LSc-OXTR$^+$ neural responses following a socially traumatic event play a pivotal role in an animal´s capacity to conquer social fear. Moreover, the discrepancies in modulation of LSc-OXTR$^+$ neurons found in the two subgroups (SEA and FEA) serve as a driver for the different levels of extinction success.

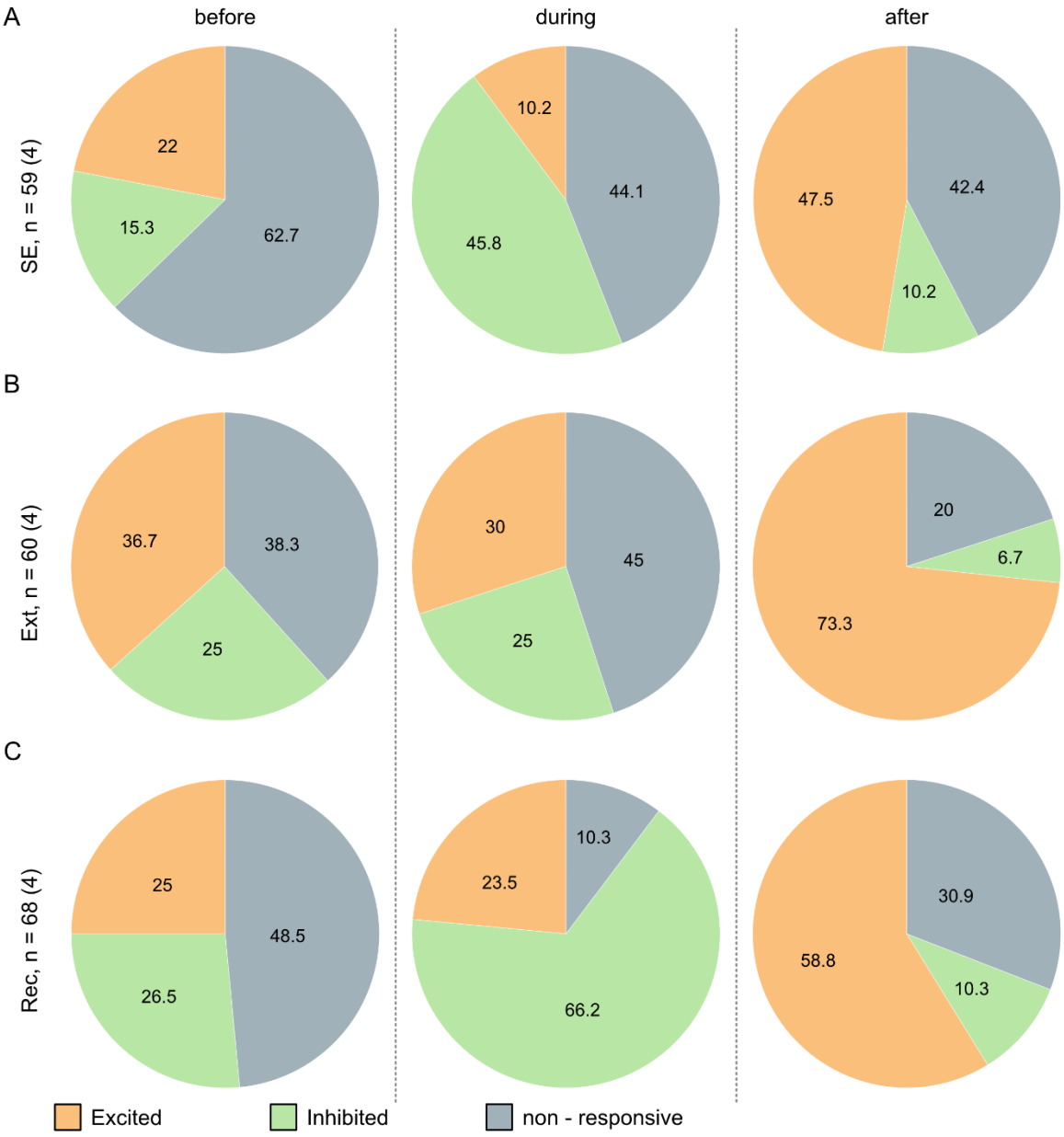

Figure 27: Proportion of modulated oxytocin receptor expressing (OXTR⁺) neurons in the caudal part of the lateral septum (LSc) before, during and after social contact during different experimental stages – slow extinction animals (SEA) only. Social contact is defined as direct nose contact with the cage of the social stimulus, before is defined as social contact -3 s and after is defined as social contact +3 s. A) Proportion of modulated neurons during social exposition (SE). B) Proportion of modulated neurons during extinction (Ext). C) Proportion of modulated neurons during recall (Rec). n = number of recorded neurons, number in brackets indicates animal number. Orange= exited-, green= inhibited- and gray= non-responsive neurons.

4 DISCUSSION

To date, exposure therapy remains the most effective therapeutic option for individuals with SAD. Nevertheless, the mechanisms underlying the gradual extinction of social fear and avoidance are not well understood. Identifying the neuronal mechanisms and brain regions involved in the extinction of social fear could pave the way for new strategies to complement exposure therapy for SAD patients. One neurotransmitter system that has been shown to enhance social fear extinction in mice is the OXT-system. Through binding to the corresponding receptor in the Lateral Septum (LS), synthetic OXT infusion has been observed to eliminate social fear expression in male mice. However, due to the complexity of brain signal processing, the effects of OXT administration on social fear extinction require a more detailed characterization. Given the potential existence of subregion specific projections and functions within the LS, it is crucial to identify the spatial distribution and resulting cellular consequences of OXTR-coupled signaling, which may lead to diverse downstream effects. Furthermore, understanding the exact temporal involvement of OXT administration in behaviors like social fear extinction is essential. Utilizing OXTR autoradiography, an increased OXTR binding in the LSc compared to the LSr was observed. Subsequent RNAscope analysis indicated that approximately 21% of LS cells express OXTR, with an increased OXTR mRNA expression in the intermediate part along the dorsal-ventral axis of the LS. Based on these findings, subsequent experiments focused on the LSc, where the highest OXTR binding was observed. Anterograde tracing techniques revealed that $OXTR^+$ neurons in the LSc project downstream to the Mhb, a region associated with decision-making and modulation of the reward system. To investigate the impact of OXT signaling specifically in the LSc on social fear extinction, synthetic OXT was administered prior to social fear extinction training. Additionally, OXTR Gi agonist atosiban and OXTR Gq agonist carbetocin were infused in the LSc to determine the downstream cellular signaling pathway. The results demonstrated that OXT administration and atosiban led to a facilitation of social fear extinction, suggesting that the effect is mediated via the OXTR-Gi coupled signaling pathway, lowering the excitability of these cells. The pharmacological findings led me speculate, that the timing of activation of $OXTR^+$ neurons in the LSc may be crucial for a successful and robust extinction of social fear. Advances in technology, particularly *in vivo* Ca^{2+} imaging combined with an OXTR-Cre mouse line, allowed tracking changes in the activity of LSc-$OXTR^+$ neurons during social interaction. These neurons were found to be specifically activated during social interaction and exhibited increased activation after experiencing a socially traumatic event compared to pre-traumatic social interaction. Additionally, differences in the modulation of LSc-$OXTR^+$ neurons,

noted in mice with varying degrees of extinction success, particularly in the context of social interactions, might contribute to the effectiveness of individual therapy outcomes.

4.1 Characterization of OXTR$^+$ Cells in the LS

In this study, I characterized the precise distribution pattern of OXTR binding along the rostral-caudal axis of the LS, as well as subregion-specific OXTR mRNA and the downstream connectivity of OXTR$^+$ neurons in the LSc. The results revealed that approximately a fifth of cells in the LS expressed OXTR mRNA (Figure 13, B). Interestingly, while OXTR binding increased towards the LSc (Figure 12), no significant differences were observed in the total mRNA transcript number or the percentage of OXTR$^+$ cells along the rostral-caudal axis (Figure 14).

Using RNAscope I could further reveal that most of the OXTR$^+$ cells throughout the LS express approximately 3-9 OXTR mRNA transcripts/cell, the proportion of very high expressing cells (20-60 dots/cell) turned out higher in the LSc (Figure 14), which might explain the increased OXTR binding in LSc found with OXTR autoradiography. However, it is important to note that the amount of mRNA does not necessarily correlate with the amount of the respective proteins. Mechanisms acting on mRNA stability or attenuation of the translation influence the turnover rate, as well as the degradation or internalization cycle of certain proteins (Cohen et al., 2013). Also mechanisms on protein level might influence the observed increase of OXTR binding towards the LSc, for example the OXTR can occur in the cell membrane in different conformations and shows different affinity for OXT as monomer or dimer (Busnelli and Chini, 2018). These regulatory mechanisms allow cells to adapt to their environment and maintain homeostasis and all of those factors influence each other in a complex and still undefined manner. The extracellular environment, particularly the presence of glia, can have a potent influence on protein turnover. For instance, glial cells either speed up or slow down the turnover rate of neuronal protein (Dörrbaum et al., 2018). Interestingly, Laura Boi (PhD student from the Neumann lab) showed, that there is a significant increase of Astrocyte density towards the LSc (unpublished data), which could correlate with the increased OXTR protein level.

The mechanisms mentioned above could account for the observed disparity between OXTR mRNA and OXTR binding along the rostral-caudal axis of the LS. However, there may also be a functional explanation for the heightened OXTR binding in the LSc. For instance, increased neuronal activity in the LSc could result in an elevated turnover of OXTR proteins. Previous studies have demonstrated that heightened activity can alter the turnover rates of various proteins in cortical neurons, thereby preparing the neurons for new functional roles (Ehlers, 2003). Another possibility is, that higher turnover of OXTR in the LSc could be an overcompensation to capture as much OXT

as possible. Interestingly another study showed, that OXT neurons from the PVN and SON mainly project to the rostral and intermediate part of the LS (Liao et al., 2020). Similar compensatory mechanisms have been observed in other systems, such as the increased expression of D2/D3 receptors in the striatum upon decreased dopamine levels in the same region (Stokholm et al., 2021).

Previous studies have frequently concentrated on either the dorsal or ventral subdivisions of the LS. For instance, the dorsal LS inhibits the ventral LS, playing a role in male aggression (Leroy et al., 2018), or SSt expressing neurons in the dorsal LS are linked to food-seeking behavior (Carus-Cadavieco et al., 2017). Conversely, the ventral LSr is implicated in social dysfunctions induced by early-life stress (Shin et al., 2018). While these studies highlight functional distinctions among LS subregions, they also underscore diverse roles of neurons with specific chemical compositions. The heterogeneity in the distribution of $OXTR^+$ cells in the LS emphazises potential subregion-dependent functional differences among $OXTR^+$ cells within the LS as well.

Another important question to consider is what alterations occur in downstream signaling, specifically after the binding of OXT to its respective receptor in the LS. As previously mentioned, the LS is predominantly composed of GABAergic neurons (Zhao et al., 2013). Certain GABAergic neurons within the LS express SSt and Nts (Köhler and Eriksson, 1984). SST and Nts signaling is involved in regulating various physiological and behavioral responses, including the modulation of social interaction and fear responses (Besnard et al., 2019; Li et al., 2023). Interestingly, I was able to identify that only a minority of $OXTR^+$ cells (about 40%) co-localize with SSt and Nts (Figure 13). While this finding does not rule out the possibility of OXTR being expressed on GABAergic neurons in the LS, it does raise questions about the downstream signal integration upon ligand binding. Understanding how OXT signaling further influences cellular mechanisms and downstream signaling is crucial to unravel the complex mechanisms underlying the effects of OXT in the LS. Further investigations are needed to elucidate the specific pathways and processes that occur after OXT binds to its receptor in the LS and how these interactions contribute to the regulation of social behaviors.

4.1.1 Downstream Target of $OXTR^+$ Neurons in the LSc

To further investigate the connectivity of OXTR neurons in the LSc, I utilized a transgenic mouse line expressing Cre specifically in $OXTR^+$ cells, along with a Cre-dependent recombinant virus expressing a synaptophysin-mCherry fusion protein in the axon terminals. This approach allowed me to label

the downstream projection sites of OXTR$^+$ neurons in the LSc. Brain-wide microscopy revealed sparse and distinct projection sites of OXTR$^+$ neurons in the LSc. Notably, these projection sites included the medial habenula (MHb), the ventral diagonal band of Broca (VDB), and the hippocampal CA2/3 region, with the highest intensity observed in the MHb (Figure 15).

The habenula is a phylogenetically old brain region and present in all vertebrate species and can be divided in into the MHb and lateral habenula (LHb) (Okamoto et al., 2012). While the LHb in zebrafish has received some attention in previous studies, the MHb has been relatively neglected so far (Viswanath et al., 2013). Nevertheless, research has shown that the habenula receives input from limbic systems, including the septal area, and communicates with the ventral tegmental area (VTA) and the raphe nuclei downstream, suggesting a modulatory role in the dopamine and serotonin systems (Herkenham and Nauta, 1977). Based on gene expression, it is believed, that the LHb and MHb serve different functions (Andres et al., 1999). However, due to their small size and high proximity, it is challenging to target one subdivision exclusively. Nevertheless, a sparse number of studies revealed an involvement of the MHb in experience dependent fear response via lesioning of that region in zebrafish (Agetsuma et al., 2010; Mathuru and Jesuthasan, 2013). Another study using selective postnatal ablation of MHb cells in transgenic mice showed deficits in cognition-dependent executive function (Kobayashi et al., 2013). Based on this finding it is speculated that the habenula plays a role in value-based decision-making by modulating dopamine and serotonin neurons downstream.

For the first time, my studies demonstrate that OXTR$^+$ neurons in the LSc project specifically to the MHb. Nevertheless, it is crucial to highlight that, although this projection was observed in multiple animals, viral spreading from the injection site to the rostral part of the LS was noted in 3 out of 4 animals. Therefore, it cannot be ruled out that OXTR$^+$ neurons in the LSr may also project to the MHb. Consequently, these observations should be interpreted with caution. Nonetheless, given the understanding of the functions associated with the LS and the MHb and the OXT system, it is tempting to speculate that the specific pathway of OXTR$^+$ LSc – MHb is involved in the processing of emotional states and the generation of specific behaviors.

4.2 Functional Involvement of OXTR Signaling in the LS in Social Fear Extinction

Regions that produce OXT have been found to project to the LS. Specifically in the intermediate part of the LSr fibers where detected (Liao et al., 2020). At least in lactating females mice this

projections predominantly originate from the SON (Menon et al., 2018). Additionally, the expression of OXTR in the septal nuclei has been described before (Gimpl and Fahrenholz, 2001; Russell and Brunton, 2009). Particularly interesting for this study was the observation, that OXT is released into the LS upon social interaction during extinction training in the SFC in SFC^-, but not in SFC^+ mice. Moreover, infusion of OXT in the LSd led to increased social investigation levels, similar to those found in unconditioned animals. Notably the coordinates for microdialysates as well as OXT infusion was set on Bregma: −0.3 mm, ±0.5 mm, −1.6 mm in this study (Zoicas et al., 2014). Since previous studies revealed, that the expression level of OXTR is a critical factor determining responses to OXT in the brain and directly influences behavioral responses and social traits (King et al., 2016; Rilling and Young, 2014), I aimed to define the effects of OXTR binding more precisely, by infusing OXT in the intermediate part of the LSc, targeting the subregion with the highest OXTR density within the LS. The results indicated that SFC^+/OXT treated animals exhibited significantly more social interaction in the beginning of extinction compared to SFC^-/Veh, demonstrating an extinction facilitating effect of OXT (Figure 16). However, it is worth mentioning that the SFC^+/OXT animals received fewer foot shocks during acquisition. Typically, animals receive 1-3 foot shocks to establish complete social avoidance, with subsequent grouping ensuring an equal distribution of foot shock between treatment and veh groups. However, rare instances may disrupt this even distribution, such as the exclusion of animals due to issues like improper cannula placement or other abnormalities, which occurred in this particular case.

Since the above discussed experiment indicates an involvement of OXT in the LSc on social fear extinction, I next aimed to clarify the molecular pathway that follows OXT binding and mediates this effect. As mentioned earlier, the OXTR is a GPCR, and the signaling cascade triggered by ligand binding depends on the engaged Gα subunit of the heterotrimeric G protein complex. The OXTR can couple to Gαq and Gαi complexes in a promiscuous manner and is capable of mediating either synergistic or opposite effects depending on the context. Two factors control the response upon OXT binding. Firstly, the local concentration of OXT plays a role, for instance Gαi-coupled complexes are activated upon high OXT concentrations and Gαq-coupled complexes are activated on lower concentrations. Secondly, the expression level of individual G protein isoforms plays a role, which can vary in different cell types and regions (Busnelli and Chini, 2018). The complete downstream effects of Gαi and Gαq signaling are not fully understood yet and most of the knowledge derives from studies in non-neuronal cells. However, some general key aspects of their functioning have been clarified. The Gαq isoform is ubiquitously expressed and, upon activation, stimulates the PLC pathway, leading to the release of calcium from internal stores. carbetocin is a functionally selective analogue capable of inducing specifically OXTR/Gαq protein coupling. Interestingly icv

administration of carbetocin has already been associated with anxiolytic effects in the EPM (Mak et al., 2012). In contrast to the Gαq isoform, the Gαi isoform is particularly highly expressed in the brain. Gαi inhibits adenylate cyclase activity and directly regulates ion channel activity, thereby closing Ca^{2+} channels. The selective agonist atosiban promotes OXTR/Gαi coupling and has been shown to inhibit cell proliferation and exhibits pro-inflammatory effects in in vitro cell cultures (Busnelli et al., 2012).

Taken together, administration of synthetic OXT, which can activate OXTR regardless to which G protein they are coupled, in the LS had an extinction facilitating effect. Upon administration of Atosiban in the LSc, conditioned animals exhibited increased social investigation during the presentation of the first stimulus during extinction compared to SFC^+/Veh treated mice. Interestingly, during recall, SFC^+/Atosiban treated animals no longer differed from unconditioned animals, indicating successful extinction memory formation, while SFC^+/Veh animals showed significantly reduced social interaction compared to that group (Figure 17). On the other hand, Carbetocin injection had no effect on social fear extinction compared to SFC^+/Veh treated animals at all (Figure 18). It should be noted that by chance atosiban-treated animals received fewer foot shocks during acquisition. Nevertheless, these results suggest that OXT binding in the LSc has an extinction-facilitating effect and stabilizes extinction memory via Gαi-coupled signaling cascades and this could be either due to an increased local concentration of OXT during extinction training, or specific accumulation of OXTR/Gαi subtypes in the LSc.

4.2.1 Biological Variations in Experimental Animals

In 2014, Zoicas et al. demonstrated the reversal of social fear expression within the SFC paradigm through intracerebroventricular (icv) and LSd administration of OXT (Zoicas et al., 2014). However, given the absence of such striking effects in the findings discussed above, I conducted a replication of the original experiments to validate the previously published impact of OXT on the extinction of social fear. To determine whether there exists a region-specific influence of OXT, animals were infused across various subregions of the LS. Surprisingly, none of the administered regions revealed any effects of OXT (Figure 20).

Furthermore, icv administration also failed to show any observable effect of OXT on social fear extinction. Moreover, animals from two distinct cohorts were utilized to mitigate any potential cohort-related influences arising from differing handling and breeding conditions. Intriguingly, animals bred at the University of Regensburg exhibited an elevated level of fear, apparent through

the complete inability of both the SFC^+/Veh and SFC^+/OXT groups to effectively overcome social fear during the course of extinction training (Figure 21).

It is worth noting that both of these experiments should be regarded as pilot studies due to the relatively small sample size. Nonetheless, the outcomes have raised compelling questions concerning the reproducibility of animal experiments.

The challenge of reproducibility and the inconsistency of experimental results, even within or between laboratories, are major issues of animal research. Strategies to address this concern are constantly under discussion (Voelkl et al., 2020). The outcomes of experiments are influenced by a combination of both internal factors, such as genotype and individual experiences, and external factors, including the experimental environment and conditions. The role of discrete experimental factors was, for example, investigated in a study where a computational approach was used to assess variability in pain responses in rats based on a previous experiment. This investigation revealed that factors such as time of day, test order, and room humidity significantly contributed to the behavioral variation (Chesler et al., 2002). Often overlooked hidden variables, like husbandry practices and environmental cycles, can exert substantial influence on experimental outcomes (Butler-Struben et al., 2022). The impact of seemingly minor changes can also be profound. For instance, transitioning to a different cage type was found to alter the effectiveness of maternal immune activation in inducing deficits in working memory and social interaction (Mueller et al. 2018). The "litter effect" is another noteworthy phenomenon, where animals from the same litter exhibit different behaviors compared to those from different litters. This effect is frequently disregarded, yet can significantly impact research outcomes (Lazic and Essioux, 2013). Characteristics of the human experimenter also introduces variability. Studies have demonstrated that the sex of the human experimenter influences mouse behavior, with increased stress susceptibility observed when handled by male experimenters (Georgiou et al., 2022). Additionally, previous research indicated that male experimenters result in higher corticosterone levels and increased anxiety-like behavior in mice (Sorge et al., 2014). Even when focusing on a single strain, results may not generalize to other strains. Extensive testing of various mouse strains revealed substantial within-strain variability in behavior under highly standardized conditions over time, highlighting the intricate interplay of genetic and environmental factors (Loos et al., 2015). The variability of phenotypes within a population of organisms reflects the combined effects of genotype and lifetime environmental response, contributing to the challenge of reproducibility in animal research.

While the current best practice involves stringent standardization of animals and their environment (Principles of laboratory animal science, 2003), this approach may reduce environmental noise but falls short in accounting for biological variation. Treatment effects often vary due to a multitude of genetic and environmental factors, which can be highly specific and unexpected, thus challenging to control. One approach to account for that is the systematic heterogenization of study samples, and conditions can be employed to artificially introduce diversity and enhance the robustness of experimental findings. Taken together, the abovementioned studies might explain the lack of effects found in the replicated experiments. However, it also becomes very clear that phenotypic variations are a factor that is very hard to determine and test for. However, it is a factor that should always carefully be considered when interpreting behavioral results.

4.3 Temporal Characterization of OXTR$^+$ Neurons in the LSc

In this experimental setup usage ot the transgenic OXTR-Cre mouse line in combination with a Cre-dependent recombinant virus expressing a GECI and delivered into the LSc, enabled specific measurement of the activity of OXTR$^+$ neurons in the LS throughout the aSFC paradigm. Intracellular calcium signaling plays a pivotal role in a diverse array of cellular processes, and neuronal activity triggers a brief influx of calcium (Roth and Ding, 2020). Thus, calcium serves as a more indirect measure of neuronal activity but acts as a reliable proxy for such measurements. However, The use of GECIs, such as GCaMP, offers a distinct advantage in providing a continuous record of neuronal activity over an extended period, even spanning several days.

Having said, that this technique was performed for the first time in our lab, we were able to perform surgery in all planned nine experimental animals with an optimal lens placement and viral transfection. In contrast to surgical approaches regularly conducted, the AAV-DJ-EF1a-DIO-GCaMP6m requires 6 weeks minimum for optimal transfection. Since animals can not group housed after surgery, to secured maintenance of the implant, this experimental setup caused a longer isolation period that normally conducted prior to experimental start. However, the long isolation period did not interfere with general social interest as seen by the high social exploratory activity during SE. Furthermore, the surgery did not affect animals, as they were daily and carefully observed after the surgery and one week prior to experiment daily handled, including microscope attachment in order to habituate them to the procedure and minimize stress for the animal on the experimental days.

4.3.1 Activity of OXTR$^+$ Neurons in the LSc During Exposure to the EPM

Exposure to the EPM typically generates a natural conflict in the mice, with a tendency to avoid the exposed and potentially dangerous open arms of the maze and favoring the enclosed arms as environment of relative safety. In line with this presumption here we could show, that the animals prefer to remain in the closed arms than venture into the open arms.

Previous studies have already demonstrated an involvement of the LS in the regulation of anxiety-related behavior measured in the EPM. Notably, septal administration of the GABA-A agonist muscimol, but also SSt diminished anxiety-like behavior, thereby increasing the number of OA entries and the time spent in the OA in rats (Trent and Menard, 2010)(Yeung and Treit, 2012). Furthermore, single-unit recording in the LS revealed a heightened neuronal firing rate when rats were exposed to the OA compared to the CA of the maze. The authors concluded, that activation of the LS suppresses fear, enabling animals to confront anxiety-provoking situations (Thomas et al., 2013). While the LS seems to be linked to anxiety-related behavior, the septal OXT system has predominantly been associated with social-related behavior (Menon et al., 2022). The presence of OXTR within the LS has been directly correlated with heightened social investigation in prairie voles (Ophir et al., 2009). Moreover, OXTR signaling has been demonstrated to mediate social memory in both, rats and mice (Horiai et al., 2020; Lukas et al., 2013). Notably, the infusion of OXT into the LS alleviates social fear and recovers social preference in female and male mice (Menon et al., 2018; Zoicas et al., 2014).

Interestingly, employing in vivo calcium imaging technique, we were able to show, that LSc-OXTR$^+$ neurons remain unresponsive both, during CA occupancy as well as OA exploration. Even investigation of the entire OA (fullOA) of the EPM, did not lead to increased activity of LSc-OXTR$^+$ neurons (Figure 22). The observed lack of responsiveness is further underscored by consistently low overall neuronal activity. While the before mentioned studies demonstrate, that the LS certainly plays a role in anxiety related behavior measured in the EPM, the LSc-OXTR$^+$ neurons don't seem to be involved in that context. These findings support the notion that septal OXT signaling is specifically involved in social behavior, with less involvement in general fear processing or risk assessment behavior.

4.3.2 Activity of OXTR$^+$ Neurons in the LSc throughout aSFC

During SE and therefore prior to acquisition of social fear, animals exhibit robust social investigation behaviors, consistent with prior observations of heightened exploratory tendencies towards

conspecifics in rodents (Blanchard et al., 2001; File and Hyde, 1978). The pattern of social behavior observed during social fear acquisition, extinction, and recall aligns with earlier studies (Toth et al., 2012), characterized by fear-induced suppression of social interactions and subsequent restoration of social behavior following repeated social stimulus presentations, akin to the attenuation of conditioned fear responses (Maren et al., 2013)(Figure 23). No discernible LSc-OXTR$^+$ neuronal activity emerges during non-social object exploration, reinforcing the notion of specific neuronal regulation in response to social behaviors. This observation is in line with investigations identifying OXTR-mediated roles in social recognition and processing in rodents (Ferguson et al., 2001; Knobloch et al., 2012). Remarkably, heightened activation of LSc-OXTR$^+$ neurons follows social fear acquisition. This finding parallels discovery in another brain region, where distinct basal AMY neuron populations triggering contextual fear conditioning by a switch of activity in mice, suggesting finely tuned neuronal responsiveness contributes to appropriate behavioral adaptations (Herry et al., 2008). Normalization of neuronal activity during extinction training further supports the role of LSc-OXTR$^+$ neurons in mediating recovery from fear induction. Similar mechanisms have been proposed already (Myers and Davis, 2002) but mostly in other regions and neurotransmitter systems, i.e. increased infralimbic activity was detected in rats using single-unit recording, but is dampened with extinction success (Milad and Quirk, 2002).

Interestingly, detailed behavioral analysis reveals two distinct animal subgroups based on their extinction training responses. This differentiation between Fast Extinction Animals (FEA) and Slow Extinction Animals (SEA) underscores the heterogeneity in coping with social fear and recovery. FEA animals rapidly respond to extinction training, while SEA animals struggle to overcome social fear during training, achieving normal social investigation only during recall (Figure 24). This variability, known as fear extinction learning variability, has been explored in humans and rodents (Milad and Quirk, 2012), highlighting individual differences in neural circuits and learning processes contributing to diverse extinction responses. Notably, while LSc-OXTR$^+$ neuronal activity decreases with heightened social investigation in FEA animals, SEA animals lack such a decrease, suggesting altered neuronal processing contributing to impaired fear extinction (Figure 24). Comparable impairment has been observed in humans, where varying therapeutic responses are often noted (Norrholm and Jovanovic, 2018). A comprehensive analysis of neuronal modulation patterns surrounding contact events uncovers insights into LSc-OXTR$^+$ neuronal dynamics during social fear modulation and interaction. Across all animals, a consistent pattern emerges encompassing pre-acquisition (SE) and post-acquisition (Ext, Rec), indicating specific responses to social stimuli in LSc-OXTR$^+$ neurons (Figure 25). Subgrouping neurons based on calcium traces reveals that approximately 50% of neurons are unmodulated before contact (= contact -3s), with half being

inhibited during contact and half activated after contact (= contact +3s). A similar study on extinction-mediating neurons in the BLA in mice demonstrated, that a specific neuronal subtype is activated during contextual fear extinction and further shows distinct modulation patterns throughout extinction training (Zhang et al., 2020). This supports the idea, that precise context-dependent modulation of specific neuronal subtypes in specific regions, plays an important role in mediating certain behaviors.

Remarkably, FEA animals exhibit substantial inhibition (87%) during social contact in extinction training (Figure 26). This unique signature can be associated with efficient fear extinction and might suggest a potential neuronal mechanism contributing to their rapid fear recovery. Clinical studies using fMRI, show that human individuals with effective fear extinction often display pronounced AMY inhibition in response to fear cues, as induced by mild shock coupled to presentation of a colored square (Phelps et al., 2004). In contrast, SEA animals show increased neuronal activation after contact during extinction training and inhibition during recall, hinting at distinct neural signaling or compensatory mechanisms reinforcing fear extinction (Figure 27). Notably, other studies have highlighted the impact of subtle factors on extinction success (Monfils et al., 2009). For example, a recently published study shows that regulation of the lncRNA Meg3 influences extinction success (Royer et al., 2022).

In conclusion, this study demonstrates that LSc-OXTR$^+$ neurons exhibit context-specific responses, with inhibition upon social interaction and increased activation following social fear acquisition. The distinct response patterns between FEA and SEA animals underscore the intricate neuronal mechanisms driving behavioral adaptations and individual responsiveness.

4.4 Summary

In this thesis, I charcterized a population of LS neurons expressing OXTR, which play a pivotal role in regulating social interaction and the extinction of social fear.

I colocalized and quantified of OXTR$^+$ cells within the LS and its subregions, revealing an approximate proportion of 20%. Notably, I also demonstrated a varied distribution pattern of OXTR at both protein and mRNA levels within the LS, with the highest levels of expression found in the intermediate caudal region. Prior studies have highlighted the predominant composition of GABAergic neurons in the LS (Zhao et al., 2013), alongside the expression of SSt and Nts (Risold and Swanson, 1997). My work, however, shows that septal OXTR$^+$ cells largely do not co-localize with Nts and SSt. Furthermore, existing evidence has associated the septum and the OXT system with

diverse facets of motivated behavior (Menon et al., 2022). Building upon this, I was able to illustrate that septal OXTR$^+$ neurons project to the Mhb, a region that has also been linked to motivated behaviors (Kobayashi et al., 2013). Taken together, the heterogeneous nature of septal OXTR$^+$ cells within the LS implies that distinct populations of these cells are involved in mediating different functions.

Earlier studies have linked OXT signaling in the LS to anxiolysis (Menon et al., 2018; Yoshida et al., 2009) and even the reversal of social fear (Zoicas et al., 2014). Building upon this, I established that OXTR-mediated signaling in the LSc specifically facilitates social fear extinction. Furthermore, treatment with the selective OXTR-Gαi agonist atosiban enhanced social investigation during extinction training and stabilized the formed extinction memory, in contrast to the ineffectiveness of carbetocin. This implies the involvement of OXTR-Gαi, but not OXTR-Gαq- mediated signaling pathways in modulating social investigation. Thus, inhibiting OXTR$^+$ cells in the LSc during extinction training seems to play a restorative role in social functioning.

In order to investigate the activity pattern of LSc-OXTR$^+$ neurons in more detail, we used calcium fluorescence, to observe real-time activity in LSc-OXTR$^+$ neurons during a modified SFC paradigm (aSFC) which includes an additional social interaction period prior to acquisition of social fear and EPM tasks. Intriguingly, these neurons remained unmodulated during exposure to the EPM and object (non-social stimulus) investigation, reaffirming their specificity to social contexts. Further investigation of modulation patterns revealed that these neurons are inhibited during social contact and become more active after contact, suggesting a specific response to social interaction. Overall, LSc-OXTR$^+$ neurons exhibited heightened activity during socially related behavior after acquiring social fear, with activity levels normalizing following successful fear extinction.

Strikingly, segregating animals into two responder groups during SFC unveiled differing responses of LSc-OXTR$^+$ neurons following social fear acquisition. In mice that rapidly overcame fear during social fear extinction, reflected by gradual increase of social interaction which did not differ from the interaction levels found during SE, LSc-OXTR$^+$ neurons showed increased inhibition during contact, while animals with slower fear extinction displayed heightened inhibition during recall, when those animals achieved successful extinction of social fear. This indicates that the activity of OXTR$^+$ neurons in the LSc is associated with individual extinction success, possibly mediated by temporal shifted or disrupted OXT secretion into the LSc.

A noteworthy point is, that the OXTR can promiscuously couple to Gαi and Gαq subunit, resulting in either decreased or increased cellular excitability (Gravati et al., 2010). For instance, the recruitment of these different subunits and therefore distinct cellular pathways is influenced by

different OXT concentrations. While Gαi-coupled complexes are activated upon high OXT concentrations, Gαq-coupled complexes are activated on lower concentrations (Busnelli et al., 2012). Considering the observation, that the LS is mainly composed of GABAergic neurons, a possible scenario could be, that the presence of a social stimulus might stimulates local OXT release and consequently the inhibition of LSc-OXTR^{+} neurons, recruiting the Gαi pathway, followed by disinhibition of downstream targets. A gradual reduction in locally available OXT through reduced local release, diffusion and peptide degradation could shift the response of the neurons towards the Gq pathway, leading to enhanced activation post-social contact. This molecular transition in LSc-OXTR^{+} neurons might mediate normal social interaction (Figure 28).

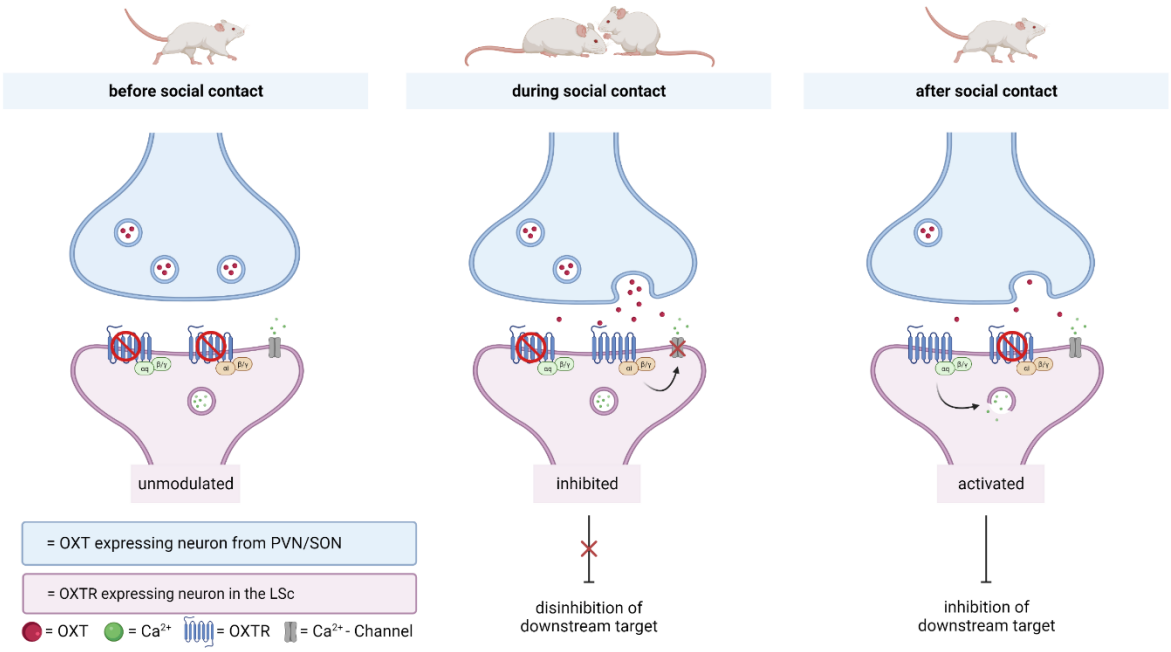

Figure 28: Oxytocin (OXT) signaling in the caudal part of the lateral septum (LSc) implicated in social interaction. Theoretical OXT- oxytocin receptor (OXTR) signaling, indicated on a schematic illustration of the mouse LS before, during and after social contact. Before social contact, no OXT secretion in the synaptic cleft, further leads to majority of neurons being unresponsive. Social contact directly leads to increased OXT secretion from stored presynaptic vesicles, which activates the OXTR-Gαi pathway, which closes calcium ion-channels and leads to decreased excitability of the postsynaptic membrane. After social contact the OXT secretion is reduced, which leads to recruitment of the OXTR-Gαq pathway, leading to secretion of calcium from internal calcium stores and increases excitability of the postsynaptic membrane.

However, the induction of social fear disrupts this signaling cascade, evident from increased LSc-OXTR^{+} activation during presentation of social stimuli post-social trauma, which gradually normalizes with extinction success. In animals quickly overcoming social fear (FEA) exaggerated OXT

release within the LSc upon social contact may trigger substantial neuronal inhibition and consequently, disinhibition of downstream targets such as the Mhb. Conversely, in slow fear extinctions animals (SEA) decreased and delayed OXT release, potentially explains heightened LSc-OXTR$^+$ activation after social contact during extinction training. It is important to consider the possibility, that co-release of other transmitters from LSc-projecting OXT neurons, or other regions projecting to these neurons, recruiting different neurotransmitter systems might be modulated post-social fear induction.

Summing up, my thesis has unraveled the heterogeneous distribution of OXTR$^+$ cells within the LS. I have also illuminated the role of OXT signaling in LSc, specifically in facilitating social fear extinction and consolidating extinction memory through the OXTR-Gαi signaling pathway. Additionally, I have elucidated a specific modulation pattern of LSc-OXTR$^+$ neurons upon social interaction and identified their activity as a marker for individual extinction success. These results shed light on the neuronal regulation of social interaction, as well as the formation of social fear extinction memories. Furthermore, these insights enhance our understanding of individual therapy success.

4.5 Future Directions

The present study has provided valuable insights into the intricate interplay between OXTR$^+$ neurons in the LSc and their role in regulating social behavior and fear extinction. Based on these results, several research avenues for future exploration and experimentation emerge, offering the potential to unravel deeper layers of the neuronal mechanisms underlying social interaction and fear processing.

Comprehensive brain connectivity: To elucidate the broader context of LSc-OXTR$^+$ neuron functions, the utilization of anterograde and retrograde tracing techniques, coupled with light sheet microscopy, can provide a comprehensive mapping of the whole brain connectivity of septal OXTR$^+$ neurons. This approach would offer insights into the specific regions influenced by LSc-OXTR$^+$ projections and region-specific quantification of the primary sources for OXT in the LS, possibly with subregion specific resolution, further unraveling the intricacies of social behavior regulation.

Single-cell RNA sequencing and functional heterogeneity: Recent advancements in single-cell RNA sequencing technology offer a powerful tool to delve deeper into the molecular and functional diversity of OXTR$^+$ neurons within the LSc. By characterizing gene expression profiles of individual neurons, researchers can identify distinct subtypes of LSc-OXTR$^+$ cells, each potentially contributing to different aspects of social behavior and fear extinction. Integrating this information with in vivo

calcium imaging data could uncover specific molecular signatures associated with different modulation patterns, shedding light on the underlying mechanisms governing diverse responses to social stimuli.

Population recording and manipulation: In order to validate the concept of response of LSc-OXTR$^+$ neurons within the aSFC paradigm, population recording could be employed, recording the activity of OXTR$^+$ neurons using acute brain slices. Investigation of the response of LSc-OXTR$^+$ neurons to different doses of OXT, atosiban, and carbetocin, utilizing an OXTR-Cre mouse line with mCherry-labeled cells, could provide insights into the specific activity patterns in response to pharmacological manipulations.

Neurotransmitter interactions and plasticity: Exploring the interactions between OXT and other neurotransmitter systems, such as dopamine and serotonin, could provide a more comprehensive understanding of the complex neural network regulating social behaviors and fear responses. Investigating the plasticity of LSc-OXTR$^+$ neurons in response to chronic social trauma or prolonged exposure to social stimuli could reveal the mechanisms underlying maladaptive responses and potential targets for therapeutic interventions.

Optogenetic and chemogenetic manipulation: One promising direction lies in the application of optogenetics, a cutting-edge technique that enables precise control of neural activity with light stimulation. By targeting specific subpopulations of LSc-OXTR$^+$ neurons, researchers can investigate their functional significance within intricate neural circuits. Optogenetic activation or inhibition of these neurons during social interactions or fear extinction tasks could elucidate the causal relationships between LSc-OXTR$^+$ neuron activity and behavioral outcomes. Moreover, optogenetic approaches can extend to investigating the role of downstream targets, such as the medial habenula, in the context of social behaviors and fear processing. While a chemogenetic approach in this context would be possible as well, one needs to consider the fact that it lacks the temporal specificity of optogenetics.

Clinical applications and precision medicine: Translating the knowledge gained from this study into clinical settings holds promise for developing individualized interventions for social anxiety and related disorders. By profiling LSc-OXTR$^+$ neuron activity in patients and correlating it with treatment outcomes, researchers could establish a basis for precision medicine approaches, tailoring therapeutic strategies to match the neural profiles of individuals.

The current study has set a basis for a multitude of future directions. By the use of state-of-the-art techniques, investigating further the cellular and functional heterogeneity of OXTR$^+$ cells in the LS

offer a multifaceted approach to unraveling the complexities of social interaction and fear processing at the neural level. With further work in this field, the understanding of social behaviors and dysfunctions, as well as individual responses could be increased and contribute to the development of more effective therapeutic strategies.

REFERENCES

1. Acarturk, C., Cuijpers, P., van Straten, A., Graaf, R. de, 2009. Psychological treatment of social anxiety disorder: a meta-analysis. Psychol. Med. 39, 241–254. https://doi.org/10.1017/S0033291708003590.

2. Agetsuma, M., Aizawa, H., Aoki, T., Nakayama, R., Takahoko, M., Goto, M., Sassa, T., Amo, R., Shiraki, T., Kawakami, K., Hosoya, T., Higashijima, S., Okamoto, H., 2010. The habenula is crucial for experience-dependent modification of fear responses in zebrafish. Nat Neurosci 13, 1354–1356. https://doi.org/10.1038/nn.2654.

3. Alfieri, V., Mattera, A., Baldassarre, G., 2022. Neural Circuits Underlying Social Fear in Rodents: An Integrative Computational Model. Frontiers in systems neuroscience 16, 841085. https://doi.org/10.3389/fnsys.2022.841085.

4. Althammer, F., Grinevich, V., 2017. Diversity of oxytocin neurons: beyond magno- and parvocellular cell types? Journal of neuroendocrinology. https://doi.org/10.1111/jne.12549.

5. Anderson, D.J., Adolphs, R., 2014. A framework for studying emotions across species. Cell 157, 187–200. https://doi.org/10.1016/j.cell.2014.03.003.

6. Andres, K.H., Dring, M. von, Veh, R.W., 1999. Subnuclear organization of the rat habenular complexes. Journal of Comparative Neurology 407, 130–150. https://doi.org/10.1002/(SICI)1096-9861(19990428)407:1<130:AID-CNE10>3.0.CO;2-8.

7. Anthony, T.E., Dee, N., Bernard, A., Lerchner, W., Heintz, N., Anderson, D.J., 2014. Control of Stress-Induced Persistent Anxiety by an Extra-Amygdala Septohypothalamic Circuit. Cell 156, 522–536. https://doi.org/10.1016/j.cell.2013.12.040.

8. Association, A.P., 2016. Neurodevelopmental disorders: DSM-5 selections. American Psychiatric Association Publishing, Arlington, VA, 1 online resource.

9. Bale, T.L., Davis, A.M., Auger, A.P., Dorsa, D.M., McCarthy, M.M., 2001. CNS region-specific oxytocin receptor expression: importance in regulation of anxiety and sex behavior. J. Neurosci. 21, 2546–2552. https://doi.org/10.1523/JNEUROSCI.21-07-02546.2001.

10. Bargmann, C.I., Marder, E., 2013. From the connectome to brain function. Nature methods 10, 483–490. https://doi.org/10.1038/nmeth.2451.

11. Barkowski, S., Schwartze, D., Strauss, B., Burlingame, G.M., Barth, J., Rosendahl, J., 2016. Efficacy of group psychotherapy for social anxiety disorder: A meta-analysis of randomized-controlled trials. Journal of anxiety disorders 39, 44–64. https://doi.org/10.1016/j.janxdis.2016.02.005.

12. Belzung, C., Lemoine, M., 2011. Criteria of validity for animal models of psychiatric disorders: focus on anxiety disorders and depression. Biology of mood & anxiety disorders 1, 9. https://doi.org/10.1186/2045-5380-1-9.

13. Besnard, A., Gao, Y., TaeWoo Kim, M., Twarkowski, H., Reed, A.K., Langberg, T., Feng, W., Xu, X., Saur, D., Zweifel, L.S., Davison, I., Sahay, A., 2019. Dorsolateral septum somatostatin interneurons gate mobility to calibrate context-specific behavioral fear responses. Nat Neurosci 22, 436–446. https://doi.org/10.1038/s41593-018-0330-y.

14. Besnard, A., Leroy, F., 2022. Top-down regulation of motivated behaviors via lateral septum sub-circuits. Mol Psychiatry 27, 3119–3128. https://doi.org/10.1038/s41380-022-01599-3.

15. Blanchard, R.J., McKittrick, C.R., Blanchard, D.C., 2001. Animal models of social stress: effects on behavior and brain neurochemical systems. Physiology & Behavior 73, 261–271. https://doi.org/10.1016/S0031-9384(01)00449-8.

16. Bludau, A., Neumann, I.D., Menon, R., 2023. HDAC1-mediated regulation of GABA signaling within the lateral septum facilitates long-lasting social fear extinction in male mice. Translational psychiatry 13, 10. https://doi.org/10.1038/s41398-023-02310-y.

17. Bondy, C.A., Jensen, R.T., Brady, L.S., Gainer, H., 1989. Cholecystokinin evokes secretion of oxytocin and vasopressin from rat neural lobe independent of external calcium. Proceedings of the National Academy of Sciences of the United States of America 86, 5198–5201. https://doi.org/10.1073/pnas.86.13.5198.

18. Bosch, O.J., Young, L.J., 2018. Oxytocin and Social Relationships: From Attachment to Bond Disruption. Current topics in behavioral neurosciences 35, 97–117. https://doi.org/10.1007/7854_2017_10.

19. Bouton, M.E., 2004. Context and behavioral processes in extinction. Learning & memory (Cold Spring Harbor, N.Y.) 11, 485–494. https://doi.org/10.1101/lm.78804.

20. Brady, J.V., Nauta, W.J., 1953. Subcortical mechanisms in emotional behavior: affective changes following septal forebrain lesions in the albino rat. Journal of Comparative and Physiological Psychology 46, 339–346. https://doi.org/10.1037/h0059531.

21. Brini, M., Calì, T., Ottolini, D., Carafoli, E., 2014. Neuronal calcium signaling: function and dysfunction. Cell. Mol. Life Sci. 71, 2787–2814. https://doi.org/10.1007/s00018-013-1550-7.

22. Brownstein, M.J., Russell, J.T., Gainer, H., 1980. Synthesis, transport, and release of posterior pituitary hormones. Science (New York, N.Y.) 207, 373–378. https://doi.org/10.1126/science.6153132.

23. Busnelli, M., Bulgheroni, E., Manning, M., Kleinau, G., Chini, B., 2013. Selective and potent agonists and antagonists for investigating the role of mouse oxytocin receptors. The Journal of pharmacology and experimental therapeutics 346, 318–327. https://doi.org/10.1124/jpet.113.202994.

24. Busnelli, M., Chini, B., 2018. Molecular Basis of Oxytocin Receptor Signalling in the Brain: What We Know and What We Need to Know. Current topics in behavioral neurosciences 35, 3–29. https://doi.org/10.1007/7854_2017_6.

25. Busnelli, M., Saulière, A., Manning, M., Bouvier, M., Galés, C., Chini, B., 2012. Functional selective oxytocin-derived agonists discriminate between individual G protein family subtypes. The Journal of biological chemistry 287, 3617–3629. https://doi.org/10.1074/jbc.M111.277178.

26. Butler-Struben, H.M., Kentner, A.C., Trainor, B.C., 2022. What's wrong with my experiment?: The impact of hidden variables on neuropsychopharmacology research. Neuropsychopharmacol 47, 1285–1291. https://doi.org/10.1038/s41386-022-01309-1.

27. Calhoon, G.G., Tye, K.M., 2015. Resolving the neural circuits of anxiety. Nature neuroscience 18, 1394–1404. https://doi.org/10.1038/nn.4101.

28. Carter, C.S., Williams, J.R., Witt, D.M., Insel, T.R., 1992. Oxytocin and social bonding. Annals of the New York Academy of Sciences 652, 204–211. https://doi.org/10.1111/j.1749-6632.1992.tb34356.x.

29. Carus-Cadavieco, M., Gorbati, M., Ye, L., Bender, F., van der Veldt, S., Kosse, C., Börgers, C., Lee, S.Y., Ramakrishnan, C., Hu, Y., Denisova, N., Ramm, F., Volitaki, E., Burdakov, D., Deisseroth, K., Ponomarenko, A., Korotkova, T., 2017. Gamma oscillations organize top-down signalling to hypothalamus and enable food seeking. Nature 542, 232–236. https://doi.org/10.1038/nature21066.

30. Chen, Z., Chen, G., Zhong, J., Jiang, S., Lai, S., Xu, H., Deng, X., Li, F., Lu, S., Zhou, K., Li, C., Liu, Z., Zhang, X., Zhu, Y., 2022. A circuit from lateral septum neurotensin neurons to tuberal nucleus controls hedonic feeding. Molecular psychiatry 27, 4843–4860. https://doi.org/10.1038/s41380-022-01742-0.

31. Chesler, E.J., Wilson, S.G., Lariviere, W.R., Rodriguez-Zas, S.L., Mogil, J.S., 2002. Influences of laboratory environment on behavior. Nat Neurosci 5, 1101–1102. https://doi.org/10.1038/nn1102-1101.

32. Choy, Y., Fyer, A.J., Lipsitz, J.D., 2007. Treatment of specific phobia in adults. Clinical Psychology Review 27, 266–286. https://doi.org/10.1016/j.cpr.2006.10.002.

33. Cohen, L.D., Zuchman, R., Sorokina, O., Müller, A., Dieterich, D.C., Armstrong, J.D., Ziv, T., Ziv, N.E., 2013. Metabolic turnover of synaptic proteins: kinetics, interdependencies and implications for synaptic maintenance. PloS one 8, e63191. https://doi.org/10.1371/journal.pone.0063191.

34. Cohen, S., Janicki-Deverts, D., Miller, G.E., 2007. Psychological stress and disease. JAMA 298, 1685–1687. https://doi.org/10.1001/jama.298.14.1685.

35. Conti, F., Sertic, S., Reversi, A., Chini, B., 2009. Intracellular trafficking of the human oxytocin receptor: evidence of receptor recycling via a Rab4/Rab5 "short cycle". American journal of

physiology. Endocrinology and metabolism 296, E532-42. https://doi.org/10.1152/ajpendo.90590.2008.

36. Cottet, M., Albizu, L., Perkovska, S., Jean-Alphonse, F., Rahmeh, R., Orcel, H., Méjean, C., Granier, S., Mendre, C., Mouillac, B., Durroux, T., 2010. Past, present and future of vasopressin and oxytocin receptor oligomers, prototypical GPCR models to study dimerization processes. Current opinion in pharmacology 10, 59–66. https://doi.org/10.1016/j.coph.2009.10.003.

37. Craske, M.G., 2010. Cognitive–behavioral therapy. American Psychological Association.

38. Cryan, J.F., Slattery, D.A., 2007. Animal models of mood disorders: Recent developments. Current opinion in psychiatry 20, 1–7. https://doi.org/10.1097/YCO.0b013e3280117733.

39. Cui, G., Jun, S.B., Jin, X., Luo, G., Pham, M.D., Lovinger, D.M., Vogel, S.S., Costa, R.M., 2014. Deep brain optical measurements of cell type-specific neural activity in behaving mice. Nature protocols 9, 1213–1228. https://doi.org/10.1038/nprot.2014.080.

40. Darwin, C., Prodger, P., Ekman, P., op. 1998. The expression of the emotions in man and animals: Essay on the history of the illustration / by Philip Prodger, 3rd ed. Oxford University Press, Oxford, New York, 472 pp.

41. Davis, M., 2006. Neural systems involved in fear and anxiety measured with fear-potentiated startle. The American psychologist 61, 741–756. https://doi.org/10.1037/0003-066X.61.8.741.

42. Demarchi, L., Pawluski, J.L., Bosch, O.J., 2021. The brain oxytocin and corticotropin-releasing factor systems in grieving mothers: What we know and what we need to learn. Peptides 143, 170593. https://doi.org/10.1016/j.peptides.2021.170593.

43. Dörrbaum, A.R., Kochen, L., Langer, J.D., Schuman, E.M., 2018. Local and global influences on protein turnover in neurons and glia. eLife 7. https://doi.org/10.7554/eLife.34202.

44. Dromard, Y., Borie, A.M., Chakraborty, P., Muscatelli, F., Guillon, G., Desarménien, M.G., Jeanneteau, F., 2023. Disengagement of somatostatin neurons from lateral septum circuitry by oxytocin and vasopressin restores social-fear extinction and suppresses aggression outbursts in

Prader-Willi syndrome model. Biological Psychiatry. https://doi.org/10.1016/j.biopsych.2023.10.016.

45. Ehlers, M.D., 2003. Activity level controls postsynaptic composition and signaling via the ubiquitin-proteasome system. Nat Neurosci 6, 231–242. https://doi.org/10.1038/nn1013.

46. Eliava, M., Melchior, M., Knobloch-Bollmann, H.S., Wahis, J., da Silva Gouveia, M., Tang, Y., Ciobanu, A.C., Del Triana Rio, R., Roth, L.C., Althammer, F., Chavant, V., Goumon, Y., Gruber, T., Petit-Demoulière, N., Busnelli, M., Chini, B., Tan, L.L., Mitre, M., Froemke, R.C., Chao, M.V., Giese, G., Sprengel, R., Kuner, R., Poisbeau, P., Seeburg, P.H., Stoop, R., Charlet, A., Grinevich, V., 2016. A New Population of Parvocellular Oxytocin Neurons Controlling Magnocellular Neuron Activity and Inflammatory Pain Processing. Neuron 89, 1291–1304. https://doi.org/10.1016/j.neuron.2016.01.041.

47. Erben, L., Buonanno, A., 2019. Detection and Quantification of Multiple RNA Sequences Using Emerging Ultrasensitive Fluorescent In Situ Hybridization Techniques. Current protocols in neuroscience 87, e63. https://doi.org/10.1002/cpns.63.

48. Evans, K.C., Wright, C.I., Wedig, M.M., Gold, A.L., Pollack, M.H., Rauch, S.L., 2008. A functional MRI study of amygdala responses to angry schematic faces in social anxiety disorder. Depression and anxiety 25, 496–505. https://doi.org/10.1002/da.20347.

49. Falkai, P., Hans-Ulrich Wittchen (Eds.), 2014. Diagnostisches und Statistisches Manual Psychischer Störungen - DSM-5 ®: Deutsche Ausgabe herausgegeben von Peter Falkai und Hans-Ulrich Wittchen, mitherausgegeben von Manfred Döpfner, Wolfgang Gaebel, Wolfgang Maier, Winfried Rief, Henning Saß und Michael Zaudig, 1st ed. Hogrefe, [Erscheinungsort nicht ermittelbar], 1364 pp.

50. Fedoroff, I.C., Taylor, S., 2001. Psychological and Pharmacological Treatments of Social Phobia: A Meta-Analysis. Journal of Clinical Psychopharmacology 21, 311. https://doi.org/aspx.

51. Ferguson, J.N., Aldag, J.M., Insel, T.R., Young, L.J., 2001. Oxytocin in the medial amygdala is essential for social recognition in the mouse. J. Neurosci. 21, 8278–8285. https://doi.org/10.1523/JNEUROSCI.21-20-08278.2001.

52. Feske, U., Chambless, D.L., 1995. Cognitive behavioral versus exposure only treatment for social phobia: A meta-analysis. Behavior Therapy 26, 695–720. https://doi.org/10.1016/S0005-7894(05)80040-1.

53. File, S.E., Hyde, J.R., 1978. Can social interaction be used to measure anxiety? British journal of pharmacology 62, 19–24. https://doi.org/10.1111/j.1476-5381.1978.tb07001.x.

54. Franklin, T.B., Silva, B.A., Perova, Z., Marrone, L., Masferrer, M.E., Zhan, Y., Kaplan, A., Greetham, L., Verrechia, V., Halman, A., Pagella, S., Vyssotski, A.L., Illarionova, A., Grinevich, V., Branco, T., Gross, C.T., 2017. Prefrontal cortical control of a brainstem social behavior circuit. Nat Neurosci 20, 260–270. https://doi.org/10.1038/nn.4470.

55. Friard, O., Gamba, M., 2016. BORIS : a free, versatile open-source event-logging software for video/audio coding and live observations. Methods Ecol Evol 7, 1325–1330. https://doi.org/10.1111/2041-210X.12584.

56. Gainer, H., Yamashita, M., Fields, R.L., House, S.B., Rusnak, M., 2002. The magnocellular neuronal phenotype: cell-specific gene expression in the hypothalamo-neurohypophysial system. Progress in Brain Research 139, 1–14. https://doi.org/10.1016/S0079-6123(02)39003-4.

57. Georgiou, P., Zanos, P., Mou, T.-C.M., An, X., Gerhard, D.M., Dryanovski, D.I., Potter, L.E., Highland, J.N., Jenne, C.E., Stewart, B.W., Pultorak, K.J., Yuan, P., Powels, C.F., Lovett, J., Pereira, E.F.R., Clark, S.M., Tonelli, L.H., Moaddel, R., Zarate, C.A., Duman, R.S., Thompson, S.M., Gould, T.D., 2022. Experimenters' sex modulates mouse behaviors and neural responses to ketamine via corticotropin releasing factor. Nat Neurosci 25, 1191–1200. https://doi.org/10.1038/s41593-022-01146-x.

58. Gimpl, G., Fahrenholz, F., 2001. The oxytocin receptor system: structure, function, and regulation. Physiological reviews 81, 629–683. https://doi.org/10.1152/physrev.2001.81.2.629.

59. Glover, G.H., 2011. Overview of functional magnetic resonance imaging. Neurosurgery clinics of North America 22, 133-9, vii. https://doi.org/10.1016/j.nec.2010.11.001.

60. Gravati, M., Busnelli, M., Bulgheroni, E., Reversi, A., Spaiardi, P., Parenti, M., Toselli, M., Chini, B., 2010. Dual modulation of inward rectifier potassium currents in olfactory neuronal cells by promiscuous G protein coupling of the oxytocin receptor. Journal of neurochemistry 114, 1424–1435. https://doi.org/10.1111/j.1471-4159.2010.06861.x.

61. Grinevich, V., Knobloch-Bollmann, H.S., Eliava, M., Busnelli, M., Chini, B., 2016. Assembling the Puzzle: Pathways of Oxytocin Signaling in the Brain. Biological Psychiatry 79, 155–164. https://doi.org/10.1016/j.biopsych.2015.04.013.

62. Grinvald, A., Hildesheim, R., 2004. VSDI: a new era in functional imaging of cortical dynamics. Nature reviews. Neuroscience 5, 874–885. https://doi.org/10.1038/nrn1536.

63. Gutkowska, J., Jankowski, M., 2012. Oxytocin revisited: its role in cardiovascular regulation. Journal of neuroendocrinology 24, 599–608. https://doi.org/10.1111/j.1365-2826.2011.02235.x.

64. Guzmán, Y.F., Tronson, N.C., Jovasevic, V., Sato, K., Guedea, A.L., Mizukami, H., Nishimori, K., Radulovic, J., 2013. Fear-enhancing effects of septal oxytocin receptors. Nat Neurosci 16, 1185–1187. https://doi.org/10.1038/nn.3465.

65. Halbach, P., Pillers, D.-A.M., York, N., Asuma, M.P., Chiu, M.A., Luo, W., Tokarz, S., Bird, I.M., Pattnaik, B.R., 2015. Oxytocin expression and function in the posterior retina: a novel signaling pathway. Invest. Ophthalmol. Vis. Sci. 56, 751–760. https://doi.org/10.1167/iovs.14-15646.

66. Harris, J.A., Hirokawa, K.E., Sorensen, S.A., Gu, H., Mills, M., Ng, L.L., Bohn, P., Mortrud, M., Ouellette, B., Kidney, J., Smith, K.A., Dang, C., Sunkin, S., Bernard, A., Oh, S.W., Madisen, L., Zeng, H., 2014. Anatomical characterization of Cre driver mice for neural circuit mapping and manipulation. Frontiers in neural circuits 8, 76. https://doi.org/10.3389/fncir.2014.00076.

67. Heimberg, R.G., Horner, K.J., Juster, H.R., Safren, S.A., Brown, E.J., Schneier, F.R., Liebowitz, M.R., 1999. Psychometric properties of the Liebowitz Social Anxiety Scale. Psychol. Med. 29, 199–212. https://doi.org/10.1017/s0033291798007879.

68. Helmchen, F., Fee, M.S., Tank, D.W., Denk, W., 2001. A miniature head-mounted two-photon microscope. high-resolution brain imaging in freely moving animals. Neuron 31, 903–912. https://doi.org/10.1016/S0896-6273(01)00421-4.

69. Herkenham, M., Nauta, W.J., 1977. Afferent connections of the habenular nuclei in the rat. A horseradish peroxidase study, with a note on the fiber-of-passage problem. The Journal of comparative neurology 173, 123–146. https://doi.org/10.1002/cne.901730107.

70. Herry, C., Ciocchi, S., Senn, V., Demmou, L., Müller, C., Lüthi, A., 2008. Switching on and off fear by distinct neuronal circuits. Nature 454, 600–606. https://doi.org/10.1038/nature07166.

71. Hope, D.A., Heimberg, R.G., Turk, C.L., 2010. Managing Social Anxiety, Workbook. Oxford University Press.

72. Horiai, M., Otsuka, A., Hidema, S., Hiraoka, Y., Hayashi, R., Miyazaki, S., Furuse, T., Mizukami, H., Teruyama, R., Tamura, M., Bito, H., Maejima, Y., Shimomura, K., Nishimori, K., 2020. Targeting oxytocin receptor (Oxtr)-expressing neurons in the lateral septum to restore social novelty in autism spectrum disorder mouse models. Scientific reports 10, 22173. https://doi.org/10.1038/s41598-020-79109-0.

73. Izard, C.E., 2009. Emotion theory and research: highlights, unanswered questions, and emerging issues. Annual review of psychology 60, 1–25. https://doi.org/10.1146/annurev.psych.60.110707.163539.

74. Jurek, B., Neumann, I.D., 2018. The Oxytocin Receptor: From Intracellular Signaling to Behavior. Physiological reviews 98, 1805–1908. https://doi.org/10.1152/physrev.00031.2017.

75. Kessler, R.C., Berglund, P., Demler, O., Jin, R., Merikangas, K.R., Walters, E.E., 2005. Lifetime prevalence and age-of-onset distributions of DSM-IV disorders in the National Comorbidity Survey Replication. Arch Gen Psychiatry 62, 593–602. https://doi.org/10.1001/archpsyc.62.6.593.

76. Kilkenny, C., Altman, D.G., 2010. Improving bioscience research reporting: ARRIVE-ing at a solution. Laboratory animals 44, 377–378. https://doi.org/10.1258/la.2010.0010021.

77. King, L.B., Walum, H., Inoue, K., Eyrich, N.W., Young, L.J., 2016. Variation in the Oxytocin Receptor Gene Predicts Brain Region-Specific Expression and Social Attachment. Biological Psychiatry 80, 160–169. https://doi.org/10.1016/j.biopsych.2015.12.008.

78. Kleinginna, P.R., Kleinginna, A.M., 1981. A categorized list of emotion definitions, with suggestions for a consensual definition. Motiv Emot 5, 345–379. https://doi.org/10.1007/BF00992553.

79. Knobloch, H.S., Charlet, A., Hoffmann, L.C., Eliava, M., Khrulev, S., Cetin, A.H., Osten, P., Schwarz, M.K., Seeburg, P.H., Stoop, R., Grinevich, V., 2012. Evoked axonal oxytocin release in the central amygdala attenuates fear response. Neuron 73, 553–566. https://doi.org/10.1016/j.neuron.2011.11.030.

80. Kobayashi, Y., Sano, Y., Vannoni, E., Goto, H., Suzuki, H., Oba, A., Kawasaki, H., Kanba, S., Lipp, H.-P., Murphy, N.P., Wolfer, D.P., Itohara, S., 2013. Genetic dissection of medial habenula-interpeduncular nucleus pathway function in mice. Frontiers in behavioral neuroscience 7, 17. https://doi.org/10.3389/fnbeh.2013.00017.

81. Köhler, C., Eriksson, L.G., 1984. An immunohistochemical study of somatostatin and neurotensin positive neurons in the septal nuclei of the rat brain. Anatomy and embryology 170, 1–10. https://doi.org/10.1007/BF00319452.

82. Kornhuber, J., Zoicas, I., 2021. Neuropeptide Y Reduces Social Fear in Male Mice: Involvement of Y1 and Y2 Receptors in the Dorsolateral Septum and Central Amygdala. International journal of molecular sciences 22. https://doi.org/10.3390/ijms221810142.

83. Krzywkowski, P., Penna, B., Gross, C.T., 2020. Dynamic encoding of social threat and spatial context in the hypothalamus. eLife 9. https://doi.org/10.7554/eLife.57148.

84. La Mora, M.P. de, Pérez-Carrera, D., Crespo-Ramírez, M., Tarakanov, A., Fuxe, K., Borroto-Escuela, D.O., 2016. Signaling in dopamine D2 receptor-oxytocin receptor heterocomplexes and its relevance for the anxiolytic effects of dopamine and oxytocin interactions in the amygdala of the rat. Biochimica et biophysica acta 1862, 2075–2085. https://doi.org/10.1016/j.bbadis.2016.07.004.

85. Labuschagne, I., Phan, K.L., Wood, A., Angstadt, M., Chua, P., Heinrichs, M., Stout, J.C., Nathan, P.J., 2010. Oxytocin attenuates amygdala reactivity to fear in generalized social anxiety disorder. Neuropsychopharmacol 35, 2403–2413. https://doi.org/10.1038/npp.2010.123.

86. Lahoud, N., Maroun, M., 2013. Oxytocinergic manipulations in corticolimbic circuit differentially affect fear acquisition and extinction. Psychoneuroendocrinology 38, 2184–2195. https://doi.org/10.1016/j.psyneuen.2013.04.006.

87. Landgraf, R., Neumann, I.D., 2004. Vasopressin and oxytocin release within the brain: a dynamic concept of multiple and variable modes of neuropeptide communication. Frontiers in neuroendocrinology 25, 150–176. https://doi.org/10.1016/j.yfrne.2004.05.001.

88. Lazic, S.E., Essioux, L., 2013. Improving basic and translational science by accounting for litter-to-litter variation in animal models. BMC neuroscience 14, 37. https://doi.org/10.1186/1471-2202-14-37.

89. LeDoux, J.E., 2000. Emotion circuits in the brain. Annual review of neuroscience 23, 155–184. https://doi.org/10.1146/annurev.neuro.23.1.155.

90. Leichsenring, F., Leweke, F., 2017. Social Anxiety Disorder. The New England journal of medicine 376, 2255–2264. https://doi.org/10.1056/NEJMcp1614701.

91. Leroy, F., Park, J., Asok, A., Brann, D.H., Meira, T., Boyle, L.M., Buss, E.W., Kandel, E.R., Siegelbaum, S.A., 2018. A circuit from hippocampal CA2 to lateral septum disinhibits social aggression. Nature 564, 213–218. https://doi.org/10.1038/s41586-018-0772-0.

92. Lewis, M., Haviland-Jones, J., 2008. Handbook of Emotions, Third Edition, 3rd ed. Guilford Publications, New York, 2876 pp.

93. Li, L., Durand-de Cuttoli, R., Aubry, A.V., Burnett, C.J., Cathomas, F., Parise, L.F., Chan, K.L., Morel, C., Yuan, C., Shimo, Y., Lin, H.-Y., Wang, J., Russo, S.J., 2023. Social trauma engages lateral septum circuitry to occlude social reward. Nature 613, 696–703. https://doi.org/10.1038/s41586-022-05484-5.

94. Liao, P.-Y., Chiu, Y.-M., Yu, J.-H., Chen, S.-K., 2020. Mapping Central Projection of Oxytocin Neurons in Unmated Mice Using Cre and Alkaline Phosphatase Reporter. Frontiers in neuroanatomy 14, 559402. https://doi.org/10.3389/fnana.2020.559402.

95. Lin, W., McKinney, K., Liu, L., Lakhlani, S., Jennes, L., 2003. Distribution of vesicular glutamate transporter-2 messenger ribonucleic Acid and protein in the septum-hypothalamus of the rat. Endocrinology 144, 662–670. https://doi.org/10.1210/en.2002-220908.

96. Loos, M., Koopmans, B., Aarts, E., Maroteaux, G., van der Sluis, S., Verhage, M., Smit, A.B., 2015. Within-strain variation in behavior differs consistently between common inbred strains of mice. Mammalian genome : official journal of the International Mammalian Genome Society 26, 348–354. https://doi.org/10.1007/s00335-015-9578-7.

97. Ludwig, M., Callahan, M.F., Neumann, I., Landgraf, R., Morris, M., 1994. Systemic osmotic stimulation increases vasopressin and oxytocin release within the supraoptic nucleus. Journal of neuroendocrinology 6, 369–373. https://doi.org/10.1111/j.1365-2826.1994.tb00595.x.

98. Lukas, M., Bredewold, R., Neumann, I.D., Veenema, A.H., 2010. Maternal separation interferes with developmental changes in brain vasopressin and oxytocin receptor binding in male rats. Neuropharmacology 58, 78–87. https://doi.org/10.1016/j.neuropharm.2009.06.020.

99. Lukas, M., Toth, I., Veenema, A.H., Neumann, I.D., 2013. Oxytocin mediates rodent social memory within the lateral septum and the medial amygdala depending on the relevance of the social stimulus: male juvenile versus female adult conspecifics. Psychoneuroendocrinology 38, 916–926. https://doi.org/10.1016/j.psyneuen.2012.09.018.

100. Luo, L., Callaway, E.M., Svoboda, K., 2008. Genetic dissection of neural circuits. Neuron 57, 634–660. https://doi.org/10.1016/j.neuron.2008.01.002.

101. Mak, P., Broussard, C., Vacy, K., Broadbear, J.H., 2012. Modulation of anxiety behavior in the elevated plus maze using peptidic oxytocin and vasopressin receptor ligands in the rat. Journal of psychopharmacology (Oxford, England) 26, 532–542. https://doi.org/10.1177/0269881111416687.

102. Maren, S., Phan, K.L., Liberzon, I., 2013. The contextual brain: implications for fear conditioning, extinction and psychopathology. Nature reviews. Neuroscience 14, 417–428. https://doi.org/10.1038/nrn3492.

103. Masis-Calvo, M., Schmidtner, A.K., Moura Oliveira, V.E. de, Grossmann, C.P., Jong, T.R. de, Neumann, I.D., 2018. Animal models of social stress: the dark side of social interactions. Stress (Amsterdam, Netherlands) 21, 417–432. https://doi.org/10.1080/10253890.2018.1462327.

104. Mathuru, A.S., Jesuthasan, S., 2013. The medial habenula as a regulator of anxiety in adult zebrafish. Frontiers in neural circuits 7, 99. https://doi.org/10.3389/fncir.2013.00099.

105. McKay, D., Tryon, W.W., 2017. Behavior Therapy: Theoretical Bases☆, in: Reference Module in Neuroscience and Biobehavioral Psychology. Elsevier.

106. McKinney, W.T., Bunney, W.E., 1969. Animal model of depression. I. Review of evidence: implications for research. Arch Gen Psychiatry 21, 240–248. https://doi.org/10.1001/archpsyc.1969.01740200112015.

107. Melzer, S., Monyer, H., 2020. Diversity and function of corticopetal and corticofugal GABAergic projection neurons. Nature reviews. Neuroscience 21, 499–515. https://doi.org/10.1038/s41583-020-0344-9.

108. Menon, R., Grund, T., Zoicas, I., Althammer, F., Fiedler, D., Biermeier, V., Bosch, O.J., Hiraoka, Y., Nishimori, K., Eliava, M., Grinevich, V., Neumann, I.D., 2018. Oxytocin Signaling in the Lateral Septum Prevents Social Fear during Lactation. Current biology : CB 28, 1066-1078.e6. https://doi.org/10.1016/j.cub.2018.02.044.

109. Menon, R., Süß, T., Oliveira, Vinícius Elias de Moura, Neumann, I.D., Bludau, A., 2022. Neurobiology of the lateral septum: regulation of social behavior. Trends in Neurosciences 45, 27–40. https://doi.org/10.1016/j.tins.2021.10.010.

110. Mens, W.B., Witter, A., van Wimersma Greidanus, T.B., 1983. Penetration of neurohypophyseal hormones from plasma into cerebrospinal fluid (CSF): half-times of disappearance of these neuropeptides from CSF. Brain Research 262, 143–149. https://doi.org/10.1016/0006-8993(83)90478-x.

111. Milad, M.R., Quirk, G.J., 2002. Neurons in medial prefrontal cortex signal memory for fear extinction. Nature 420, 70–74. https://doi.org/10.1038/nature01138.

112. Milad, M.R., Quirk, G.J., 2012. Fear extinction as a model for translational neuroscience: ten years of progress. Annual review of psychology 63, 129–151. https://doi.org/10.1146/annurev.psych.121208.131631.

113. Mitre, M., Marlin, B.J., Schiavo, J.K., Morina, E., Norden, S.E., Hackett, T.A., Aoki, C.J., Chao, M.V., Froemke, R.C., 2016. A Distributed Network for Social Cognition Enriched for Oxytocin Receptors. J. Neurosci. 36, 2517–2535. https://doi.org/10.1523/JNEUROSCI.2409-15.2016.

114. Mohr, E., Bahnsen, U., Kiessling, C., Richter, D., 1988. Expression of the vasopressin and oxytocin genes in rats occurs in mutually exclusive sets of hypothalamic neurons. FEBS letters 242, 144–148. https://doi.org/10.1016/0014-5793(88)81003-2.

115. Mohr, E., Richter, D., 2003. Local synthesis of the rat Vasopressin precursor in dendrites of in vitro cultured nerve cells. Molecular Brain Research 114, 115–122. https://doi.org/10.1016/S0169-328X(03)00137-2.

116. Monfils, M.-H., Cowansage, K.K., Klann, E., LeDoux, J.E., 2009. Extinction-reconsolidation boundaries: key to persistent attenuation of fear memories. Science (New York, N.Y.) 324, 951–955. https://doi.org/10.1126/science.1167975.

117. Moreno-López, Y., Martínez-Lorenzana, G., Condés-Lara, M., Rojas-Piloni, G., 2013. Identification of oxytocin receptor in the dorsal horn and nociceptive dorsal root ganglion neurons. Neuropeptides 47, 117–123. https://doi.org/10.1016/j.npep.2012.09.008.

118. Morris, J.F., Pow, D.V., 1991. Widespread release of peptides in the central nervous system: quantitation of tannic acid-captured exocytoses. The Anatomical record 231, 437–445. https://doi.org/10.1002/ar.1092310406.

119. Myers, K.M., Davis, M., 2002. Behavioral and neural analysis of extinction. Neuron 36, 567–584. https://doi.org/10.1016/S0896-6273(02)01064-4.

120. National Institute of Mental Health, 2023. Social Anxiety Disorder: More Than Just Shyness. https://www.nimh.nih.gov/health/publications/social-anxiety-disorder-more-than-just-shyness (accessed 21 April 2023).

121. Neumann, I.D., 2003. Brain mechanisms underlying emotional alterations in the peripartum period in rats. Depression and anxiety 17, 111–121. https://doi.org/10.1002/da.10070.

122. Norrholm, S.D., Jovanovic, T., 2018. Fear Processing, Psychophysiology, and PTSD. Harvard review of psychiatry 26, 129–141. https://doi.org/10.1097/HRP.0000000000000189.

123. Öhman, A., 2008. Fear and anxiety: Overlaps and dissociations, pp.709-728.

124. Okamoto, H., Agetsuma, M., Aizawa, H., 2012. Genetic dissection of the zebrafish habenula, a possible switching board for selection of behavioral strategy to cope with fear and anxiety. Developmental neurobiology 72, 386–394. https://doi.org/10.1002/dneu.20913.

125. Olds, J., Milner, P., 1954. Positive reinforcement produced by electrical stimulation of septal area and other regions of rat brain. Journal of Comparative and Physiological Psychology 47, 419–427. https://doi.org/10.1037/h0058775.

126. Oliveira, Vinícius Elias de Moura, Lukas, M., Wolf, H.N., Durante, E., Lorenz, A., Mayer, A.-L., Bludau, A., Bosch, O.J., Grinevich, V., Egger, V., Jong, T.R. de, Neumann, I.D., 2021. Oxytocin and vasopressin within the ventral and dorsal lateral septum modulate aggression in female rats. Nat Commun 12, 2900. https://doi.org/10.1038/s41467-021-23064-5.

127. Ophir, A.G., Zheng, D.-J., Eans, S., Phelps, S.M., 2009. Social investigation in a memory task relates to natural variation in septal expression of oxytocin receptor and vasopressin receptor 1a in prairie voles (Microtus ochrogaster). Behavioral neuroscience 123, 979–991. https://doi.org/10.1037/a0016663.

128. Orban, P.C., Chui, D., Marth, J.D., 1992. Tissue- and site-specific DNA recombination in transgenic mice. Proceedings of the National Academy of Sciences of the United States of America 89, 6861–6865. https://doi.org/10.1073/pnas.89.15.6861.

129. Ostrowski, N.L., Young, W.S., Lolait, S.J., 1995. Estrogen increases renal oxytocin receptor gene expression. Endocrinology 136, 1801–1804. https://doi.org/10.1210/endo.136.4.7895693.

130. Parfitt, G.M., Nguyen, R., Bang, J.Y., Aqrabawi, A.J., Tran, M.M., Seo, D.K., Richards, B.A., Kim, J.C., 2017. Bidirectional Control of Anxiety-Related Behaviors in Mice: Role of Inputs Arising from the Ventral Hippocampus to the Lateral Septum and Medial Prefrontal Cortex. Neuropsychopharmacol 42, 1715–1728. https://doi.org/10.1038/npp.2017.56.

131. Paxinos, G., Franklin, K.B.J., 2019. Paxinos and Franklin's the mouse brain in stereotaxic coordinates. Academic Press, an imprint of Elsevier, London, 1 Online-Ressource.

132. Phelps, E.A., Delgado, M.R., Nearing, K.I., LeDoux, J.E., 2004. Extinction learning in humans: role of the amygdala and vmPFC. Neuron 43, 897–905. https://doi.org/10.1016/j.neuron.2004.08.042.

133. Popik, P., Vos, P.E., van Ree, J.M., 1992. Neurohypophyseal hormone receptors in the septum are implicated in social recognition in the rat. Behavioural Pharmacology 3, 351???358. https://doi.org/10.1097/00008877-199208000-00011.

134. Powers, M.B., Sigmarsson, S.R., Emmelkamp, P.M.G., 2008. A Meta–Analytic Review of Psychological Treatments for Social Anxiety Disorder. International Journal of Cognitive Therapy 1, 94–113. https://doi.org/10.1521/ijct.2008.1.2.94.

135. 2003. Principles of laboratory animal science.

136. Purves, D., Augustine, G.J., Fitzpatrick, D., Hall, W.C., LaMantia, A.-S., Whie, L.E., Mooney, R.D., Platt, M.L. (Eds.), op. 2012. Neuroscience, 5th ed. Sinauer, Sunderland (Mass.), 1 vol. (XVI-759-[60] p.).

137. Raam, T., McAvoy, K.M., Besnard, A., Veenema, A.H., Sahay, A., 2017. Hippocampal oxytocin receptors are necessary for discrimination of social stimuli. Nat Commun 8, 2001. https://doi.org/10.1038/s41467-017-02173-0.

138. Reber, S.O., Neumann, I.D., 2008. Defensive behavioral strategies and enhanced state anxiety during chronic subordinate colony housing are accompanied by reduced hypothalamic vasopressin, but not oxytocin, expression. Annals of the New York Academy of Sciences 1148, 184–195. https://doi.org/10.1196/annals.1410.003.

139. Reversi, A., Rimoldi, V., Marrocco, T., Cassoni, P., Bussolati, G., Parenti, M., Chini, B., 2005. The oxytocin receptor antagonist atosiban inhibits cell growth via a "biased agonist" mechanism. The Journal of biological chemistry 280, 16311–16318. https://doi.org/10.1074/jbc.M409945200.

140. Rhodes, C.H., Morrell, J.I., Pfaff, D.W., 1981. Immunohistochemical analysis of magnocellular elements in rat hypothalamus: distribution and numbers of cells containing neurophysin, oxytocin, and vasopressin. The Journal of comparative neurology 198, 45–64. https://doi.org/10.1002/cne.901980106.

141. Richardson, M.P., Strange, B.A., Dolan, R.J., 2004. Encoding of emotional memories depends on amygdala and hippocampus and their interactions. Nat Neurosci 7, 278–285. https://doi.org/10.1038/nn1190.

142. Rilling, J.K., Young, L.J., 2014. The biology of mammalian parenting and its effect on offspring social development. Science (New York, N.Y.) 345, 771–776. https://doi.org/10.1126/science.1252723.

143. Risold, P.Y., Swanson, L.W., 1997. Chemoarchitecture of the rat lateral septal nucleus. Brain research. Brain research reviews 24, 91–113. https://doi.org/10.1016/S0165-0173(97)00008-8.

144. Rizzi-Wise, C.A., Wang, D.V., 2021. Putting Together Pieces of the Lateral Septum: Multifaceted Functions and Its Neural Pathways. eNeuro 8. https://doi.org/10.1523/ENEURO.0315-21.2021.

145. Roth, R.H., Ding, J.B., 2020. From Neurons to Cognition: Technologies for Precise Recording of Neural Activity Underlying Behavior. BME frontiers 2020, 7190517. https://doi.org/10.34133/2020/7190517.

146. Royer, M., Pai, B., Menon, R., Bludau, A., Gryksa, K., Perry, R.B.-T., Ulitsky, I., Meister, G., Neumann, I.D., 2022. Transcriptome and chromatin alterations in social fear indicate association of MEG3 with successful extinction of fear. Mol Psychiatry 27, 4064–4076. https://doi.org/10.1038/s41380-022-01481-2.

147. Ruscio, A.M., Brown, T.A., Chiu, W.T., Sareen, J., Stein, M.B., Kessler, R.C., 2008. Social fears and social phobia in the USA: results from the National Comorbidity Survey Replication. Psychol. Med. 38, 15–28. https://doi.org/10.1017/s0033291707001699.

148. Russell, J.A., Brunton, P.J., 2009. Oxytocin (Peripheral/Central Actions and their Regulation), in: Encyclopedia of Neuroscience. Elsevier, pp. 337–347.

149. Russell, J.T., 2011. Imaging calcium signals in vivo: a powerful tool in physiology and pharmacology. British journal of pharmacology 163, 1605–1625. https://doi.org/10.1111/j.1476-5381.2010.00988.x.

150. Rydén, G., Sjöholm, I., 1969. HALF-LIFE OF OXYTOCIN IN BLOOD OF PREGNANT AND NON-PREGNANT WOMEN. Acta Endocrinologica 61, 425–431. https://doi.org/10.1530/acta.0.0610425.

151. Sakurai, K., Zhao, S., Takatoh, J., Rodriguez, E., Lu, J., Leavitt, A.D., Fu, M., Han, B.-X., Wang, F., 2016. Capturing and Manipulating Activated Neuronal Ensembles with CANE Delineates a Hypothalamic Social-Fear Circuit. Neuron 92, 739–753. https://doi.org/10.1016/j.neuron.2016.10.015.

152. Sareen, L., Stein, M., 2000. A review of the epidemiology and approaches to the treatment of social anxiety disorder. Drugs 59, 497–509. https://doi.org/10.2165/00003495-200059030-00007.

153. Schindelin, J., Arganda-Carreras, I., Frise, E., Kaynig, V., Longair, M., Pietzsch, T., Preibisch, S., Rueden, C., Saalfeld, S., Schmid, B., Tinevez, J.-Y., White, D.J., Hartenstein, V., Eliceiri, K., Tomancak, P., Cardona, A., 2012. Fiji: an open-source platform for biological-image analysis. Nature methods 9, 676–682. https://doi.org/10.1038/nmeth.2019.

154. Sheehan, T., Numan, M., 2000. The Septal Region and Social Behavior, in: The Behavioral Neuroscience of the Septal Region. Springer, New York, NY, pp. 175–209.

155. Sheehan, T.P., Chambers, R.A., Russell, D.S., 2004. Regulation of affect by the lateral septum: implications for neuropsychiatry. Brain research. Brain research reviews 46, 71–117. https://doi.org/10.1016/j.brainresrev.2004.04.009.

156. Sheintuch, L., Rubin, A., Brande-Eilat, N., Geva, N., Sadeh, N., Pinchasof, O., Ziv, Y., 2017. Tracking the Same Neurons across Multiple Days in Ca2+ Imaging Data. Cell Reports 21, 1102–1115. https://doi.org/10.1016/j.celrep.2017.10.013.

157. Shin, S., Pribiag, H., Lilascharoen, V., Knowland, D., Wang, X.-Y., Lim, B.K., 2018. Drd3 Signaling in the Lateral Septum Mediates Early Life Stress-Induced Social Dysfunction. Neuron 97, 195-208.e6. https://doi.org/10.1016/j.neuron.2017.11.040.

158. Singewald, N., Schmuckermair, C., Whittle, N., Holmes, A., Ressler, K.J., 2015. Pharmacology of cognitive enhancers for exposure-based therapy of fear, anxiety and trauma-related disorders. Pharmacology & Therapeutics 149, 150–190. https://doi.org/10.1016/j.pharmthera.2014.12.004.

159. Slattery, D.A., Neumann, I.D., 2008. No stress please! Mechanisms of stress hyporesponsiveness of the maternal brain. The Journal of physiology 586, 377–385. https://doi.org/10.1113/jphysiol.2007.145896.

160. Sorge, R.E., Martin, L.J., Isbester, K.A., Sotocinal, S.G., Rosen, S., Tuttle, A.H., Wieskopf, J.S., Acland, E.L., Dokova, A., Kadoura, B., Leger, P., Mapplebeck, J.C.S., McPhail, M., Delaney, A., Wigerblad, G., Schumann, A.P., Quinn, T., Frasnelli, J., Svensson, C.I., Sternberg, W.F., Mogil, J.S., 2014. Olfactory exposure to males, including men, causes stress and related analgesia in rodents. Nat Methods 11, 629–632. https://doi.org/10.1038/nmeth.2935.

161. Steimer, T., 2002. The biology of fear- and anxiety-related behaviors. Dialogues in clinical neuroscience 4, 231–249. https://doi.org/10.31887/DCNS.2002.4.3/tsteimer.

162. Stein, M.B., 2022. Pharmacotherapy for social anxiety disorder in adults.

163. Stein, M.B., Goldin, P.R., Sareen, J., Zorrilla, L.T.E., Brown, G.G., 2002. Increased amygdala activation to angry and contemptuous faces in generalized social phobia. Arch Gen Psychiatry 59, 1027–1034. https://doi.org/10.1001/archpsyc.59.11.1027.

164. Stokholm, K., Thomsen, M.B., Phan, J.-A., Møller, L.K., Bay-Richter, C., Christiansen, S.H., Woldbye, D.P.D., Romero-Ramos, M., Landau, A.M., 2021. α-Synuclein Overexpression Increases Dopamine D2/3 Receptor Binding and Immune Activation in a Model of Early Parkinson's Disease. Biomedicines 9. https://doi.org/10.3390/biomedicines9121876.

165. Taylor, A.H., Whitley, G.S., Nussey, S.S., 1989. The interaction of arginine vasopressin and oxytocin with bovine adrenal medulla cells. The Journal of endocrinology 121, 133–139. https://doi.org/10.1677/joe.0.1210133.

166. Terrillon, S., Durroux, T., Mouillac, B., Breit, A., Ayoub, M.A., Taulan, M., Jockers, R., Barberis, C., Bouvier, M., 2003. Oxytocin and vasopressin V1a and V2 receptors form constitutive homo- and heterodimers during biosynthesis. Molecular endocrinology (Baltimore, Md.) 17, 677–691. https://doi.org/10.1210/me.2002-0222.

167. Thomas, E., Burock, D., Knudsen, K., Deterding, E., Yadin, E., 2013. Single unit activity in the lateral septum and central nucleus of the amygdala in the elevated plus-maze: a model of exposure therapy? Neuroscience letters 548, 269–274. https://doi.org/10.1016/j.neulet.2013.05.078.

168. Tomizawa, K., Iga, N., Lu, Y.-F., Moriwaki, A., Matsushita, M., Li, S.-T., Miyamoto, O., Itano, T., Matsui, H., 2003. Oxytocin improves long-lasting spatial memory during motherhood through MAP kinase cascade. Nat Neurosci 6, 384–390. https://doi.org/10.1038/nn1023.

169. Toth, I., Neumann, I.D., Slattery, D.A., 2012. Social fear conditioning: a novel and specific animal model to study social anxiety disorder. Neuropsychopharmacol 37, 1433–1443. https://doi.org/10.1038/npp.2011.329.

170. Trent, N.L., Menard, J.L., 2010. The ventral hippocampus and the lateral septum work in tandem to regulate rats' open-arm exploration in the elevated plus-maze. Physiology & Behavior 101, 141–152. https://doi.org/10.1016/j.physbeh.2010.04.035.

171. Vega-Quiroga, I., Yarur, H.E., Gysling, K., 2018. Lateral septum stimulation disinhibits dopaminergic neurons in the antero-ventral region of the ventral tegmental area: Role of GABA-A alpha 1 receptors. Neuropharmacology 128, 76–85. https://doi.org/10.1016/j.neuropharm.2017.09.034.

172. Viswanath, H., Carter, A.Q., Baldwin, P.R., Molfese, D.L., Salas, R., 2013. The medial habenula: still neglected. Frontiers in human neuroscience 7, 931. https://doi.org/10.3389/fnhum.2013.00931.

173. Voelkl, B., Altman, N.S., Forsman, A., Forstmeier, W., Gurevitch, J., Jaric, I., Karp, N.A., Kas, M.J., Schielzeth, H., van de Casteele, T., Würbel, H., 2020. Reproducibility of animal research in light of biological variation. Nature reviews. Neuroscience 21, 384–393. https://doi.org/10.1038/s41583-020-0313-3.

174. Wahis, J., Baudon, A., Althammer, F., Kerspern, D., Goyon, S., Hagiwara, D., Lefevre, A., Barteczko, L., Boury-Jamot, B., Bellanger, B., Abatis, M., da Silva Gouveia, M., Benusiglio, D., Eliava, M., Rozov, A., Weinsanto, I., Knobloch-Bollmann, H.S., Kirchner, M.K., Roy, R.K., Wang, H., Pertin, M., Inquimbert, P., Pitzer, C., Siemens, J., Goumon, Y., Boutrel, B., Lamy, C.M., Decosterd, I., Chatton, J.-Y., Rouach, N., Young, W.S., Stern, J.E., Poisbeau, P., Stoop, R., Darbon, P., Grinevich, V., Charlet, A., 2021. Astrocytes mediate the effect of oxytocin in the central amygdala on neuronal activity and affective states in rodents. Nat Neurosci 24, 529–541. https://doi.org/10.1038/s41593-021-00800-0.

175. Waltenspühl, Y., Schöppe, J., Ehrenmann, J., Kummer, L., Plückthun, A., 2020. Crystal structure of the human oxytocin receptor. Science Advances 6, eabb5419. https://doi.org/10.1126/sciadv.abb5419.

176. Wang, J., Tian, Y., Zeng, L.-H., Xu, H., 2020. Prefrontal Disinhibition in Social Fear: A Vital Action of Somatostatin Interneurons. Frontiers in cellular neuroscience 14, 611732. https://doi.org/10.3389/fncel.2020.611732.

177. Willner, P., 1984. The validity of animal models of depression. Psychopharmacology 83, 1–16. https://doi.org/10.1007/BF00427414.

178. Wright, E.C., Hostinar, C.E., Trainor, B.C., 2020. Anxious to see you: Neuroendocrine mechanisms of social vigilance and anxiety during adolescence. European Journal of Neuroscience 52, 2516–2529. https://doi.org/10.1111/ejn.14628.

179. Xu, H., Liu, L., Tian, Y., Wang, J., Li, J., Zheng, J., Zhao, H., He, M., Xu, T.-L., Duan, S., Xu, H., 2019. A Disinhibitory Microcircuit Mediates Conditioned Social Fear in the Prefrontal Cortex. Neuron 102, 668-682.e5. https://doi.org/10.1016/j.neuron.2019.02.026.

180. Yeung, M., Treit, D., 2012. The anxiolytic effects of somatostatin following intra-septal and intra-amygdalar microinfusions are reversed by the selective sst2 antagonist PRL2903. Pharmacology, biochemistry, and behavior 101, 88–92. https://doi.org/10.1016/j.pbb.2011.12.012.

181. Yoshida, M., Takayanagi, Y., Inoue, K., Kimura, T., Young, L.J., Onaka, T., Nishimori, K., 2009. Evidence that oxytocin exerts anxiolytic effects via oxytocin receptor expressed in serotonergic neurons in mice. J. Neurosci. 29, 2259–2271. https://doi.org/10.1523/JNEUROSCI.5593-08.2009.

182. Zhang, X., Kim, J., Tonegawa, S., 2020. Amygdala Reward Neurons Form and Store Fear Extinction Memory. Neuron 105, 1077-1093.e7. https://doi.org/10.1016/j.neuron.2019.12.025.

183. Zhao, C., Eisinger, B., Gammie, S.C., 2013. Characterization of GABAergic neurons in the mouse lateral septum: a double fluorescence in situ hybridization and immunohistochemical study using tyramide signal amplification. PloS one 8, e73750. https://doi.org/10.1371/journal.pone.0073750.

184. Zhou, P., Resendez, S.L., Rodriguez-Romaguera, J., Jimenez, J.C., Neufeld, S.Q., Giovannucci, A., Friedrich, J., Pnevmatikakis, E.A., Stuber, G.D., Hen, R., Kheirbek, M.A., Sabatini, B.L., Kass, R.E., Paninski, L., 2018. Efficient and accurate extraction of in vivo calcium signals from microendoscopic video data. eLife 7. https://doi.org/10.7554/eLife.28728.

185. Zoicas, I., Slattery, D.A., Neumann, I.D., 2014. Brain oxytocin in social fear conditioning and its extinction: involvement of the lateral septum. Neuropsychopharmacol 39, 3027–3035. https://doi.org/10.1038/npp.2014.156.

186. Zych, A.D., Gogolla, N., 2021. Expressions of emotions across species. Current Opinion in Neurobiology 68, 57–66. https://doi.org/10.1016/j.conb.2021.01.003.

ACKNOWLEDGEMENTS

Zuallererst möchte ich mich bei meiner Betreuerin Prof. Dr. Inga Neumann bedanken. Für das Vertrauen, dass von Anfang an in mich gesetzt wurde, aber auch die Freiheit die mir gegeben wurde um eigene Konzepte und Ideen zu entwickeln. Ich hatte immer das Gefühl gefordert, aber auch stark gefördert zu werden. Neben der wissenschaftlichen Unterstützung wurde auch immer ein Fokus auf die persönliche Interaktion gelegt, was für mich ein einzigartiges Arbeitsumfeld geschaffen hat, in dem ich sehr gewachsen bin. Vielen Dank dafür und ich freue mich sehr den Lehrstuhl und die Forschung weiter begleiten zu dürfen.

Ein großer Dank gilt auch Prof. Dr. Tatiana Korotkova, die mir ein einzigartiges Kollaborationsprojekt ermöglicht hat und natürlich Francisco de los Santos, der mit mir zusammen an diesem Projekt gearbeitet hat. Vielen Dank, für die Unterstützung, die großartige Zusammenarbeit und die warmherzige Atmosphäre, die ich in Köln erleben durfte.

Natürlich möchte ich mich auch bei meinen Betreuern bedanken, besonders bei Dr. Rohit Menon für die konstruktiven Gespräche und natürlich auch in das Vertrauen und die Freiheit die mir gegeben wurde. Rohit hat immer an mich geglaubt und mir dadurch sehr viel Sicherheit in meinem Handeln und Entscheidungen gegeben. Auch Prof. Dr. Veronica Egger und Dr. Jan Deussing möchte ich für ihre Unterstützung und vor allem die Auseinandersetzung mit meinem Projekt danken.

Ein riesen Dank geht auch an das ganze Team am Lehrstuhl Neumann. Der technischen Assistenz möchte ich für die Unterstützung im Labor danken, vor allem Rodrigue, der mit mir viele OPs durchgeführt hat und vor allem durch seine stets wunderbare Laune die gute Stimmung auch an schlechten Tagen aufrechterhält. An Dr. Oliver Bosch, der immer bereit ist sich in die Probleme aller Studenten mit einzudenken und auch bürokratisch zu unterstützen. Das bringt mich direkt zu Eva, die jeden Tag den Papierkrieg im Hintergrund für uns führt, danke auch dafür. Auch meinen Kollegen möchte ich danken, vor allem Dr. Katarina Gryksa-Zotz. Sie war mir durch all die Zeit nicht nur eine moralische Stütze, sondern hat mir auch alles gezeigt was ich wissen musste um selbständig im Labor arbeiten zu können, egal ob es sich um das Schreiben eines Tierversuchsantrags handelte, oder eine PCR, Kathi hatte immer eine unglaublich geduldige Art ihr Wissen zu teilen und ist definitiv (für alle Studenten) eine Stütze im Labor. Auch all meinen anderen Kollegen möchte ich danken, für den beständigen Austausch und die Unterstützung. Allgemein schätze ich die Bereitschaft von allen am Lehrstuhl Probleme und Fragen gemeinsam zu lösen enorm. Ein besonderer Dank geht auch an die Studentinnen Karina und Franzi die mich toll unterstützt haben.

Vielleicht der wichtigste Dank zum Schluss, dieser Dank geht an meine Freunde und meine Familie. Die Doktorarbeit war eine intensive Erfahrung, mit Höhen, aber auch vielen Tiefen. Ich schätze zutiefst wie viel Zeit und Energie mein privates Umfeld mir in dieser Zeit geschenkt hat und mich durch alle Gefühlslagen begleitet hat. Am allerwichtigste möchte ich hier meinem Mann Dr. Maximilian Schäfer danken, der mich in so vielerlei Hinsicht unterstützt und immer an mich geglaubt hat, der jede Stimmungslage ertragen und sich jeden Vortrag und jedes Poster angehört hat.

Diese Seite wird den Menschen die mich auf diesem Weg begleitet haben nur in Ansätzen gerecht und ich möchte zuletzt noch einmal betonen, wie Dankbar ich meinem arbeits- und privaten Umfeld für die Unterstützung bin die mir zuteilwurde. Abschließend noch einmal Danke an dich Inga, für die Möglichkeit diesen Weg zu beschreiten.

DECLARATION

Herewith, I declare that this is my own work and I did not make use of any other sources and auxiliary means besides those listed in the bibliography.

Regensburg, 23.11.2023

X

Theresa Schäfer